Master's thesis

NTNU
Norwegian University of Science and Technology
Faculty of Natural Sciences
Department of Biotechnology and Food Science

Torill Hagen

Expansion of skeletal muscle cells using stirred bioreactors

One step closer to *in vitro* meat production

Master's thesis in Food and Technology
Supervisor: Eirin Marie Skjøndal Bar, Mona Elisabeth Pedersen and Sissel Beate Rønning
May 2019

NTNU
Norwegian University of Science and Technology

Torill Hagen

Expansion of skeletal muscle cells using stirred bioreactors

One step closer to *in vitro* meat production

Master's thesis in Food and Technology
Supervisor: Eirin Marie Skjøndal Bar, Mona Elisabeth Pedersen and Sissel Beate Rønning
May 2019

Norwegian University of Science and Technology
Faculty of Natural Sciences
Department of Biotechnology and Food Science

Abstract

The world's populations are expected to increase rapidly the coming years and global demand for meat will rise and result in increased energy consumption, environmental pollution and more animal suffering. Cultivation of meat *in vitro* is under development to give a potentially more sustainable and efficient alternative to today's livestock production. Technically, it is possible to grow meat in the laboratory, which Mark Post demonstrated by producing the first *in vitro* hamburger in 2013. However, a lot of work remains to make this a cost-effective product on the market. Up-scaling of muscle cells using bioreactor and cell culture with edible microcarriers is a step in this direction. Today, the commercial microcarriers are made of non-edible synthetic materials, which requires a removal step in the harvesting of bovine muscle cells from the microcarriers, making the production process more complex.

The main goal of this study was to isolate primary muscle cells from sirloin and cultivate the cells in 2D systems, and in up-scaled 3D systems with edible microcarriers. In collaboration with the ongoing research project "GrowPro-Sustainable bio-production of animal proteins for human consumption" at Nofima AS in Ås, we isolated skeletal muscle cells and cultivated them in 2D systems, spinner flasks and a benchtop bioreactor to measure the cell growth. We monitored different parameters like cell density, cell viability and biochemical processes during cultivation of muscle cells in 2D and 3D systems. To potentially achieve a more sustainable and efficient up-scaled production, two edible microcarriers were made of eggshell membrane (ESM) and collagen from residual raw materials of turkey, and was placed in the spinner flasks. Two commercial microcarriers, Cytodex 1 and 3, were also used in spinner flasks.

Light and fluorescence microscopy was used to characterise the skeletal muscle cells development over the time-course of 8 days. Biochemical processes in 2D and 3D cell culture systems, such as DNA, protein, glucose, lactate, ammonia and L-glutamine, were measured using assay kits. The edible collagen beads were made using liquid nitrogen and they were cross-linked with riboflavin to make them more stable.

The muscle cells in 2D systems were proliferating and spontaneously differentiated over the time-course of 8 days. The cell growth on Cytodex 1 and 3 gave similar trends in growth, however Cytodex 1 appeared to give a higher cell density. The muscle cells were attaching on both of the edible microcarriers, however, the muscle cells on ESM de-attached after new beads were added after day 6. The collagen beads appeared to be a suitable matrix for the muscle cells to proliferate on. The up-scaled production in the benchtop bioreactor was more stable due to the large access of nutrients and growth area, shown from the measured biochemically processes. This study arrives one step closer to the *in vitro* meat production, however, there are many challenges that must be solved before it reaches a consumer's market.

Sammendrag

Det forventes at verdens befolkning vil øke raskt de kommende årene, samtidig vil den globale etterspørselen av kjøtt stige og igjen føre til økt energiforbruk, miljøforurensning og mer slaktning av dyr. Dyrking av kjøtt *in vitro* er under utvikling for å gi et potensielt mer bærekraftig alternativ til dagens kjøttproduksjon. Teknisk sett er det mulig å dyrke kjøtt på laboratoriet, som Mark Post demonstrerte ved å produsere den første *in vitro*-hamburgeren i 2013. Likevel gjenstår det mye før dette kan bli et kostnadseffektivt produkt på markedet. Oppskalering av muskelcelledyrking i bioreaktorer med mikrobærere, er et skritt i denne retningen. I dag er de kommersielle mikrobærere laget av ikke-spiselig syntetiske materialer, som krever at cellene blir fjernet fra kulene under høstingen, noe som gir en mer kompleks produksjonsprosess.

Hovedmålet med denne studien var å isolere primære muskelceller fra storfe og dyrke cellene både i 2D-systemer, og i oppskalerte 3D-systemer med spiselige mikrobærere. I samarbeid med det pågående forskningsprosjektet «GrowPro-Sustainable bio-production of animal proteins for human consumption» ved Nofima AS på Ås, isolerte vi muskelceller og dyrket dem i 2D-systemer, spinner-flasker og i en bioreaktor for å måle cellevekst. Vi kontrollerte ulike parametere som celletetthet, celle-viabilitet og biokjemiske prosesser under celledyrking i 2D- og 3D-systemer. For å oppnå en mer bærekraftig og effektiv oppskaleringsproduksjon ble to spiselige mikrobærere, laget av eggeskallmembran (ESM) og kollagen fra restråstoff av kalkun, plassert i spinner-flasker. To kommersielle mikrobærere, Cytodex 1 og 3, ble også plassert i spinner-flasker.

Lys- og fluorescensmikroskopi ble brukt til å karakterisere utviklingen av muskelcellene i løpet av en periode på 8 dager. De biokjemiske prosessene; DNA, protein, glukose, laktat, ammoniakk og L-glutamin, ble målt i 2D- og 3D-systemene. De spiselige kollagenkulene ble laget med flytende nitrogen og kryssbundet med riboflavin for å stabilisere kulene.

Muskelcellene i 2D-systemene prolifererte og spontandifferensierte seg over perioden på 8 dager. Celleveksten på Cytodex 1 and 3 hadde lignende utfall, men Cytodex 1 viste seg å gi en høyere celletetthet. Muskelcellene festet seg på begge de spiselige mikrobærerne, men ESM pulveret mistet muskelcellene etter at det nye mikrobærerne ble tilsatt etter dag 6. Kollagenkulene viste seg å være en egnet matrise for muskelcellene å proliferere på. Den oppskalerte produksjonen i bioreaktoren ga et mer stabilt miljø for cellene, grunnet stor tilgang til næringsstoffer og tilgjengelig vekstareal, vist ved de målte biokjemiske prosessene. Selv om denne studien leder oss et skritt nærmere *in vitro* kjøttproduksjon, er det fortsatt mange utfordringer som må løses før det når forbrukermarkedet.

Preface

This thesis is the final work of my master studies at the Norwegian University of Science and Technology. The master thesis project was an integrated part of the ongoing research project ‘‘GrowPro-Sustainable bio-production of animal proteins for human consumption’’ at Nofima AS in Ås. It presents the results of a study towards innovative food production, to solve the issue of the rising food demands and to reduce environmental damage of livestock production.

I would like to thank my main supervisor, Associate Professor Eirin Marie Skjøndal Bar, who have been incredibly engaged and encouraging throughout my work. I would also like to give a big thanks to my supervisors at Nofima, Senior Scientist Mona Elisabeth Pedersen and Scientist Sissel Beate Rønning, for giving me all that knowledge, good guidance and high availability during result retrieval and writing my thesis. Thank you to Nofima AS and NTNU Biotechnology for sponsoring my 3 months stay in Ås, to perform the data retrieval for my thesis.

At last, I must give great gratitude to my family for supporting me throughout this spring, and not least for having proofread my master. Thanks to all my friends for your support and pleasant breaks, giving me motivation for continuing working until the end. This master thesis has been a very exciting, demanding and incredibly educational process, and has given me so many useful experiences that I will bring forward in life.

Thanks!

Trondheim, 25. May 2019

Torill Hagen

Table of content

Abbreviations

AEBSF	4-(2-aminoethyl) benzene-sulfonyl fluoride
ATP	Adenosine triphosphate
BR	Broad range
CREMPS	Cysteine-rich eggshell membrane proteins
CI	Confidence interval
DEAE	Diethylaminoethyl cellulose
Diff	Differential
DMEM	Dulbecco's modified eagle medium
DMSO	Dimethyl sulfoxide
DNA	Deoxyribonucleic acid
ECL	Entactin-collagen-laminin
ECM	Extracellular Matrix
EDTA	Ethylenediaminetetraacetic acid
ESM	Eggshell membrane
FBS	Fetal bovine serum
Fungizone	Amphotericin B
GIDH	Glutamate hydrogenase
GLT	Glutaminase
HS	High-sensitivity
LAF	Laminar flow
MRF	Myogenic regulatory factor
NAD/NADH	Nicotinamiade adenine dinucleotide
NP-40	Nonidet P-40
OD	Optical density
PBS	Dulbecco's phosphate buffered saline
PenStrep	Penicillin streptomycin
pH	Potential hydrogen
PM	Proliferation medium
RCF	Relative centrifugal force
RPM	Rotations per minute
SLPM	Standard liters per minute
TCA	Tricarboxylate acid
TCD	Total cell density
UV	Ultra violet
VCD	Viable cell density

1. Introduction

1.1. Background

The global population is growing and combined with changes in socio-demographics, the pressure on the world´s resources to provide more food is increasing (Henchion et al., 2017). General meat production is one of the major influencers on global environmental changes, with 30 % use of global ice-free terrestrial land and 8 % of global freshwater (Tuomisto and de Mattos, 2011), while producing 15 % of global greenhouse gas (GHG) emissions (Gerber et al., 2013), which is more than the global transportation sector. Between 2010 and 2050 it has been predicted that the consumption of livestock production will increase by 70 % (Gerber et al., 2013). Feed production areas for livestock are converted from forests, contributing to severe deforestation and degradation of natural habitat (Tuomisto et al., 2014). Beef has the highest environmental footprints of all livestock production, proving the importance of turning to other solutions that can reduce these numbers (Tuomisto, 2019).

The thought of one day producing meat outside its animal in a laboratory environment is not a new one. Winston Churchill approached the opportunity of cultured meat, as early as 1931 in an essay titled "50 Years Hence": "We shall escape the absurdity of growing a whole chicken in order to eat the breast or wing, by growing these parts separately under a suitable medium" (Galusky, 2014). Cultured meat could be an alternative source for protein and for deceasing the environmental harms stemming from livestock production (Penn, 2018). The aim of cultured meat is to grow muscle tissue in a laboratory that would be used as food, while no animal has to suffer (Tuomisto et al., 2014). Several researchers have tried to predict the environmental footprint of cultured meat, despite its novelty (Tuomisto and de Mattos, 2011; Tuomisto et al., 2014; Schaefer and Savulescu, 2014). Cultured meat have the potential to reduce land, water- and energy use, which would help the population growth while lowering food-based ecological impacts, including climate change (Penn, 2018). The cultured meat production systems can also remove a number of the problems associated with livestock production systems, such as animal welfare issues, nutrition-related diseases, food-borne illnesses and resource use (Bhat et al., 2015).

However, a number of challenges are to be faced before cultured meat becomes an up-scaled production system (Bhat et al., 2015). The quality control of mammalian cells, along with maintaining sterility in the culture, pollution prevention or disease and controlled stem cell donor breeding are important issues to consider (Post, 2012). The concerns about sustainability, animal welfare and environmental burden around beef production have been growing in recent years due to its intensification of livestock slaughtering, and the rapid increase in global population. To produce cultured meat for a global market, large-scale production must be more cost-efficient and sustainable.

1.2. Aims of this thesis

The main goal of this study was to isolate primary muscle cells from sirloin and cultivate the cells in 2D systems, and in up-scaled 3D systems with edible microcarriers. To achieve this goal, we first looked at how the skeletal muscle cells proliferate and differentiate in 2D and in up-scaled 3D systems. Different fermentation systems, such as spinner flasks and a benchtop bioreactor, was used to compare the development of the muscle cells. Secondly, edible microcarriers were made, of dry powdered eggshell membrane (ESM) and collagen beads from residual raw materials of turkey, to see if this could be a more sustainable substitute to synthetic microcarriers. At last, different parameters were monitored and controlled during cultivation of muscle cells in 2D and 3D systems. To achieve this, I implemented a literature study to identify which parameters were relevant to measure, followed by practical measurements to identify biological parameters, such as cell density, cell viability and cell growth and medium consumption.

2. Theory

2.1. State of the art

Both in European countries and in the Unites States (US) research has been dedicated to experiment with cultured meat for several years (Matheny, 2005). In 2002, the US developed research through a National Aeronautic and Space Administration (NASA) funded cultured meat experiment in New York (Hukill, 2006). Cultured meat in the European Union (EU) gained popularity in 2006, and then they established the *in vitro* meat consortium in 2007, "an international alliance of environmentally concerned scientists striving to facilitate the establishment of large-scale process industry for the production of muscle tissue for human consumption and attraction of funding to fuel these efforts" (Goodwin and Shoulders, 2013; Haugdahl, 2014). The first *in vitro* symposium was held in Norway in 2008, after the *in vitro* meat consortium was created (Midgley, 2008). In 2013, the first hamburger made *in vitro* was cooked and tasted in Riverside Studios in London. The five-ounce hamburger was created by scientist Mark Post at Maastricht University in the Netherlands and cost more than $330 000. Professor Mark Post stated that supermarkets would likely sell cultured meat in 10 to 20 years, while first as a luxury item according to both him and other experts (Bhat et al., 2015).

2.2. The skeletal muscle

Meat is post-mortem skeletal muscle containing around 90 % myofibres and 10 % connective tissue and fat cells (Listrat et al. 2016; Post and Hocquette, 2017). The satellite cells in skeletal muscle are placed beneath the mature muscle fibres' basal lamina, and are considered the most important source of regeneration from muscle injury (figure 1). The satellite cells consist of both myogenic and non-myogenic cell populations and are heterogeneous (Sinha et al., 2017). The heterogeneous organ, post-natal muscle, consists of extracellular matrix (ECM) and multi-nucleated muscle fibres. It is highly adaptive to external stimuli, which enables different functional requirements (Stern and Mozdziak, 2019). When the muscle is injured or exercised, the quiescent satellite cells are activated and begins to proliferate, differentiate and fuse cells together to make multinuclear myofibres to repair the damaged muscle, or to form new myofibres (Meiliana et al., 2015). There are two phases of muscle growth; (1) hypertrophy, which is increase in muscle cell size, and (2) hyperplasia, which is increase in cell number (Stern and Mozdziak, 2019). Muscle fibre number is increasing during embryonic development in early staged muscles with the same fibre number as adult muscles, and post-natal muscle growth is therefore due to hypertrophy of existing fibres (Wigmore and Stickland, 1983).

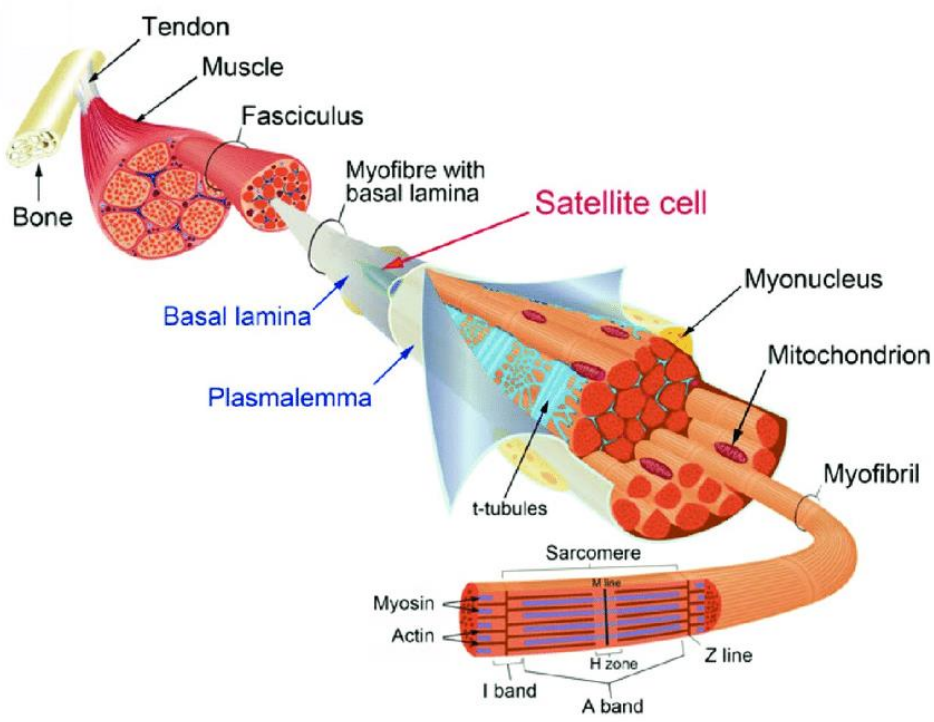

Figure 1: Structure of the skeletal muscle and satellite cell niche. *Ultra-structure of the skeletal muscle (Meiliana et al., 2015)*

The satellite cell is self-renewed, when one daughter cell is proliferating or becoming quiescent, while another commit to differentiation, with either stochastic or asymmetric cell distribution (figure 1) *(Zammit et al., 2006)*. The development from mesodermal precursor to myoblast cells before differentiation into multi-nucleated muscle fibres correlates to signalling systems control and specific transcription factors in each development steps. MyoD, myf-5, myogenin and myf-6/MRF4/herculin are the myogenic basic helix-loop-helix transcription factors playing a key role in controlling the skeletal muscle development (figure 2). The skeletal muscles must be adherent to develop growth, and need an ECM that also plays a key role in alignment and differentiation of myoblasts (Bach et al., 2004). ECM is coated on muscle fibres and are composed of two layers: an internal layer located in basal lamina, that is linked directly to the plasma membrane of myofibres, and an external layer in reticular lamina (Sanes, 2003). ECM is composed of mostly of collagen, and provides the tissue elastic properties, structure support during contractions and helps the myofibres in transmission to tendon. The ECM provides not only structural support but also participates in signalling (Grzelkowska-Kowalczyk, 2016). The ECM must have a biocompatible material and be bioresorbable. The two different matrices used in tissue engineering are either synthetic or biologically-derived biomaterial. Collagen is the most commonly used biomaterial for muscle cells to attract (Bach et al., 2004).

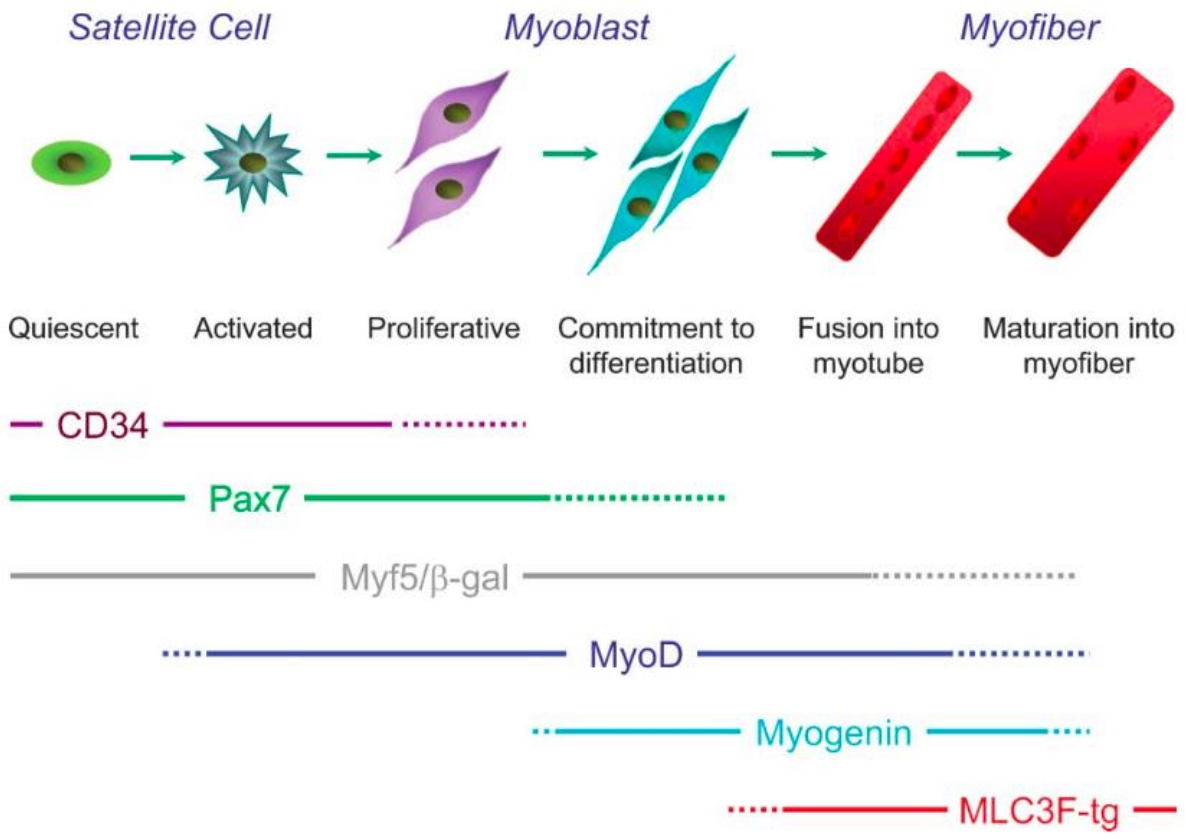

Figure 2: Satellite cell development to myofibres. *The satellite cells in adult muscles are normally quiescent and are activated by trauma or exercise (the self-renewing satellite cells are not included in this illustration). When they are activated, the satellite cells proliferate into myoblast before committing to differentiation and fusing together to form myotubes. Then, the myotubes matures into myofibres. CD34, Pax7 and Myf5/b-gal are expressed in the quiescent stage. MyoD-expression erupts rapid and affects the satellite cells activation, while myogenin later express the commitment to differentiation. The MLC3F-tg have a temporal expression pattern which becomes sarcomeric in late differentiation stages (Zammit et al., 2006).*

2.2.1. Biochemical processes

Lactic acid is almost constantly produced in the muscle fibres of living animals. The produced lactic acid is either converted to pyruvic acid oxidatively through the tricarboxylate acid (TCA) cycle, or moved out of the fibre if the muscle lacks oxygen (figure 3). The skeletal muscle use glucose as an energy source, and when the muscle breaks down the glucose into two pyruvate molecules, it generates the two pyruvate molecules further to three adenosine triphosphate (ATP) molecules. Additionally, two NAD+ molecules reduces to NADH and must be reoxidised to maintain the ratio of glycolysis (Puolanne, 2002). The skeletal muscle consists of fibrillary proteins, actin and myosin, that contributes to develop muscle contraction, which is a process that requires energy in the form of ATP. Fast muscles depend on anaerobic metabolism or glycolysis and can rapidly generate ATP, which means that they can quickly contract. Slow muscles use the aerobic metabolism and consist of a high concentration of oxidative and capillary enzymes that provide better resistance to fatigue (Argilés et al., 2016).

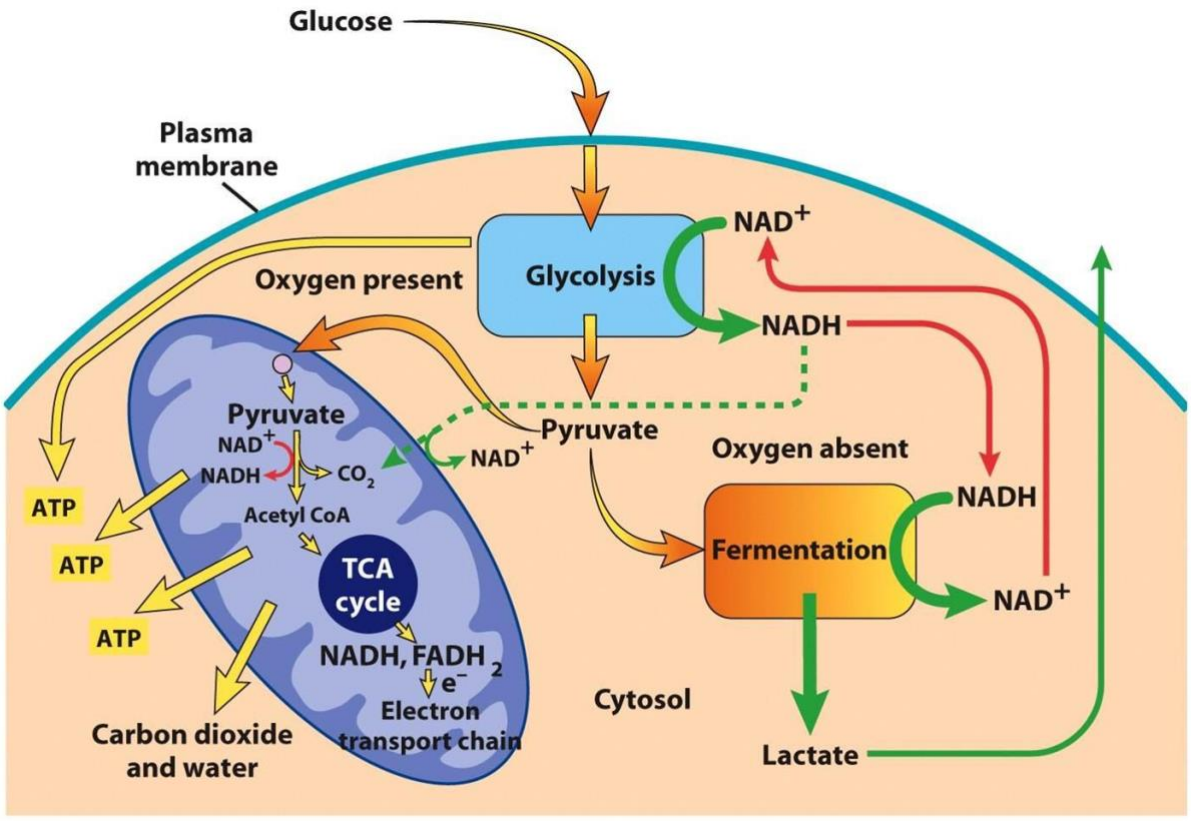

Figure 3: Overview of carbohydrate metabolism in a skeletal muscle cell *(Wiley and sons, 2008).*

Cultivating meat *in vitro,* lacks the organ system that maintains homoeostasis, a stable internal environment for the organ, and therefore needs a strictly and carefully monitored metabolism. To prevent the acidification by lactic acid in the medium, the myocytes must be metabolised aerobically. There must be sufficient oxygen available and this is an important parameter to prevent hypoxia (loss in oxygen). Medium acidification and hypoxia are detrimental to the cells. Culturing meat requires also that the harmful waste products are removed, which can be done by changing the medium after a few days (Datar and Betti, 2010). Skeletal muscle cells can, unlike other cell type, adopt to hypoxic conditions.

An essential component in specific cell culture media is L-Glutamine. It is a necessary amino acid in mammalian mediator metabolism, and closely associated with ammonia metabolism and with aerobic metabolism via the tricarboxylic acid cycle. Two major problems with this amino acid upon incorporation into growth media is; firstly, that L-glutamine is unstable and spontaneously converts to L-glutamate and free ammonium ions. Secondly, these free ammonium ions are very toxic to the cell. A solution can be to add L-glutamine immediately before use (Megazyme, 2018). Ammonia breaks down from protein, more accurately from the deamination of amino acids, from the dietary sources. When measuring ammonia, it is often referred to as the sum of ammonia (NH_3) and ammonium (NH^+_4), with a pK_a of 9.1-9.2 in blood at 37 °C. This indicates that 99 % of the ammonia is in the ionised form in physiological conditions (Stern and Mozdziak, 2019).

When low serum medium is presented to the myoblast cultures, the most common response is differentiation. However, some cells stop cycling and these cells reappear after cloning. This

indicates that when the cells are challenged with mitogenesis, a cellular device may reflect a stage leading to silence rather than differentiation in the cell cycle (Zammit et al., 2006).

2.3. The technology of *in vitro* meat

The process of culturing meat begins with harvesting myosatellite cells from a small sample of muscle of an animal, by e.g. using a biopsy needle (figure 4). The muscle cells can be placed in cell culture flasks uncoated, so that the fibroblasts attaching to the plastic surface faster, can be excluded. The isolated myosatellite cells will start to proliferate and produce myoblasts, which will begin to form a new colony of cells. To get the myoblasts under control, standard cell culture techniques by diluting and spreading the cells over larger spaces are commonly used (Post, 2018). The next step is to proliferate the cells by providing medium that contains all necessary nutrients and energy sources required for the proliferation and differentiation (Alexander et al., 2017). The medium often contains glucose, amino acid, minerals, vitamins, buffer and a percentage of serum. Fetal bovine serum (FBS) is the most commonly used serum supplement made from calf fetus blood (Gstraunthaler, 2003). The energy sources, such as glucose, are often made from plant origin and are easy to purify and extract. Vitamins are typically extracted or synthesized from plants and the amino acids are usually fermented from bacteria (Post, 2014).

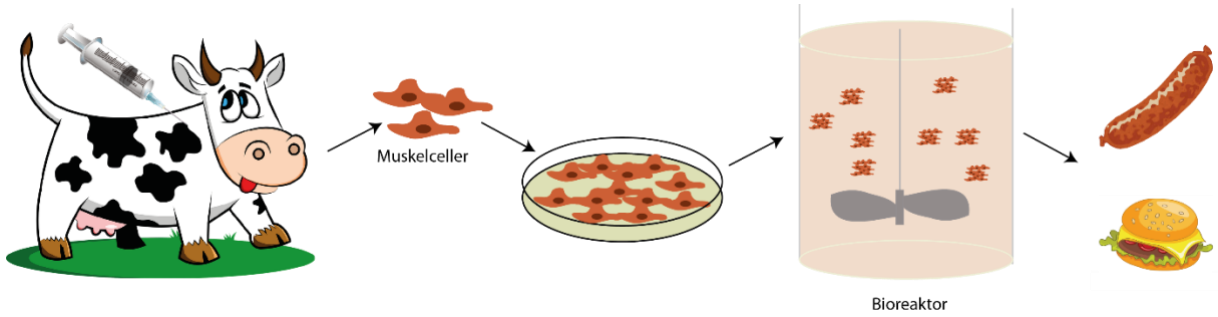

Figure 4: Schematic of a culture meat production *(figure by Sissel Beate Rønning, Nofima).*

The myoblasts will not replicate forever, but have a limited capacity of maximum 45 doublings reported for human cells (Hughes et al., 2016). Like most mammalian cells, the myoblasts are anchorage-dependent, meaning the cells grow while holding on to a surface, such as plastic bottom of a culture flask, a petri dish or microcarriers. After muscle cells have proliferated, they can be transferred to larger fermentation systems, e.g. benchtop bioreactors, to make the process faster with automatic stirring and several microcarriers to give a larger surface area for the cells to grow on (Moritz et al., 2015). The bioreactor provides optimal conditions for the different cells and are filled with sterile medium to promote further cell growth. When the cell density goal is reached, binding protein are added to reduce the development of easily settling aggregates of cells. This happens quickly after the stirring has stopped. The next step is harvesting the cells, after which the cells are pressed and customised for the desired use, e.g. sausage or hamburger (Van der Weele and Tramper, 2014).

2.4. Bioreactors

To provide a large number of cells and at the same time reach an efficiency in number of cell grown per unit of medium, large scale cell production is necessary. It is very important with resource efficiency and cost-efficiency in food production (Verbruggen et al., 2018). The stirred-tank bioreactor with cells grown on microcarriers is a commonly used method for scalable cell culture systems (figure 5). The variation in the fermentation systems is large, the smallest can hold a few millilitres and the largest can support volumes up to several thousand litres (WuXi, 2018). The microcarriers provides a larger surface for cell growth compared with tissue culture flasks (Nienow, 2006). The bioreactor also provides the cells better aeration, transfers precise nutrient supply, decreases consumable costs and supports long term cell culture (Gupta et al., 2016). Before using the large scale tank bioreactor it is common to use a smaller model such as smaller laboratory scale spinner flask (Verbruggen et al., 2018). This is one of the oldest and most commonly used reactor systems in cultured meat production, and a very simplified bioreactor compared to the large scale tank bioreactor (Gupta et al., 2016). Although the stirred-tank bioreactor is the most commonly used, there exists other bioreactors such as e.g. membrane bioreactor, packed bed and fluidised bed bioreactors. Bioprocess monitoring and control is essential when using a bioreactor (Landgrebe et al., 2010).

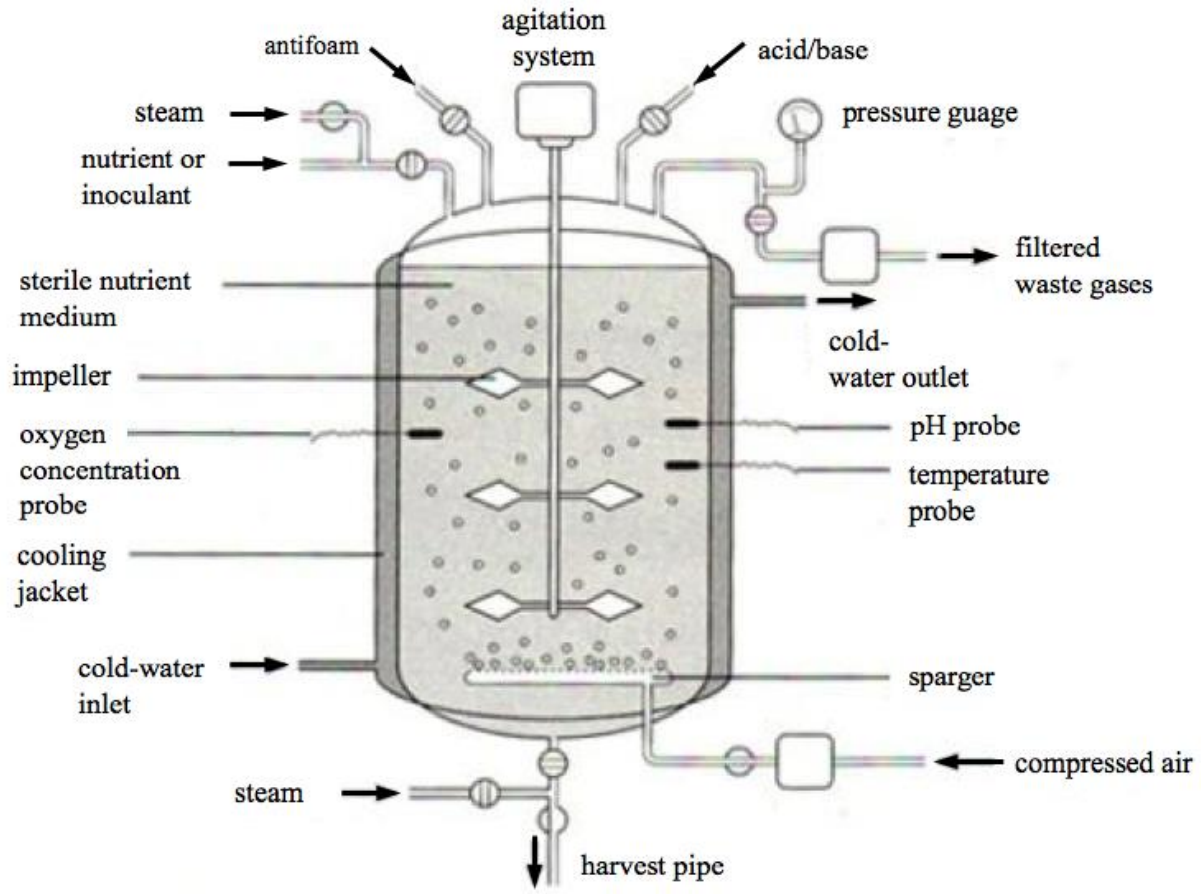

Figure 5: General structure of stirred-tank bioreactor *(Biomate, n.d.).*

It is important to monitor multiple critical constituents and metabolic indicators such as glucose, glutamine, glutamate, lactate, ammonium, osmolality, viability, viable cell density (VCD) and

total cell density (TCD) (López-Meza et al., 2016). Naturally, glucose has been the most critical monitored constituent due to its role as the primary source of nutrients for the cells. The major nutrients consumed by proliferating mammalian cells are glucose and glutamine, but how these and other contribute to cell mass is unknown (Hosios et al., 2016). Culture protocols have been largely developed leading to gradual optimization, through trial and error. However, there still lacks a theoretical basis for a systematic approach. Stem cells produced from skeletal muscles have been generated in the last 15 years, but mainly for potential medical implants. While research on tissue-muscle cells for human consumption has just begun (Post, 2012).

2.5. Microcarriers

Microcarrier culturing is a technique which makes it viable for the high yield culture of anchorage-dependent cells to maximise the growth rate and cell yield. There are a wide variety of commercial microcarriers for culturing of different cell types. The different types of microcarriers varies on the basic supporting matrix materials like dextran, collagen, cellulose, glass and polystyrene (Healthcare, 2009).

The three main categories of microcarriers are: (1) nonporous and microporous microcarriers, (2) microcarriers with matrix made of dextran, polystyrene or respectively, and (3) macroporous microcarriers made of cellulose or gelatin. On the solid and microporous microcarriers, the cells usually grow as monolayers on the outer surface on the carrier. While with the nonporous microcarriers, the cells are directly exposed to the bulk medium, oxygen supply and facilitating nutrients (Badenes et al., 2016). Although the microporous microcarrier has a structure with small pores (≤10 μm) of which the cells are unable to penetrate, it allows free exit of nutrients and metabolites throughout the entire cell surface (Dos Santos et al., 2013). Unlike the microporous microcarrier, the macroporous microcarrier allows cells to potentially enter inside the surface, because of its sponge-like structure with larger pores (10-15 μm). This function provides a larger surface area for the cells to grow, and can imitate a cell niche that also can protect the cells from shear in a bioreactor system (Badenes et al., 2016).

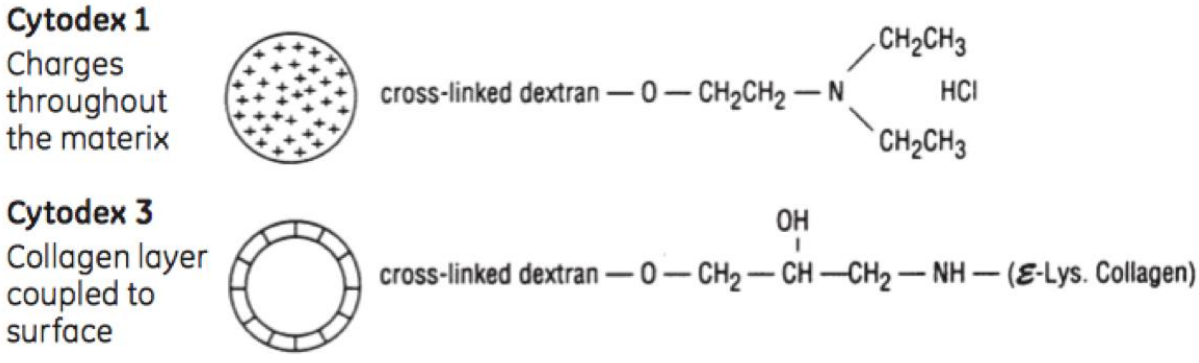

Figure 6: Schematic of two types of Cytodex *(Healthcare, 2009).*

Cytodex™ has been specifically developed for cultivation of different animal cells in culture volumes, from a few ml to more than 6000 l. Using Cytodex in simple suspension culture systems provides yields of several million cells per ml. Cytodex 1 has a positively charged DEAE groups (N, N-diethylaminoethyl) scattered throughout the matrix, of the microcarrier,

shaped from a replacement of a cross-linked dextran matrix (figure 6) (Healthcare, 2009). It is often used to culture mesenchymal stem cells in stirred tank bioreactors and using a non-porous polystyrene microcarrier (Verbruggen et al., 2018). Cytodex 3 is coated with a cross-linked dextran matrix with a thin layer of denatured collagen through a chemically coupling. This microcarrier is optimised for cells that may be challenging to culture *in vitro*, and especially for cells with an epithelial-like morphology (Healthcare, 2009). Both Cytodex 1 and 3 are microporous microcarriers (Badenes et al., 2016). In studies, the Cytodex 1 has measured higher cell proliferation than Cytodex 3 (Souza et al., 2005).

3. Materials and Methods

The methods used for cultivating the skeletal muscle cells and measuring the biochemical processes were chosen based on earlier experiments done at Nofima AS in Ås. All the materials used in the methods are listed in appendix with full name and suppliers (appendix 1). Statistical significants (tukey's multiple comparisons test) was performed on all the measured parameters with more than one replication using Graphpad (appendix 2).

3.1. Bovine primary cell culture

3.1.1. Isolating myoblast cells from bovine cattle

The myoblast, or satellite cells, were isolated from freshly slaughtered bovine sirloin, provided by Notura located in Lillehammer, Norway (Veiseth-Kent et al., 2019). To reduce the risk of contamination, the experiments were completed in a laminar flow (LAF)-bench as a sterile environment that was washed with ethanol 75 % before and after usage. Cells were isolated from inside the sirloin because there were no bacteria there, unlike on the outside surface of the sirloin. Satellite cells were isolated through enzymatic digestion of skeletal muscle with collagenase and with 0.05 % Trypsin to separate the myosatellite cells from other tissue structures (Will et al., 2015). The cells from one isolated batch had the same genetic material as from the bovine cattle. To keep the myoblast's innate signalling pathway under cell growth, the number of myoblast passages should be kept low (Yablonka-Reuveni and Day, 2011). The isolated myosatellite cells were transferred to uncoated plastic cell culture flasks to separate the fibroblast (that attaches to the surface faster) from the myoblasts.

Material:

- 0.05 % Trypsin-EDTA
- Dulbecco's phosphate buffered saline (PBS)
- Collagenase medium:
    - Penicillin streptomycin (PenStrep)
    - Dulbecco's modified eagle medium (DMEM)
    - Amphotericin B (Fungizone)
    - Collagenase
- Falcon tube
- Shaking water bath
- Entactin-collagen-laminin (ECL)-coated cell culture flasks (T-25)
- Seeding medium:
    - DMEM
    - FBS
    - PenStrep
    - Fungizone
- Proliferation medium (PM), 12 % FBS:

    - DMEM
    - FBS
    - PenStrep
    - Fungizone
- Sterile biopsy needle
- Sirloin taken from bovine (freshly slaughtered)
- Cell filter (100 mm)

Protocol:

- The collagenase medium was made with 200 ml DMEM, 1 ml PenStrep, 1 ml Fungizone and 142 mg collagenase, and sterile filtered before usage.
- Marked 5 falcon tubes with I, II, III, IV, V x10 and added:

I	10 ml Collagenase medium
II	1 ml FBS
III	2 ml FBS
IV	2 ml FBS
V	2 ml FBS

- The cells were isolated from tissue samples (1-2 g) extracted from bovine sirloin, using biopsy needle and added to the tubes (I) with collagenase medium.
- Then the tubes with tissue samples were incubated for 60 min at 37 °C in a shaking water bath at 70 rpm.
- Centrifuged the tissue samples for 10 s at 550 RCF and the supernatant was filtered while transferred to new tubes (II).
    - Centrifuged the new tubes (II) for 5 min at 550 RCF before the supernatant was removed.
- Pellet in tubes (I) was re-suspended in 20 ml Trypsin and incubated for 15 min at 37 °C in a shaking water bath at 70 rpm. Moved the tubes around every 5 min.
- Centrifuged the incubated tubes (I) again for 10 s at 550 RCF and the supernatant was filtered while transferred to new tubes (III).
- These steps were repeated till tubes (III-V) had removed supernatant.
- The 4 tubes (II-V) was merged together by re-suspended the pellets with 3 ml seeding medium.
- Sowed out the merged pellets to T-25 flasks to remove fibroblasts that attaches to plastic.
- Incubated the T-25 flasks for 60 min at 37 °C.
- Afterwards the medium was transferred to ECL-coated T-25 flask placed in the incubator cabinet for 48 h, before new proliferations medium was added.

3.1.2. Coating cell culture flasks and 6 well plates

The cell culture flasks are coated before adding the cells for better attachment on the surface. The cell culture flask and wells are coated with ECL which is a cell attachment matrix consisting of several proteins in ECM. ECM is a non-cellular component surrounding all cells *in vivo*, consisting of collagens, proteoglycans and glycoproteins (Shuttleworth, 1998). To effectively grow muscle cells *in vitro,* cells need to be introduced to an environment similar to *in vivo* (Godfrey, 2009). The ECM provide physically separating the stem cell pool from other tissue resident cells and interstitial matrix as one of its key roles. (Thomas et al., 2015). It also affects the proliferation and differentiation of the cells (Rønning et al., 2013).

Material:

- ECL
- Cell scrape
- Cell culture flasks (T-175)
- 6 well plate
- DMEM
- PBS

Protocol:

- ECL was directly added on the bottom of the cell culture flasks and partitioned with a cell scrape, while ECL was mixed with DMEM to coat the 6 well plates and the 3 floored multi flask.

Unit	**Unit volume**	**ECL**	**DMEM**
6 Well Plate	10 cm^2	30 µl	4 ml
Cell culture flask (T-25)	25 cm^2	25 µl	Cell scrape
Cell culture flask (T-75)	75 cm^2	75 µl	Cell scrape
Cell culture flask (T-175)	175 cm^2	175 µl	Cell scrape
Cell culture multi flask (3 floors)	525 cm^2	525 µl	60 ml

- Incubated the coated 6 well plate on a LAF-bench for 2-4 h.
- Medium was removed and washed with PBS before the cells were added.

3.1.3. Long time storage of muscle cells using liquid nitrogen

The isolated cells were frozen down when the cells were approximately 80 % confluent. Cryopreservation of the cells is an important step before long-term storage in liquid nitrogen. The cells will change their functional characteristics, properties and at worst be contaminated over time, so this method is to prevent these changes and ensure a career-long scours of cells (Tirabassi, 2017). Tissue culture grade dimethyl sulfoxide (DMSO) is a cryoprotective agent and the most common ingredient to use in freezing medium. Cryoprotective agent decrease the freezing point of the medium and give the medium a slower cooling rate. It also prevents the risk of crystallization, which can damage and lead to cell death (ThermoFisher, 2019b).

Material:

- PBS
- Trypsin
- PM
- Cell culture flasks (T-175)
- Tubes
- FBS
- DMSO
- Freezer container

Protocol:

- When the flasks with isolated cells were 80 % confluent, the cells were divided as in: "3.1.5. Splitting cells culture".
- After centrifuging the cells for 5 min at 550 RCF the cells were counted
- Resuspended with 1 ml freezing mixture:
    - 0.2 ml PM
    - 0.4 ml FBS
    - 0.4 20 % DMSO
- Transferred to a marked eppendorf tubes and directly placed in freezing containers that were placed in a -80 °C freezer for 24 h.
- After 24 h, the frozen cells were transferred to the liquid nitrogen tank for long-term storage.

3.1.4. Thawing and preparation of muscle cells

The primary satellite muscle cells from freshly slathered bovine sirloin and stored in liquid nitrogen with 20 % DMSO and FBS, were used in all the experiments (Rønning et al., 2013). Proliferation medium of mostly DMEM was used for cell growth, and contained 12 % FBS, which have essential components for cell proliferation and maintenance such as growth factors, spreading, trace elements, transport proteins, vitamins and hormones (Van der Valk et al., 2018). It also contained PenStrep as an addition of antibiotics to reduce the risk of infection from unwanted bacteria in the medium, and fungizone to prevent yeast and multicellular fungi contamination of cell culture. (Ryu et al., 2017; ThermoFisher, 2019a). 2 % Ultroser™ G was used in the proliferation medium instead of FBS as a serum free substitute, when it arrived in the laboratory.

Material:

- Isolated muscle cells
- Water bath
- Proliferation medium
- Coated cell culture flasks (T-175)
- Falcon tube (50 ml)

Protocol:

- Isolated muscle cells were retrieved from the liquid nitrogen tank and thawed on the bench.
- Medium was heated to 37 °C in a shaking water bath.
- The cells were added to 28 ml medium (to give around 30 ml mixture) and turned twice to make a homogenised solution.
- The mixture was added to the pre-coated flasks and incubated at 37 °C for 2 days.

3.1.5. Splitting cell culture

Once the cells were 70-90 % confluent they were ready to split. Trypsin was used to release the cells from the coated flasks. This proteolytic enzyme is a member of the serine protease family and the most common used enzyme to detach cells from adherent substrate. The pre-heated Trypsin at 37 °C, speed up the detachment because the optimum activity is achieved. Long-term incubation with trypsin will damage the cells by striping the surface protein of the cells and lead to cell death (Merck, 2019a). The cells are usually split from cell culture flask (T-25) to larger flasks (T-75) and (T-175), or from one flask (T-175) to two flasks (T-175). Cell culture multi flask (3 floors) were used for the bioreactor experiments to get a large number of cells more effectively and in less space.

Material:

- PBS
- 0.05 % Trypsin-EDTA
- PM
- Cell culture flasks (T-175)
- Falcon tubes

Protocol:

- Preheat Trypsin, sterile PBS and proliferation medium to 37 °C in a shaking water bath.
- Medium was removed from the cell culture flask and washed with 10 ml PBS.
- 4 ml Trypsin was added to the T-175 cell culture flask and incubated for 10 min at 37 °C.
- The flask was knocked on the side to disengaged the cells from the surface and a microscope was used to ensure that all the cells had disengaged from the surface.
- 2 ml PM was added and pumped over the cells to get all the cells off the surface, and it was added to a centrifuge tube.
- The samples were centrifuged for 5 min at 550 RCF to separate the cells from the Trypsin. After centrifuging the supernatant was removed.
- The pellet was re-suspended with 2 ml PM and added to T-175 cell culture flask for cell growth.

3.1.6. Analysing the total amount of cells

The semi-automated Countess™ system was used to viable cell-count, consisting of a hemocytometer to count the cells based on the trypan blue exclusion technique (Cadena-Herrera

et al., 2015). Only the cells with compromised membrane (dead cells) become stained and the cells with intact membranes (live cells) become excluded (Invitrogen™, 2019). Trypan blue staining is a widely-used method to identify live and dead cells, and was used in all the experiments. This method is also used to determine the cell viability quickly and accurately to see if the cells will survive and expand, or take a few days to grow (Gibco™, 2019). Counting of the cells were performed to get a quantitative result for all the experiment.

Material:

- Cell suspension
- Eppendorf tubes
- Trypan blue stain (0.4 %) (T10282)
- Cell counter plate
- Semi-automated Countess™ cell counter

Protocol:

- Transferred 10 µl of the cell suspension to an eppendorf tube.
- Added 10 µl trypan blue stain (0.4 %) to the eppendorf tube and carefully mixed.
- 10 µl of the mix was transferred to a cell counter plate and placed in the Countess™ automated cell counter.

3.2. Skeletal muscle cells grown in 2D systems

The experiment lasted over 8 days and the sampling was taken on day 1, 3, 5 and 8. Cell growth in 2D systems is a well-known technique. The nuclear density of *in vitro* meat production is higher compared to the *in vivo* condition, but *in vitro* meat production lacks the cytoskeleton architecture. Therefore, the protein source in the cells is much lower and the cells are immature. However, after the myoblast fusion, the cells mature and produce sufficient amount of protein (Gharaibeh et al., 2008).

Material:

- Coated 6 well plate
- PM
- Isolated cells
- Incubator cabinet
- Inverted laboratory microscope (Leica DM IL LED)

Protocol:

- Added 4 ml PM to 4 coated 6 well plate, one for each day sampling.
- 60 000 cells were mixed with the medium in each well and placed in an incubator cabinet at 37 °C for 8 days.
- Day 1, 3, 5 and 8: All the medium from the wells was collected in three tubes for analysing glucose and three tubes for analysing lactate (figure 7).
- 1 ml new PM was refilled to each well.
- Pictures with microscope (Leica DM IL LED) was taken from well 1 and 2.

- The rest of the sampling were taken as in figure 7.

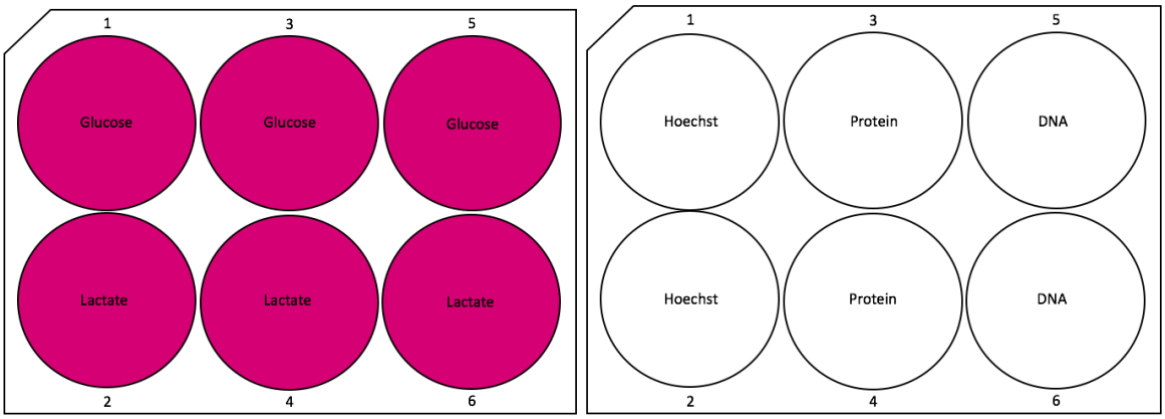

Figure 7: Model of the sampling portioning from the 6 well plate. *The left figure, showing the sampling with the supernatant. The right figure, showing the sampling with the muscle cells.*

3.2.1. Analysis of muscle cells in 2D systems

Qubit™ dsDNA (Broad-Range) assay

Qubit 3.0 fluorometer was used to measure the amount of DNA concentration in all the experiments (Techonlogies, 2014). Double-stranded DNA (dsDNA) was stained with a fluorescent dye and measured based on its fluorescence intensity. Qubit measures intact dsDNA and is thus generally considered useful for controlling DNA quality before next generation sequencing (Nakayama et al., 2016). The Qubit dsDNA broad–range (BR) assay kit measured DNA quickly and was used to prepare the samples from 2D systems and the spinner flask experiments (Probes, 2015). The measurement of dsDNA in Qubit depends on the salt concentration in the sample, and if there is a low salt concentration it can lead to low ratio of the Qubit quantity to the ex-ND value (Q/E ratio) (Nakayama et al., 2016).

Material:

- PBS
- Buffer RLT plus (RNeasy Plus lysis buffer)
- Qubit™ dsDNA BR buffer
- Qubit™ reagent
- Qubit™ dsDNA BR assay kit
- Samples
- Tubes
- Incubation cabinet
- Centrifuge
- Qubit 3.0 fluorometer

Protocol:

- Washed the samples twice with PBS.
- Added 350 ml RLT and froze the samples, or directly measured the samples on the Qubit 3.0 fluorometer.
- Thawed the frozen samples on the bench.

- The sample were mixed for 10-15 s.
- Incubated for 15 min at 50 °C.
- Centrifuged the samples for 1 min at 13 000 RCF.
- Buffer mix was made with 199 µl BR buffer x n samples + n samples µl reagent.
- Made the standards:
    - Standard 1: 190 µl buffer mix + 10 µl reagent I from the assay kit
    - Standard 2: 190 µl buffer mix + 10 µl reagent II from the assay kit
- Added 180 µl buffer mix to new eppendorf tubes for DNA reading + 20 µl supernatant from the samples.
- Mixed all the samples and standards for 10 s.
- Used the Qubit 3.0 fluorometer (BR) to quantify the total amount of DNA concentration in each sample.

Bio-Rad protein assay

The Bio-Rad protein assay was used to measure total protein concentration with a method based on the Bradford dye-binding. The method became popular because it was sensitive, relatively low priced, rapid and specific for protein (Compton and Jones, 1985). It is a simple colorimetric assay used for samples with a protein concentration between 200-1400 µg/ml (20-140 µg total). The Coomassie brilliant blue G-250 dye was used to bind primarily basic and aromatic amino acid residues, and changed colour as a response to various concentration of protein. Interference with the assay could be caused by several detergents and basic protein buffers, and cause chemical-dye or chemical-protein interactions. The dying reaction was determined rapid in 96-well microplates and analysed using a microplate reader with a 750 nm absorbance (Bio-Rad, 2019).

Material:

- PBS
- NP-40 lysis buffer
- 4-(2-aminoethyl) benzene-sulfonyl fluoride (AEBSF)
- Phosphatase cocktail
- Ice
- DC reagent A, B and S
- RC reagent I and II
- 96 well plate
- Microplate reader (Synergy H1)

Protocol:

- Washed the 1 ml fresh sample two times with PBS.
- Made lysis buffer:
    - 0.5 ml NP-40 lysis buffer
    - 2.5 µl AEBSF
    - 5 µl phosphatase cocktail
- Added 150 µl lysis buffer to the samples and left it for 10 min on ice before freezing it down at - 80 °C.

- Thawed the samples on the bench.
- Made different concentrations of the standard based on 2 mg/ml:
    - Diluted: 2 – 1 – 0.5 – 0.25 – 0.125 – 0.06125 mg/ml
- Added 2 x 25 µl of the standard, blank and the supernatant of the samples to eppendorf tubes.
- Incubated all the tubes at 50 °C for 10 min.
- Added 125 µl RCI to all the tubes.
- Mixed and incubated the tubes 1 min on the bench.
- Added 125 µl RCII to all the tubes.
- Mixed and centrifuged for 5 min at 4 °C with 13 000 RCF.
- Made reagent A:
    - 127 µl x n samples DC reagent A + 2 % reagent S (1:51)
- After centrifuging the tubes, the supernatant was removed and dried on the bench for 45 min.
- Added 127 µl reagent A to all the tubes, mixed and incubated the tubes for 5 min on the bench.
- Mixed the tubes again.
- Added 1 ml reagent B and mixed all the tubes.
- Incubated the samples for 15 min on the bench.
- Added 200 µl of the samples to a 96 well plate.
- Measured the protein with the microplate reader (Synergy H1) at 750 nm absorbance.

Hoechst staining of muscle cells

The NucBlue™ or Hoechst 33342 is a counterstain that emits blue fluorescence when bound to adenine-thymine-rich regions on minor grooves of DNA (MedChemExpress, 2019). It stains the cell nuclei and is very sensitive to DNA conformation and chromatin state on cells. Therefore, it can detect damaged nuclei (Invitrogen™, 2005). The blue fluorescence hoechst dye is light sensitive and must be kept away from the light as much as possible. It was used to characterised and count the number of cells, to quantify the development of cell growth in all the experiments. Zeiss Zen software was used to captured the images with stained nuclei (figure 8).

Material:

- NucBlue™ live cell stain ReadyProbes™ reagent
- 6-well plate with muscle cells
- Fluorescence microscope (Axio observer. Z1)

Protocol:

- Two droplets of NucBlue™ were added into each well with 1 ml PM and cells.
- The well was added to a rocker board for 20 min.

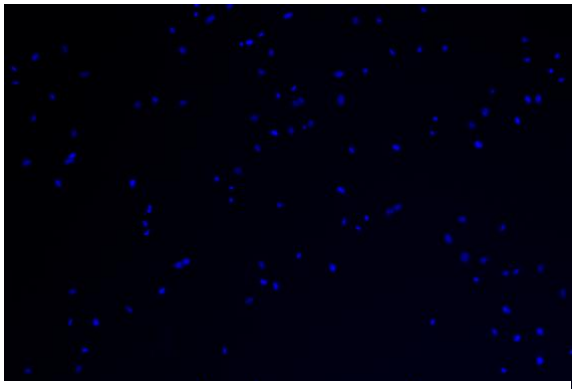

Figure 8: NucBlue™ stained skeletal muscle cells. *Taken with a fluorescence microscope and Zeiss Zen software.*

- Pictures were taken with a fluorescence microscope and analysed using Zeiss Zen software and ImageJ.

Glucose assay

The glucose assay kit (Colorimetric) (ab65333) is designed to measure glucose in various biological samples. The assay was also suitable for detecting the glucose level during fermentation processes, such as bioreactors. The assay kit consists of an enzyme mix (lyophilised) that reacts with the dye when it specifically oxidises glucose. The amount of colour and glucose presenting in the sample were proportional. Glucose is an important fuel source to produce ATP in the muscle cells and was presented through the proliferation medium, which consists mostly of glucose (Abcam, 2019).

Material:

- Glucose assay buffer
- Glucose probe
- Glucose enzyme mix
- Glucose standard (100 nmol/µl)
- Sample solutions
- 96 well plate
- Distilled water

Protocol:

- Heated the glucose probe in a water bath at 37 °C for 5 min before use.
- Suspended glucose enzyme mix with 220 µl glucose assay buffer and kept it on ice.
- Prepared 1 ml of 1 nmol/µl glucose standard by diluting 10 µl of glucose standard in 990 µl glucose assay buffer.
- Made a standard curve by using the 1 nmol/µl glucose standard as described in the table in tubes and adding 50 µl to the well in the end:

Standard #	1 nmol/µl Glucose standard (µl)	Assay buffer (µl)	Final volume in well (µl)
1	0	150	50
2	6	144	50
3	12	136	50
4	18	132	50
5	24	126	50
6	30	120	50

- Added 2 µl samples and 48 µl glucose assay buffer to the sample wells.
- Made the glucose reaction mix and prepared 50 µl for each reaction:
    - 46 µl glucose assay buffer
    - 2 µl glucose probe
    - 2 µl glucose enzyme mix
- Added 50 µl of the reaction mix into each standard and sample well.

- Mixed and incubated the wells for 30 min at 37 °C protected from light.
- Measured the absorbance in a microplate reader at OD 570 mm.
- Calculated the results with the formula under:

$$Glucose\ concentration = \left(\frac{Sa}{Sv}\right) * D$$

Lactate

Lactate or lactic acid ($C_3H_6O_3$) is produced during the metabolism of glucose (Rabi et al., 2017). Under the catalytic effect of lactate dehydrogenase on lactate hydrogenase to a pyruvate, the lactic acid is oxidised by nicotinamiade adenine dinucleotide (NAD) (Martinello et al. 2011). The Reflectoquant® lactic acid test was used to measure the total lactic acid (sum of D- and L-lactic acid) in the medium from all the experiments. Lactate was determined using the reflectometer, RQflex® 10, showing NADH formed in the process when blue formazan was reduced from a tetrazolium salt in the present of diaphorase. It measures the light reflection from the strip added to the RQflex® 10 reader. This method can be used to analyse the lactate level in food after pre-treatments, beverages, e.g. fruit/vegetable juice, wine and beer after dilution (Merck, 2019b).

Material:

- Clean H_2O
- Samples
- Tubes
- Lactate test strip
- RQflex plus 10 reader

Protocol:

- Collected 1.5 ml fresh sample and froze it down at -18 °C.
- Thawed all the samples when the experiment was finished.
- Diluted the samples 20 times in clean H_2O.
- Added the lactate strip into the sample for 2 s. before transferring it to the RQflex plus 10 reader for 298 s.
- After 300 s, the result was shown and noted.
- This was repeated for all the samples.

3.3. Microcarriers

Microcarriers are particles supporting the cells, and can be made of various materials of different shapes, such as polystyrene, gelatin and dextran (Fernandes et al., 2007). Microcarriers are usually used in cell culture systems, such as bioreactors, to give the cells more surface space to grow on. This method makes it possible to introduce up-scaling of the cell production in a more efficient and less expensive way. Cytodex™ microcarriers was developed specifically by Amersham Biosciences (apart of GE Healthcare) for a different animal cell production in culture volumes ranging from a few millilitres to several thousand litres, with the possibility of

yields up to 200 mill cells per millilitre (Healthcare, 2005). Other microcarriers with a natural material, e.g. collagen and ESM, can also be used to get a 3D environment to proliferate primary cells on. The collagen beads in the spinner flask experiments were prepared from collagen pad of turkey using liquid nitrogen, followed by dehydration and cross-linking (Tebb et al., 2006). The eggshell matrix consists of highly cross-linked type I and V collagens layered in thick fibres that compose a pair of non-mineralised matrix layers, called the shell membrane.

3.3.1. Preparing the microcarriers

Preparation of Cytodex 1 and Cytodex 3
Cytodex 1 and 3 arrives as dry powder, so before use they were hydrated and sterilised. The easiest method for sterilization is autoclaving of the microcarriers (Healthcare, 2009).

Material:
- Cytodex 1 and Cytodex 3
- PBS
- High-pressure steam steriliser
- Tubes

Protocol:
- Soaked 500 mg beads with 50 ml PBS for 3 h on the bench.
- Removed the supernatant and added 50 ml fresh PBS.
- Autoclaved the beads before usage in a high-pressure steam steriliser.

Sifting and preparation of eggshell membrane
The dry ESM powder were sifted to get more control over the variation of the spheres. The spheres were also washed and sterilised with PBS and ethanol to reduce the risk of unwanted bacterial infection in the microcarrier culture.

Material:
- ESM powder
- Shaker
- Strainer (100 µm-400 µm)
- PBS
- Ethanol 70 %

Protocol:
- The ESM powder was washed with water, freeze dried and milled at 250 µm before it was part of this experiment.
- 10 g of ESM were weighed.
- Sifted the powder first through a 400 µm strainer and then a 100 µm strainer using a shaker to get a refined powder between 100-250 µm.
- The strained ESM powder was weighed to 50 mg in four falcon tubes.

- Sterilised with 10 ml 70 % ethanol for 10 min.
- Washed three times with 10 ml PBS.
- Stored in refrigerator with 10 ml PBS.

Making the collagen beads

Collagen is one of the major components in ECM. Collagen has been fabricated into microspheres due to its natural abundance within the animal body, and its biodegradability and biocompatibility (Yao et al., 2013).

Material:

- Isolated collagen pad from turkey
- 20 mM acetic acid
- 500 ml measuring cup
- Magnetic stirrer and bar
- Liquid nitrogen
- Polystyrene box
- Falcon tubes and stand
- 10 ml syringe with 6 mm needle
- Alpha 1-2 LD plus entry laboratory freeze dryer (Prat no. 101530)

Protocol:

- Added 45 ml 20 mM acetic acid to 450 mg of the collagen pad and stirred it on a magnetic stirrer for 24 h at 4 °C.
- Cryotechnique was used to prepare the spherical microcarriers. This was performed by adding 50 ml falcon tubes with 30 ml of liquid nitrogen in a polystyrene box, with liquid nitrogen around to keep the temperature down.
- Falcon tubes was refilled so it always was around 30 ml liquid nitrogen or never completely evaporate.
- The syringe was filled with dissolved collagen and droplets were poured into the liquid nitrogen in the falcon tubes one at a time to form beads.
- The tube was put on the bench to allow the nitrogen to completely evaporate.
- The collagen beads were then freeze dried for two days at -50 °C, before use.

Cross-linking and sterilizing of the collagen beads

Cross-linking of the collagen beads was used to stabilise the beads, as they dissolved in medium over a few days. Cross-linking reagents are molecules that consists of more than two reactive ends, that can chemically bind to particular functional groups on proteins or other molecules. Cross-linking have been used to increase the strength and stiffness of the material. Cross-linking can stabilise the protein-protein interaction on microcarriers, to establish surface immobilization (Bertolo et al., 2015). Riboflavin is a water-soluble B-vitamin, that has been used in cross-linking of eye and dental treatments. Riboflavin is an essential constituent in all living cells and non-cytotoxic (Seciu et al., 2016).

Material:

- Riboflavin powder
- UV radiator
- Tubes
- PBS
- Ethanol 70 % and 96 %
- Collagen beads

Protocol:

- Added 1 g riboflavin powder to 99 ml ethanol 70 % to get a 1 % mixture of riboflavin.
- 50 mg collagen beads were added to a glass beaker with 5 ml 1% riboflavin.
- Exposed the collagen beads to UV radiation at 2.94 mw/cm^2 for 5 min.
- The collagen beads were then washed four times with PBS and soaked in 96 % ethanol for 10 min, before washed four times with PBS again to get as much of the riboflavin and ethanol removed.
- 10 ml of PBS was added to each falcon tube and stored at 4 °C before further cell experiment was performed.

Selecting the most stable collagen beads

Before the spinner flask experiment with different beads, the homemade collagen beads were cross-linked with three different treatments to see which became most stable. The collagen beads were exposed for 5 min, 15 min and 30 min in a UV radiator to cross-link the beads. The protocol of cross-linking the beads were the same as described earlier.

Material:

- DMEM
- Cross-linked collagen beads with different UV-treatment
- Tubes
- Magnet stirrer
- Incubation cabinet at 37 °C

Protocol:

- The cross-linked collagen beads were placed in three tubes with a magnetic stirrer and 5 ml DMEM.
- Stored the beads with stirring at 100 RCF, in an incubation cabinet at 37 °C for 5 days.
- Looked at the beads every day to see if it would keep its form.

3.3.2. Characterisation of microcarriers

Picro sirius red staining has been used traditionally with polarised light to easily differentiate the collagen fibres from the background (Abcam, 2018). The sirius red have a sulphonic acid group that reacts with basic amino groups of hydroxylysine and lysine, and guanidine group of arginine (Bhutda et al., 2016). The method relies on molecule-binding parallel to cationic collagen fibres with the elongated, anionic structure in the dye (Wegner et al., 2017). It attracts

all types of collagen isoform, by being an anionic dye. This method was used to characterise the different microcarrier's size and shape. The collagen appears as pink to red fibres in light microscope (Bhutda et al., 2016).

Material:

- Soaked Cytodex 1 and 3
- ESM powder (100-250 µm)
- Cross-linked and not cross-linked collagen beads
- Phosphomolybdic acid, solution A
- Picro sirius red F3BA, solution B
- 0,1 N hydrochloric acid, solution C
- Distilled water
- Ethanol 70 %
- Glass microscope slides and coverslips
- Light microscope (Leica DMIL LED, type: 11090 137001)

Protocol:

- 50 µl of each bead and a few collagen beads were transferred to falcon tubes.
- Removed the supernatant.
- Added 100 µl of solution A and mixed.
- Washed the beads with distilled water.
- Added 100 µl of solution B and mixed.
- Incubated it for 1 h on the bench.
- Removed the supernatant.
- Added 100 µl of solution C and waited 2 min.
- Washed with ethanol 70 % and waited 2 min.
- Added 20 µl of the beads to microscope glass.
- Used the light microscope and Leica Application Suite (version 4) software to characterising the microcarriers.

3.4. Skeletal muscle cells grown in 3D systems

3.4.1. Spinner flasks

Spinner flasks have been used to provide larger surface area per unit volume medium on microcarriers, in comparison to cell culture flask (Verbruggen et al., 2018). The spinner flask experiment went on for 8 days and the samples were taken on day 1, 3, 6 and 8. The first day the stirring was off so the cells had time to attach to the beads. The collagen beads were added to a reduced cell suspension and incubated in 24 h at 37 °C for cell attachment before rotation, because the collagen beads were floating unlike the other microcarriers. On day 6 the medium was replaced to give the cells fresh nutrition and remove the toxins that the cells produce. New beads were also added on day 6 to give the cells more space to grow and to postpone the differentiation of the cells.

Material:

- Spinner flasks
- Magnet plate and glass mini bars
- Prepared microcarriers
    - Cytodex 1
    - Cytodex 3
    - ESM powder
    - Collagen beads
- PM 12 % FBS
- PM 2 % Ultroser/FBS
- Thermostatic cabinet
- Autoclaved 100 ml bottles with blue cap
- Isolated cells

Protocol for Cytodex 1, 3 and ESM:

- Added 100 ml PM, 500 mg of Cytodex 1 and 3, 50 mg of ESM and 1 mill cells to each autoclaved spinner flask with a glass stirring bar in it on day 0.
- Incubated the flasks with loose hook at 37 °C for 8 days.
- Waited 24 h to start the stirring at 100 rpm.
- Day 1, 3, 6 and 8: 5 ml of beads and medium from the edge of the bottom was transferred to a 15 ml falcon tube, before it was divided for further analysis.
    - 1.5 ml to lactate (supernatant)
    - 0.5 ml to glucose (supernatant)
    - 1 ml x2 to DNA (with beads)
    - 1 ml to protein (with beads)
    - 0.5 ml to hoechst (with beads)
- Day 6 the PM 12 % FBS was replaced with 100 ml PM 2 % ultroser/FBS.
- The same amount of beads from day 1 were added on day 6.
- Waited 24 h to start the stirring at 100 rpm.

Protocol for the collagen beads:

- Placed the beads with PM 12 % FBS into the spinner flask.
- Removed the medium leaving 10 ml, just to cover the beads.
- Incubated the flask with loose hook at 37 °C at 8 days.
- Waited 24 h to start the stirring at 100 rpm.
- Added 90 ml PM 12 % FBS on day 1.
- Day 1, 3, 6 and 8: 5 ml of beads and medium were taken out from the solution, and transferred to a 15 ml falcon tube, before it was divided for further analysis.
    - 1.5 ml to lactate (supernatant)
    - 0.5 ml to glucose (supernatant)
    - 1 ml x2 to DNA (mixed)
    - 1 ml to protein (mixed)
    - 0.5 ml to hoechst (mixed)
- Day 6 the PM 12 % FBS was replaced with 10 ml PM 2 % ultroser/FBS.

- The same amount of beads on day 1 were added on day 6.
- Waited 24 h to start the stirring at 100 rpm.
- Added 90 ml PM 2 % ultroser/FBS on day 7.

3.4.2. Benchtop bioreactor

Stirred tank bioreactor has been a commonly used tool to grow cells on microcarriers for efficiency of cost and cell culture resources. The usage of microcarriers for cell growth was to provide a larger surface area per medium volume compared to a cell culture flasks. In this experiment, Cytodex 1 was used as a matrix for the cell. Cytodex 1 is frequently used to culture stem cells in stirred bioreactors (Verbruggen et al., 2018). The experiment went over 8 days and the samples were taken on day 0, 1, 3, 6, 7 and 8. Day 6, the beads that got stuck to the walls were taken out with a cell scrape, and new beads og medium were added to give the cells more space to proliferate.

Material:

- Benchtop bioreactor
- PM 12 % FBS
- PM 2 % Ultroser/FBS
- Soaked and autoclaved Cytodex 1
- Isolated cells
- Sample syringe
- Tubes

Protocol:

- Prepared all the bioreactor components.
- Autoclaved the bioreactor capsule.
- Added 400 ml of PM 12 % FBS to the sterile capsule in a fume hood.
- Mixed the beads and medium before adding the beads in the middle of the container.
- Added 13 mill cells to the middle and pipette the rest of the medium to get 600 ml in total.
- Added all tubes with gases and solution to the benchtop bioreactor and turn on setpoint based on an optimal environment for the cells:

Parameter	**Setpoint**	**Mode**	**Units**
pH	7.80	On	pH
Dissolved Oxygen	35.0	On	%
Agitation	45.0	On	RPM
Temperature	37.0	On	°C

- The gas flow that were used to stabilised the setpoints shown in the table under:

Air	%
CO2	%
Gas Flow	SLPM
N2	%
O2	%
Base	mL/m

- The parameters were stabilizing for one hour before the first sampling was taken.
- Day 0, 1, 3, 6, 7 and 8: 7.5 ml of the solution in the bioreactor was taken out with a sterile sample syringe and transferred to a falcon tube.
- Waited till the beads felled down and divided the samples:
    - 1.5 ml to lactate (supernatant)
    - 1.5 ml to ammonia (supernatant)
    - 0.5 ml to glucose (supernatant)
    - 0.5 ml to L-glutamine (supernatant)
    - 1 ml x2 to DNA (mixed)
    - 1 ml to protein (mixed)
    - 0.5 ml to hoechst (mixed)
- On day 6 the bioreactor was paused and placed in a fume hood to change the medium and add more beads.
    - The beads that were stuck to the walls were removed with a cell scrape
    - The medium was removed and replaced with 600 ml of PM 2 % Ultroser/FBS
    - 3 g new beads were added in the middle of the capsule
    - Started the bioreactor again and it stabilised itself with the same setpoint as before after a few hours

3.4.3. Analysis of spinner flask and benchtop bioreactor

Qubit 1X dsDNA (High-Sensitivity/Broad Range) assay

The Qubit 1X dsDNA assay kit was used to measure total amount of DNA concentration in the spinner flasks with high-sensitivity (HS) and with BR in the benchtop bioreactor using the Qubit 3.0 fluorometer. This method was designed to be selective for double-stranded DNA (dsDNA) over RNA and to be accurate for sample concentrators from 10 pg/µl to 100 ng/µl. Common contamination are well tolerated in the assay, such as free nucleotides, salts, solvents, detergents or protein (Invitrogen™, 2017).

Material:

- PSB
- RLT
- HS buffer
- Qubit™ assay tubes
- Samples
- Qubit 3.0 fluorometer

Protocol:

- Washed the samples twice with PBS, vortexed and centrifuged the samples in between. The samples with collagen beads were just turned a few times for mixing.
- Added 350 ml RLT and mixed.
- Froze the sample at -80 °C.
- Thawed the frozen samples on the bench.
- The sample were mixed for 10-15 s.
- Incubated for 15 min at 50 °C.
- Centrifuged the samples for 1 min at 13 000 RCF.
- Added 180 µl of HS buffer to the fluorometer tubes for DNA reading + 20 µl supernatant from the samples.
- Mixed all the samples for 10 s.
- Used the Qubit 3.0 Fluorometer (HS) to quantify DNA in the samples.

Protein, glucose and lactate measurements

The measurements for protein, glucose and lactate was gone exactly like as in 2D systems.

Hoechst staining

Protocol:

- One droplets of NucBlue™ were added to the 500 µl of sample in an eppendorf tube.
- The sample was placed on a rocker board for 30-40 min.
- Pictures were taken with a fluorescence microscope and analysed using Zeiss Zen software and ImageJ.

Ammonia and L-glutamine assay

The Megazynes L-glutamine/ammonia (rapid) assay was used for the simultaneous determination of L-glutamine and ammonia ions in cell culture media. Megazyme™ has developed a kit for measuring L-glutamine and ammonia with recombinant enzyme, that are rapid and has a simple format (Megazyme, 2018). The principle is that the number of $NADP^+$ formed by the combined action of glutaminase (GLT) and glutamate hydrogenase (GIDH) is balanced with the amount of glutamine and ammonia in the sample volume (Nzytech™, 2014). Measuring the NADPH consumption by decreasing the absorbance at 340 nm (Megazyme, 2018). The results were calculated before presented in figure 33 with the formula under:

$$\Delta A_{ammonia} = (A_1 - A_2)_{ammonia\ sample} - (A_1 - A_2)_{ammonia\ blank}$$

$$\Delta A_{(L\text{-}glutamine\ +\ ammonia)} = (A_1 - A_2)_{L\text{-}glutamine\ sample} - (A_1 - A_2)_{L\text{-}glutamine\ blank}$$

$$\Delta A_{L\text{-}glutamine} = \Delta A_{(L\text{-}glutamine\ +\ ammonia)} - \Delta A_{ammonia}$$

Material:

- Solution 1: Buffer (11 ml, pH 4.9) plus sodium azide (0.02 % w/v) as a preservative
- Solution 2: Buffer (25.5 ml, pH 8.0) plus sodium azide (0.02 % w/v) as a preservative
- Solution 3: NADPH, lyophilised powder
- Suspension 4: Glutaminase suspension (1.1 ml)
- Suspension 5: Glutamate dehydrogenase (2.2 ml)
- Solution 6: Ammonia standard solution (5 mL, 0.04 mg/ml) in 0.02 % (w/v) sodium azide
- Solution 7: L-glutamine control powder (0.30 g in 1 l distilled water)
- Sample solutions
- 96 well plate
- Microplate reader at 340 mm
- Distilled water

Protocol for Ammonia:

- Kept the blank sample empty from the beginning.
- Added 10 µl sample solution and solution 6 (standard) to the 96 well plate.
- Mixed and incubated the solutions for 5 min at room temperature.
- Added to the wells:

	Blank sample (µl)	Sample solution and standard (µl)
Distilled water	182	172
Solution 2	30	30
Solution 3	20	20

- Mixed all the wells and reed the absorbance of solutions (A_1) after approximately 4 min at OD 340 mm in a plate reader.
- Then started the reaction by adding 2 µl suspension 5 (GIDH) to each well.
- Mixed and reed the absorbance of solution (A_2) at the end of the reaction (approximately 5 min).
- Reed the absorbance a few more times with 1 min interval, till the reaction stopped.

Protocol for L-glutamine:

- Added 20 µl solution 1 and 2 µl suspension 4 to the blank sample.
- Added 10 µl sample solutions and solution 6 (standard) to the 96 well plate with:
    - 20 µl solution 1
    - 2 µl suspension 4
- Mixed and incubated the solutions for 5 min at room temperature.

- Added to the wells:

	Blank sample (µl)	Sample solution and standard (µl)
Distilled water	160	150
Solution 2	30	30
Solution 3	20	20

- Mixed all the wells and reed the absorbance of solutions (A_1) after approximately 4 min at OD 340 mm in a microplate reader.
- Then started the reaction by adding 2 µl suspension 5 (GIDH) to each well.
- Mixed and reed the absorbance of solution (A_2) at the end of the reaction (approx. 5 min.)
- Reed the absorbance a few more times with 1 min interval, till the reaction stopped.

4. Results

4.1. Growth of bovine skeletal muscle cells in 2D systems

4.1.1. Cell proliferation and cell number

Bovine skeletal muscle cells were cultivated in 6 wells plates. Cell proliferation was characterised using light microscopy and the cell number using fluorescence microscope during a time-course of 8 days. The light microscopy was used to monitor cell proliferation and differentiation, and to examine cell morphology over the time-course. On day 1, the cells were evenly distributed and after five days they started to fuse and had developed myotubes (figure 9, arrowhead on day 5). Although no differentiation medium (with lower serum volume and insulin) was added, the cells still performed spontaneously differentiation on day 8 (figure 9, arrowhead on day 8).

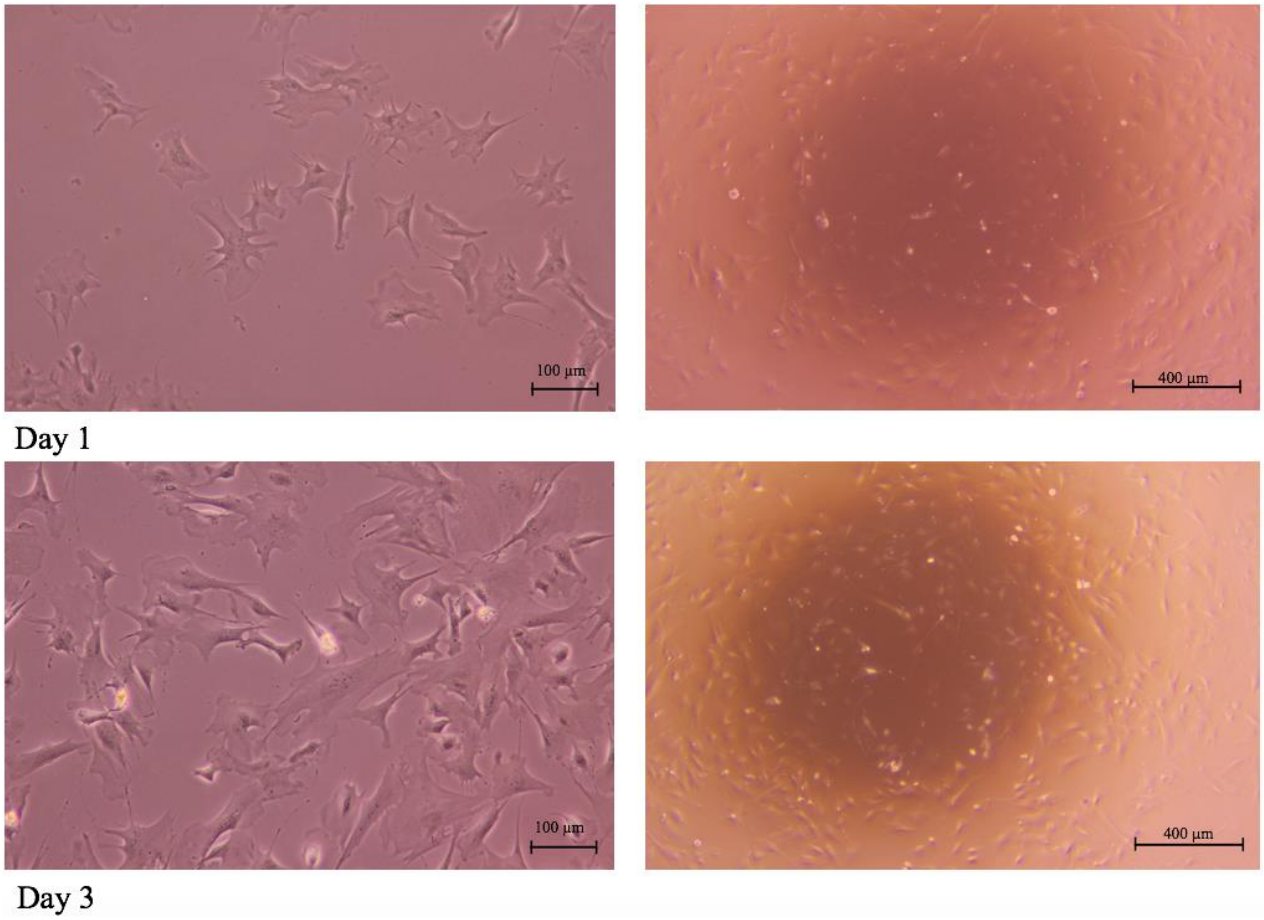

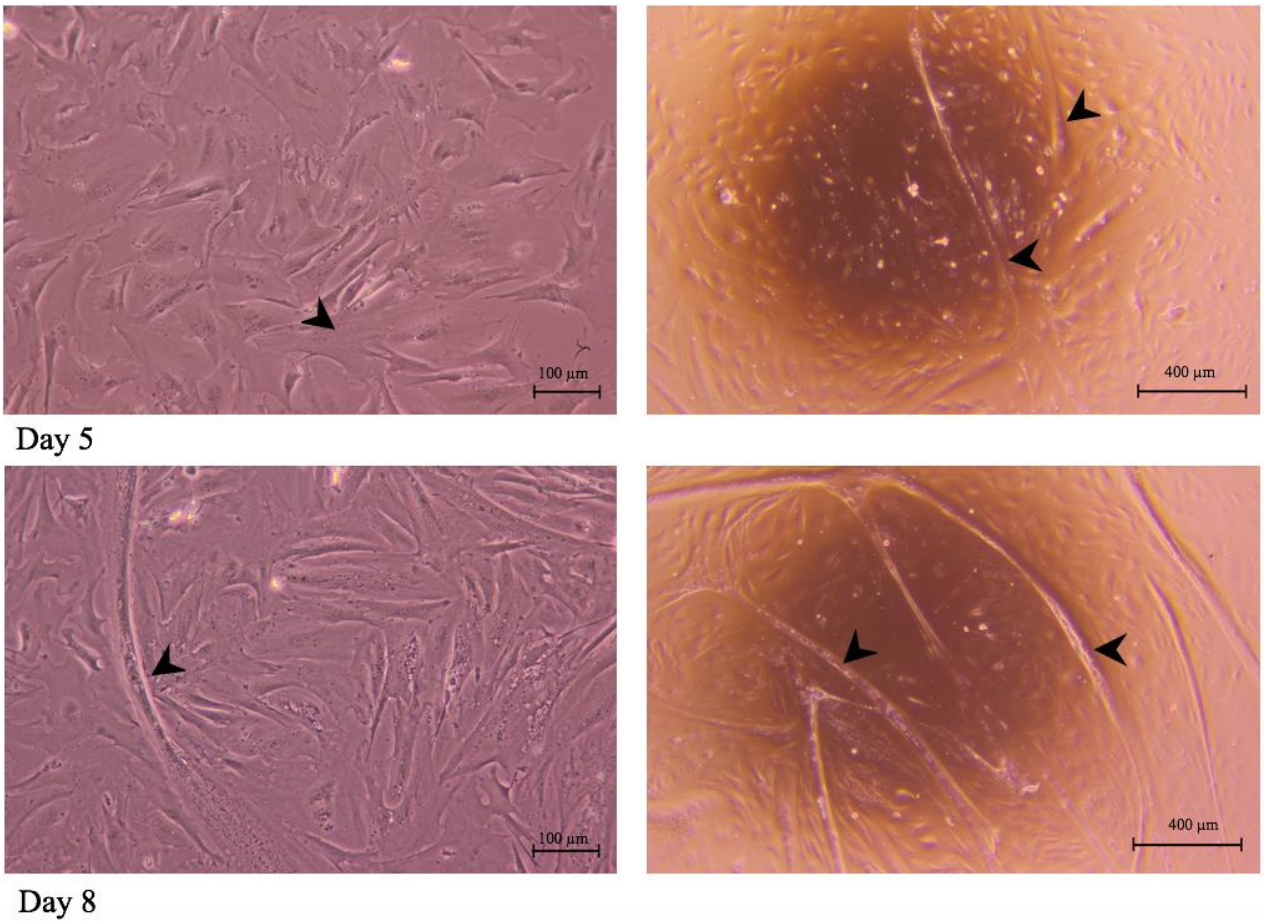

Figure 9: Proliferation and differentiation of skeletal muscle cells in 2D systems. *The muscle cells proliferated and differentiated in 2D systems over a time-course of 8 days. Arrowhead on day 5 points to the cells merging together, and on day 8 to spontaneously differentiation of the cells. The images selected were representative of a group of images from 3 independent experiments. Pictures were taken using light microscope with a 4x (left) and 10x (right) magnification.*

Hoechst staining of the muscle cells nuclei were used to analyse the cell proliferation, differentiation and cell number. In figure 10 the cells on day 1 were evenly divided and proliferated every day till day 8. After 8 days, the cell density was high compared to day 1. The stained cell nuclei that were closely aligned, showed spontaneous differentiation of the cells.

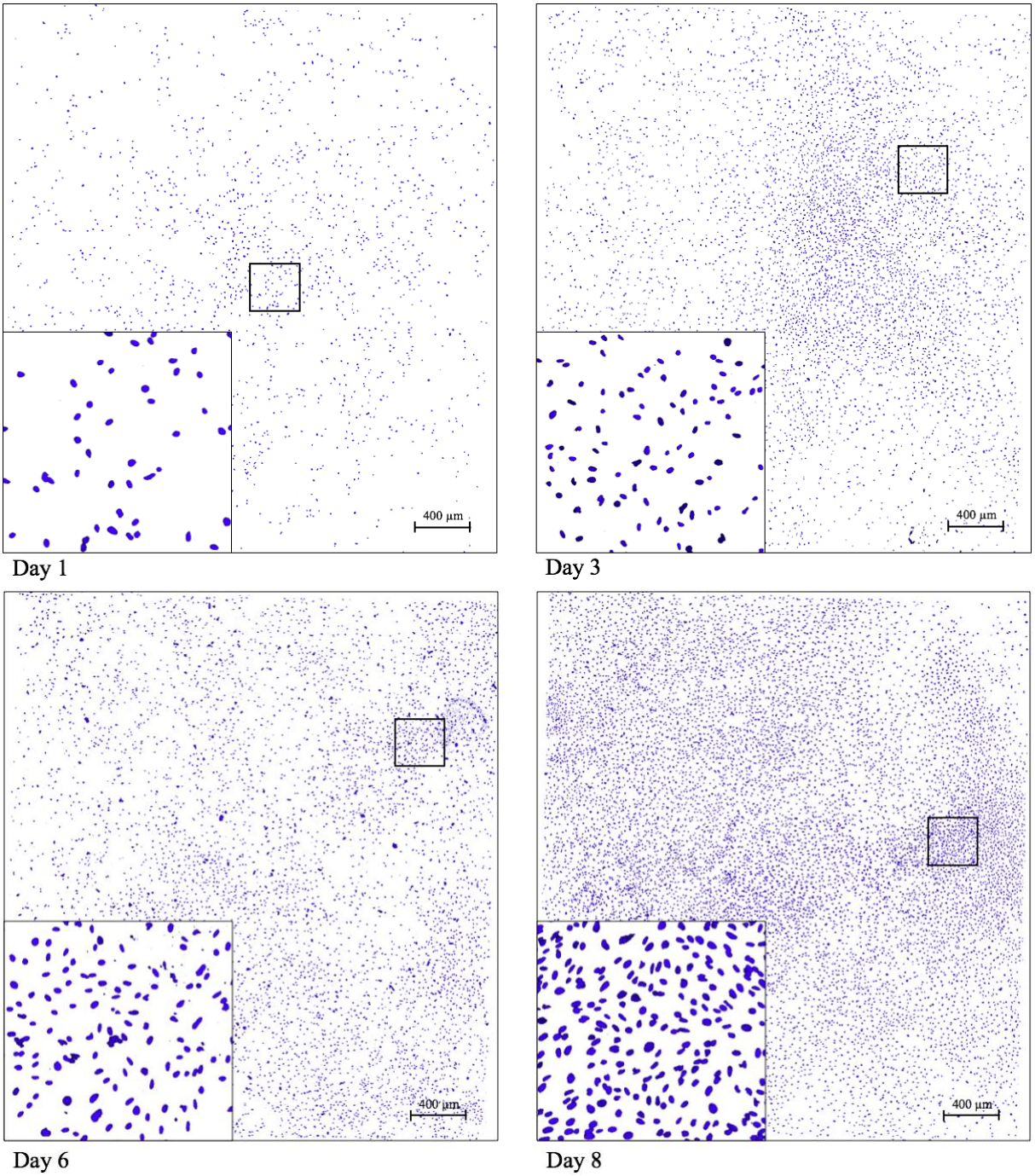

Figure 10: Hoechst stained skeletal muscle cell nuclei in 2D systems. *The muscle cells proliferated and differentiated in 2D systems over a time-course of 8 days. A total of 24 images were assembled using fluorescence microscope with a 5x magnification and Zeiss Zen software. The most representative images were presented from multiple images of 3 independent experiments. The image background was edited using Thresholds colour in ImageJ.*

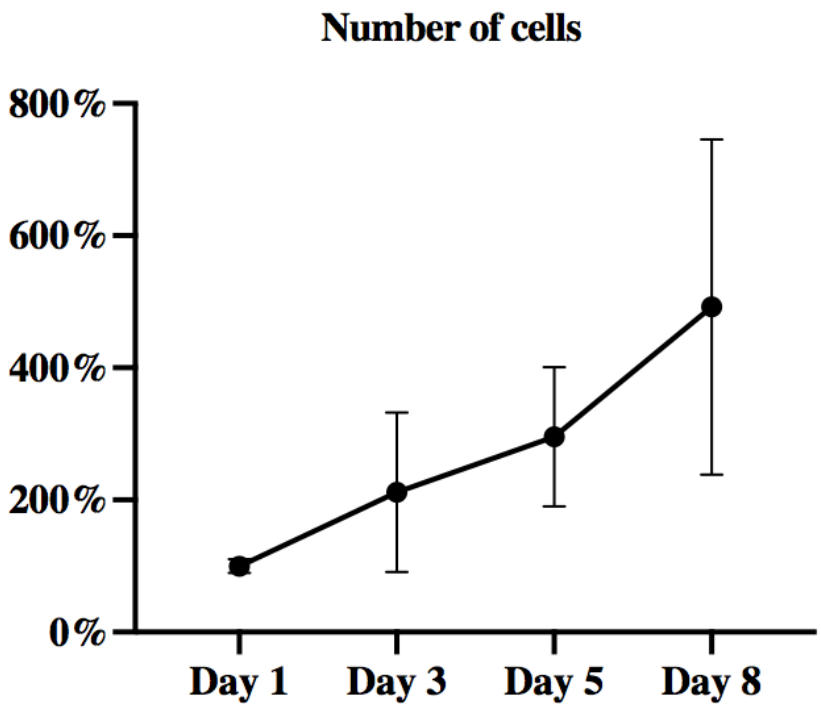

Figure 11: Number of cells in 2D systems. *The number of muscle cells proliferated and differentiated in 2D systems over a time-course of 8 days, were quantified using images as presented in figure 10 and the semi-automatic counting system in ImageJ. The data was assembled from 3-5 images of two independent experiments, and normalised to day 1 in percent.*

The muscle cells in 2D systems showed an increase in number of cells from day 1 to 8 (figure 11). The standard deviation on day 8 was large and therefore it was an uncertainty in the cell number this day. Using t-test between each measurement it was only day 1 and day 8 that gave a statistical significant with a significant level of 0.05 (appendix 2).

4.1.2. Biochemial measurements in 2D systems

DNA concentration

The DNA concentration results was analysed using the Qubit™ dsDNA (BR) assay kit with a Qubit 3.0 fluorometer and converted to percent to see how much the concentration changed over a period of 8 days. The samples used to measure DNA concentration was frozen before use.

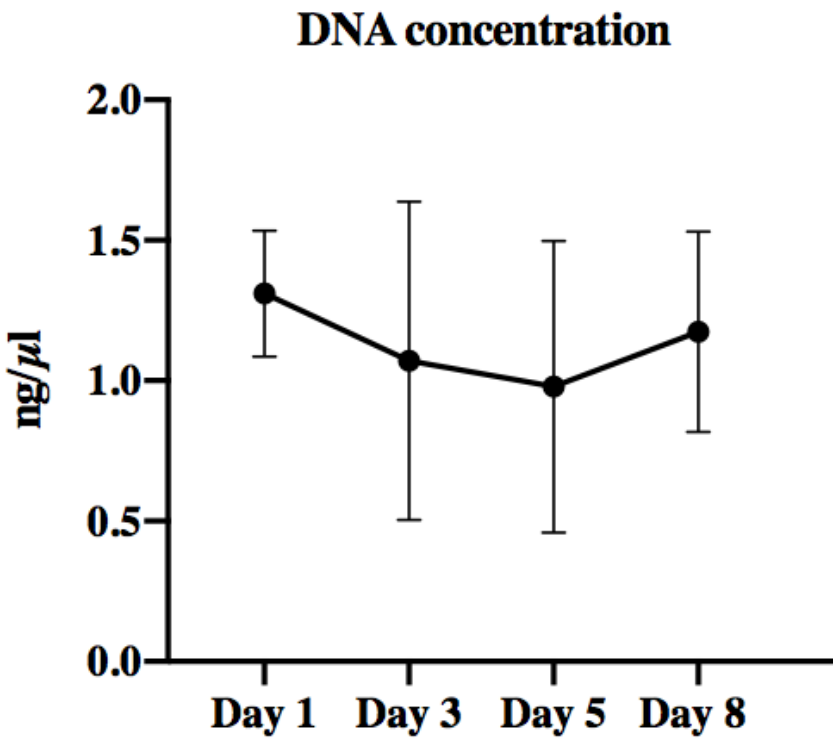

Figure 12: Total DNA concentration (ng/µl) of muscle cells in 2D systems. *The concentration was measured with frozen samples taken over a time-course of 8 days. Qubit™ dsDNA assay kit with a Qubit 3.0 fluorometer (broad range) was used to collect the results. The results from the graph above were assembled from two replications of two independent experiments.*

The total DNA concentration of muscle cells in 2D systems are shown in the graph above (figure 12). The DNA concentration was first decreasing and then rising after day 5. There was a large scatter in the results over the time-period, shown in the large standard deviations. No statistical significance was found between the different days (appendix 2).

Protein production

The total protein concentration was measured using Bio-Rad DC™ protein assay kit I with frozen samples in a microplate reader. The total protein concentration was calculated relative to a standard line.

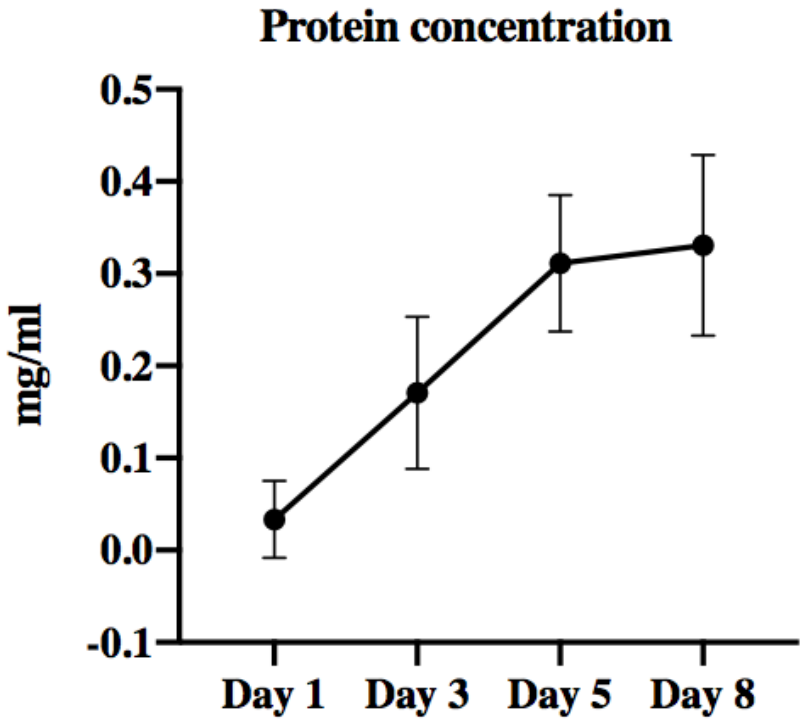

Figure 13: Total protein concentration (mg/ml) of muscle cells in 2D systems*. The concentration was measured with frozen samples taken over a time-course of 8 days. Bio-Rad DC™ protein assay kit I was used to measure the protein concentration. The graph shows the average from three replications of three independent experiments.*

The total protein concentration was increasing from day 1 to day 8 (figure 13). There was a statistical significance between all the days except from between day 5 and 8 with a significant level of 0.05 (appendix 2).

Glucose consumption and lactate level

The total glucose level was measured using glucose assay kit (Colorimetric) and a microplate reader with frozen samples over a time-course of 8 days. The results of the total lactate levels were given straight from the reflectometer (RQflex plus10) with lactate strips, while total glucose levels were calculated relative to a standard line.

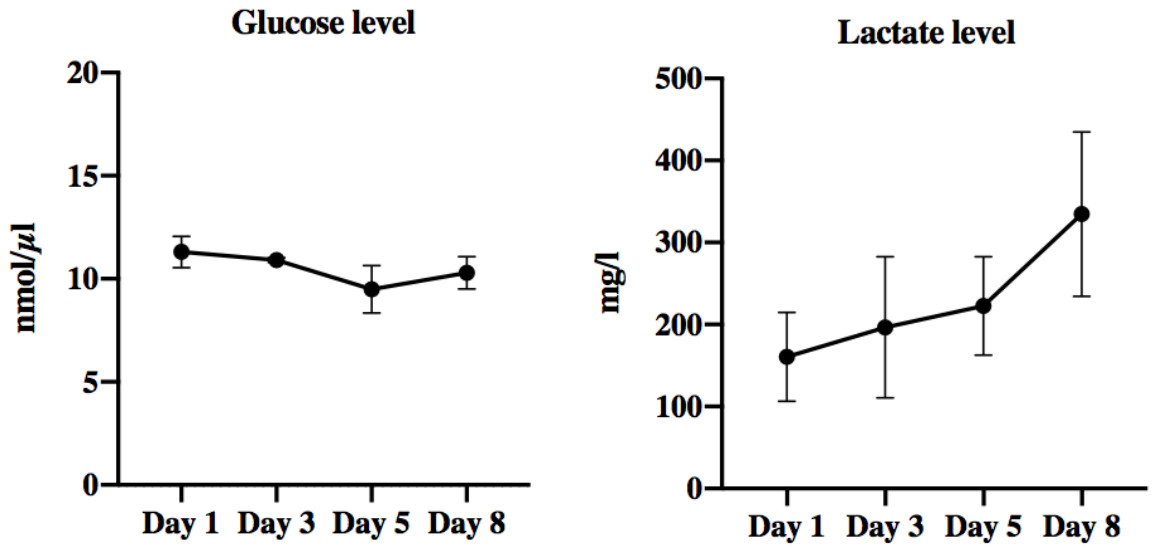

Figure 14: The total glucose (nmol/µl) and lactate (mg/l) level in medium with muscle cells in 2D systems*. Both the glucose and lactate level were measured with frozen samples taken over a time-course of 8 days. Total glucose levels were obtained with glucose assay kit, and the total lactate levels were measured with reflectometer (RQflex plus 10). The results from both graphs were calculated from one replication of three independent experiments.*

The glucose level in the left graph remained stable throughout the period, with just a small decrease on day 5. The total lactate level was increasing in all the experiments (figure 14). However, neither in the glucose or lactate results a statistical significance was found between any days (appendix 2). The graph to the right in figure 14 showed that the cells were producing lactate, indicating proliferation of the cells.

4.2. Up-scaling from 2D systems to spinner flasks with 3D microcarriers in cell culture

4.2.1. Characterisation of microcarriers

The microcarriers (Cytodex 1, Cytodex 3, ESM and collagen beads) were characterised with picro sirius red staining and light microscopy to evaluate the morphology. The average size of the beads was calculated on the diameter of Cytodex 1 and 3, while ESM and collagen beads were measured by the longest navigable straight-line on the beads (figure 15).

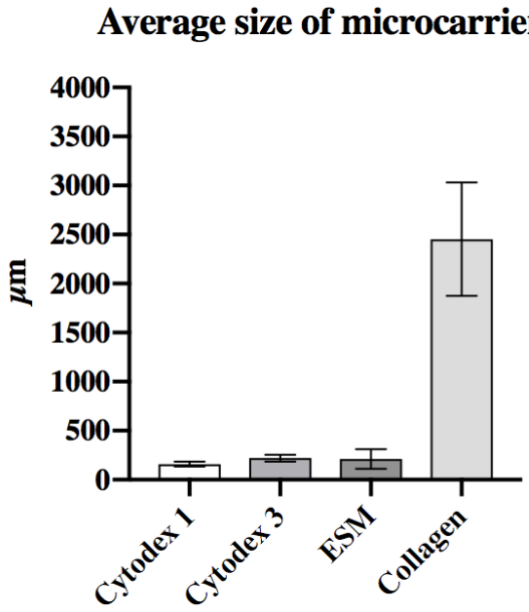

Figure 15: Average size (µm) of the microcarriers. *Diameter of Cytodex 1 and 3 were measured, while ESM and collagen beads were measured at the longest ends of the beads.*

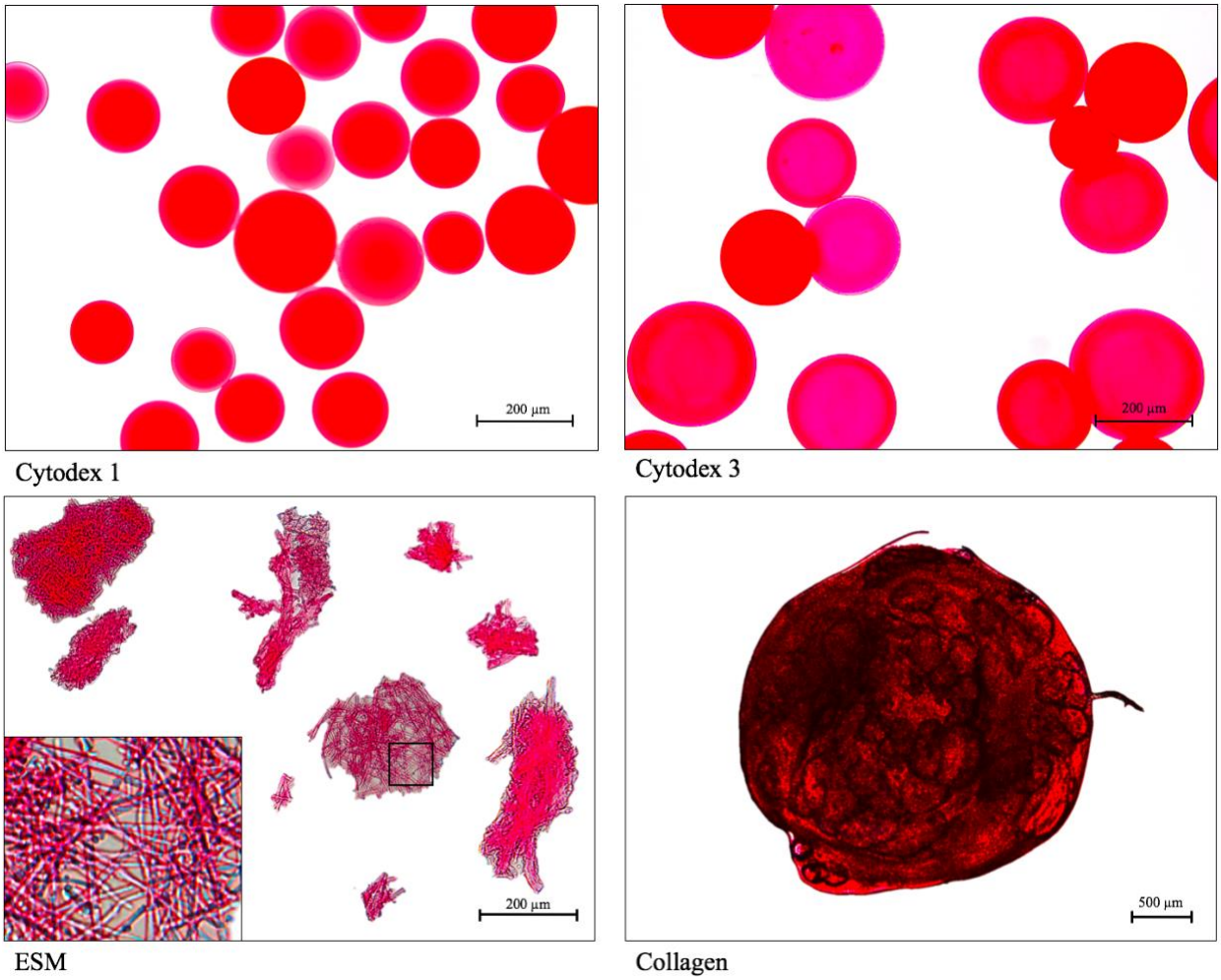

Figure 16: Characterisation of the different microcarriers*. Cytodex 1, Cytodex 3, ESM powder and collagen beads stained with picocuries red. The backgrounds were edited white with thresholder in ImageJ, and the image with ESM was assembled from several images.*

The commercial microcarriers, Cytodex 1 and 3, had a circular shape and smooth surface, while the ESM and collagen beads had a more uneven surface (figure 16). There were different variations in size within the beads and between the different microcarriers (figure 15). The collagen and ESM beads had a large variation in size and shape. The ESM powder had a shape of collagen fibres crossing. The collagen beads had a larger surface with several small holes, like a sponge (figure 17). Statistical significance was calculated between the different beads with a significance level of 0.05, and only the collagen beads were statistical significance from all the other microcarriers.

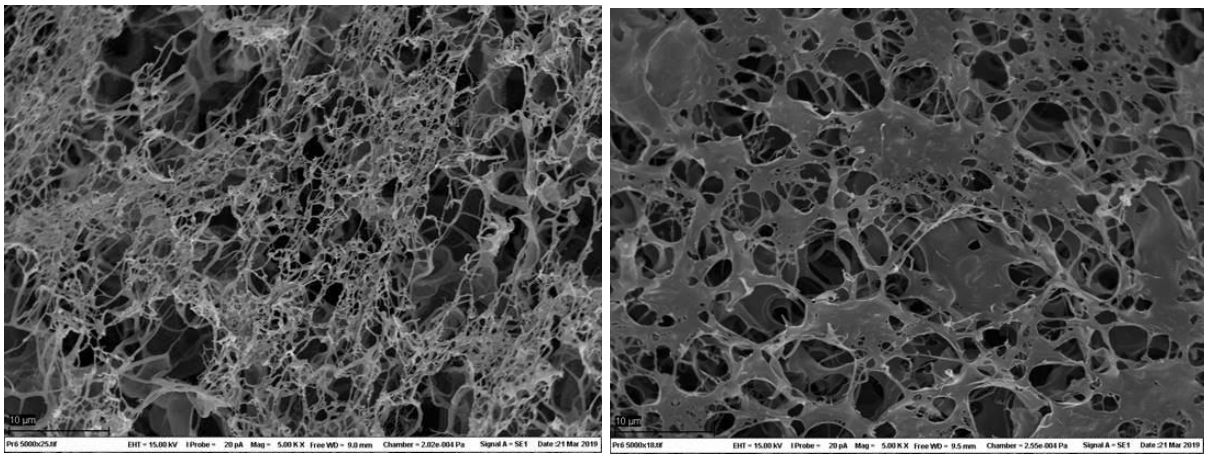

Figure 17: SEM images of the collagen beads surface *(Images by Vibeke Høst, Nofima).*

4.2.2. Proliferation and number of muscle cells on miccrocarriers in spinner flasks

The muscle cells nuclei were stained with hoechst and characterised with a fluorescence microscope and Zeiss Zen software to observe the proliferation of the cells on the microcarriers in spinner flasks. Nuclei staining with hoechst (blue) was performed on the cells, but unspecific staining was also observed on the microcarriers. After day 6 the medium was changed and new microcarriers were added to the all the spinner flasks to prevent cell aggregation and give them more surface to proliferate on. Every sampling day (day 1, 3, 6 and 8) an average of six images were taken to characterise viable cells on the microcarriers, and the most representative images were presented under from two independent experiments.

Cytodex 1

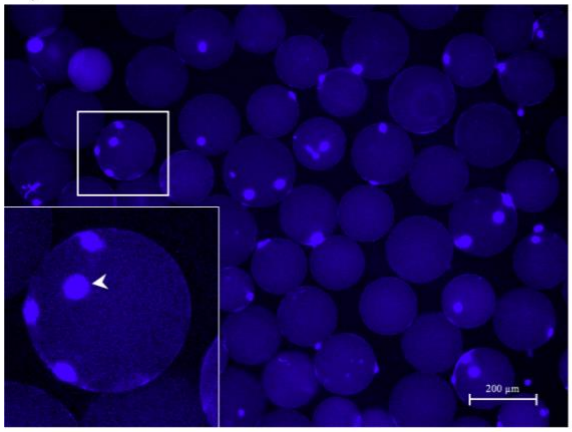

Day 1

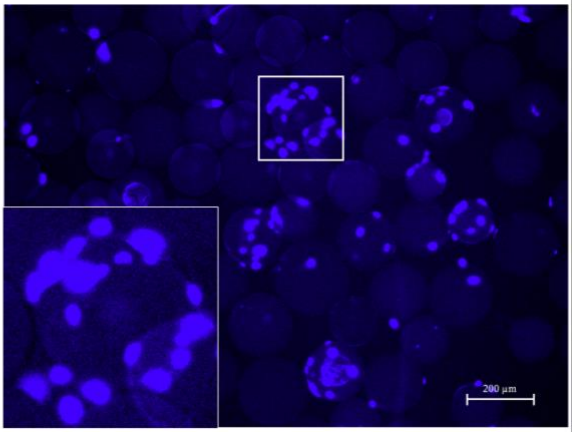

Day 3

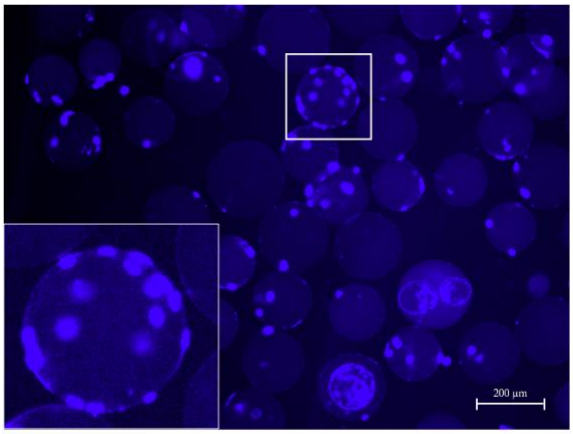

Day 6

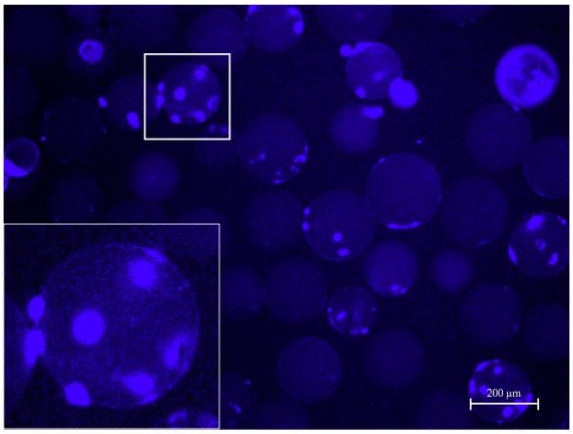

Day 8

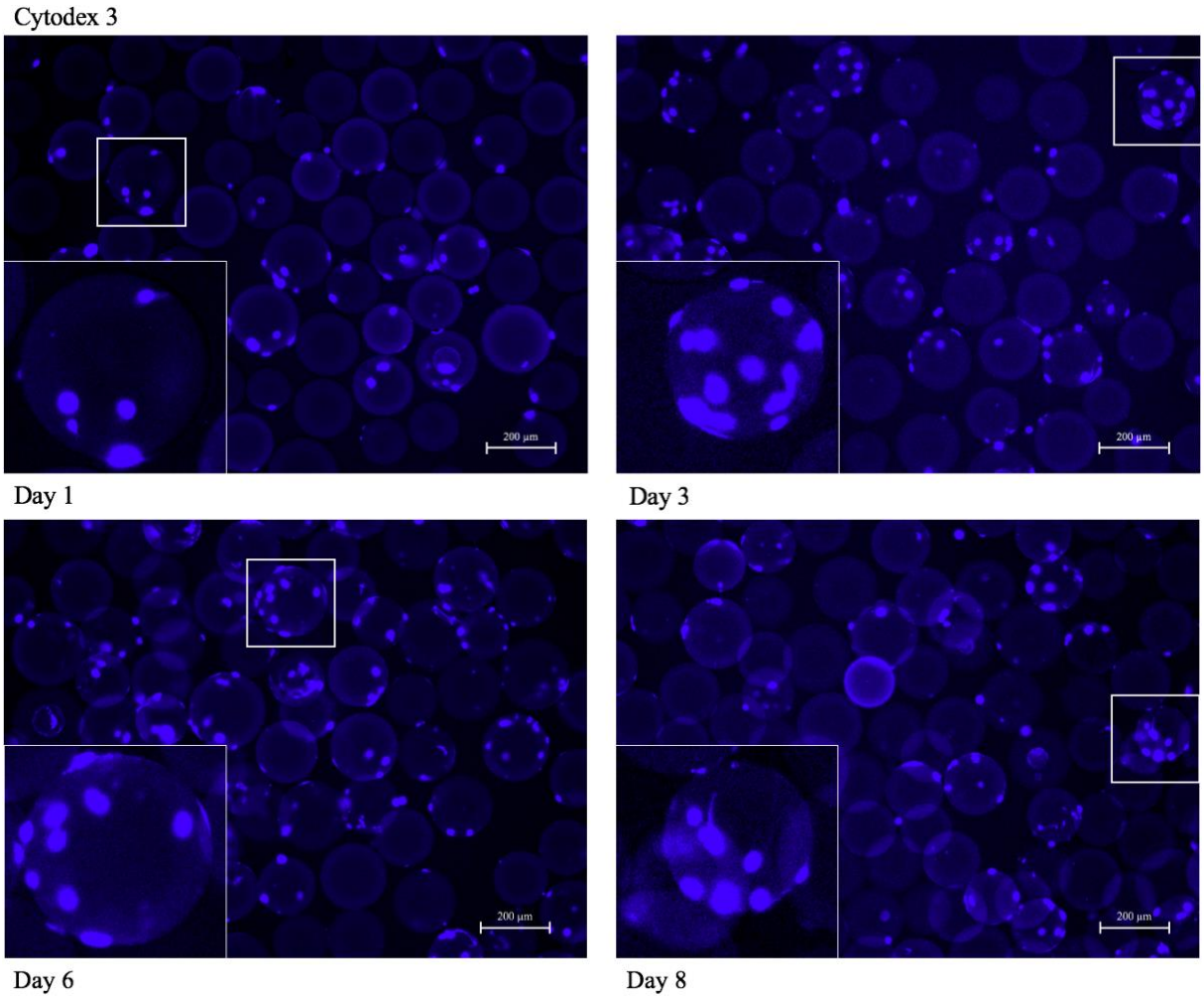

Figure 18: Hoechst stained muscle cell nuclei on Cytodex 1 and 3 in spinner flask. *Proliferation of muscle cells on Cytodex 1 and 3 in spinner flasks over a time-course of 8 days. The medium was changed and new microcarriers were added after day 6. The representative images were selected from a group of images from two independent experiments. Images were taken using the Zeiss Zen software and fluorescence microscope with 5x magnification.*

Figure 18 showed muscle cells attachment and proliferation on both Cytodex 1 and 3. Both images (day 8) clearly outline the number of empty beads added after day 6 (figure 18).

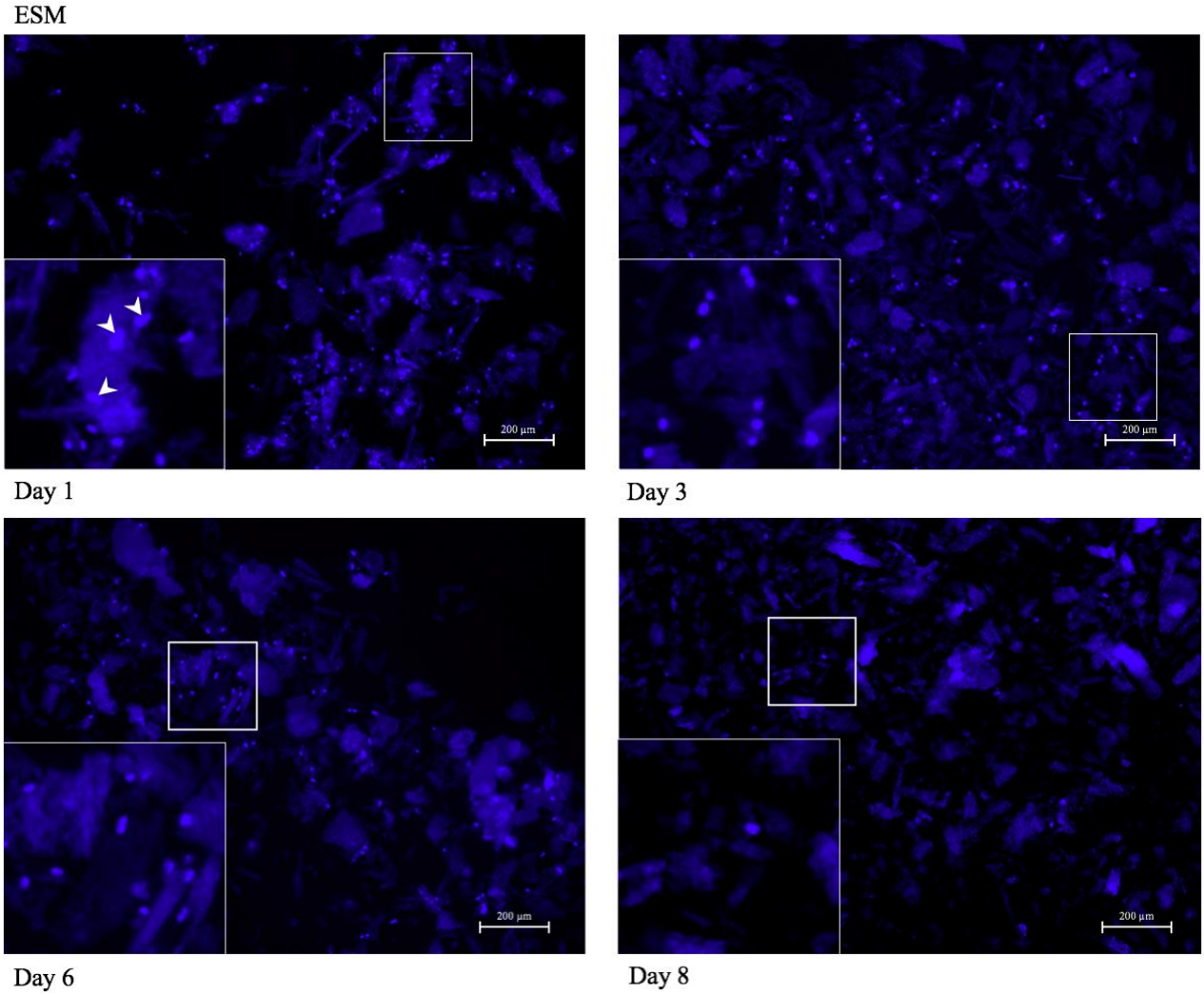

Figure 19: Hoechst stained muscle cell nuclei on eggshell membrane (ESM) in spinner flask. *Muscle cells on ESM powder in spinner flask over a time-course of 8 days. The white arrowhead points at stained muscle cell nuclei on the ESM. The medium was changed and new microcarriers were added after day 6. The representative images were selected from a group of images from 2 independent experiments. Images were taken using the Zeiss Zen software and fluorescence microscope with 5x magnification.*

Up to day 6, the muscle cells were attached to the ESM powder. However, after the new powder was added the cell number dropped considerably (figure 19). The muscle cells were decreasing every sampling day.

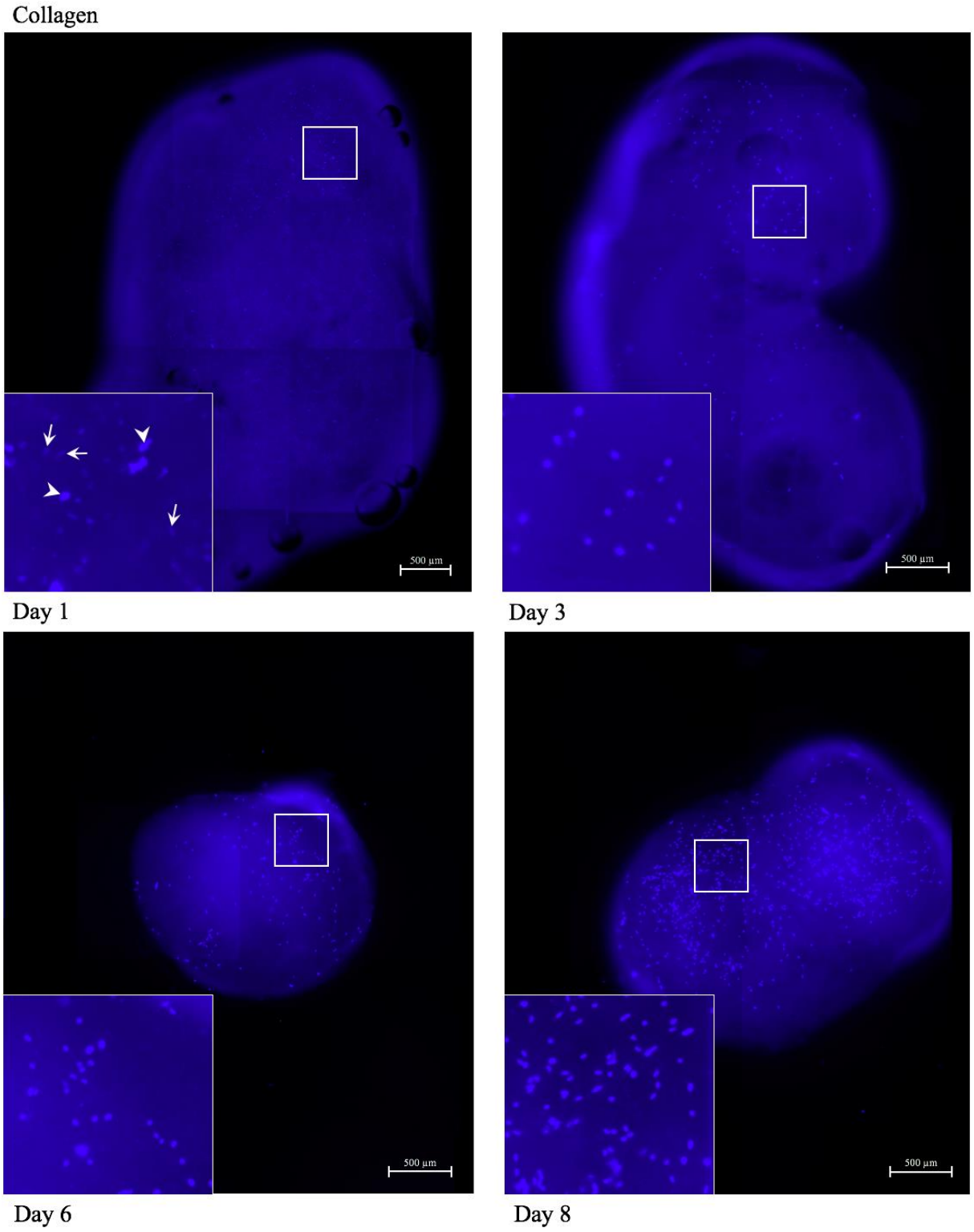

Figure 20: Hoechst stained muscle cell nuclei on collagen beads in spinner flask. *Proliferation of muscle cells on collagen beads in spinner flasks over a time-course of 8 days. The white arrowheads points at stained muscle cells nuclei and the white arrows points to unknown background noise. The medium was changed and new microcarriers were added after day 6. A total of 24 images were assembled using Zeiss Zen software and fluorescence microscope with a 5x magnification. The representative images were selected from a group of images from two independent experiments.*

The muscle cells were attaching to the collagen beads and proliferated over a period of 8 days. After the new beads were added some of the spheres had still a large number of muscle cells attached. The collagen beads had unknown background dots that only were shown on day 1 (figure 20, arrows), which was not cells according to images from electron microscope taken by Senior Engineer Vibeke Høst at Nofima AS in Ås (figure 17).

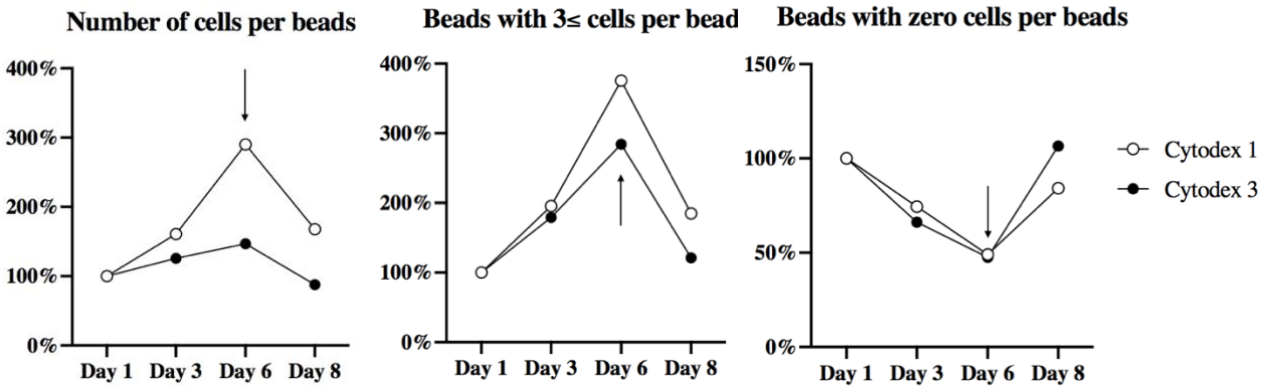

Figure 21: Number of cells, beads with 3≤ cells and empty beads in spinner flasks. *The amounts were compared to the total number of beads over a time-course of 8 days. The results were collected from one replicate of one images, with a total of 24 images assembled using Zeiss Zen software and fluorescence microscope with a 5x magnification, of two independent experiment every sampling day, taken with fluorescence microscope, using ImageJ. The black arrow indicates when the medium was changed and new beads were added, after day 6. The numbers were converted to percent and normalised to day 1.*

Number of muscle cell, cells with 3≤ cells and beads with zero cells were counted from one image (24 images merge together) taken by fluorescence microscope on every sampling day, and compared to the total amount of beads (figure 21). This was done to get a better picture of how the cells interacted with the beads over time and to get a clearer result on whether the cells proliferated or died. The number of beads with 3≤ cells attached were increasing till day 6, and after the new beads were added the cell number and number of beads with more cells dropped. Cytodex 1 got a higher increase in cell number than Cytodex 3. The number of empty beads were decreasing till day 6 and then increased till day 8, as a reaction of the new batch of beads that were added after day 6. The amount of empty beads were very similar for both Cytodex 1 and 3.

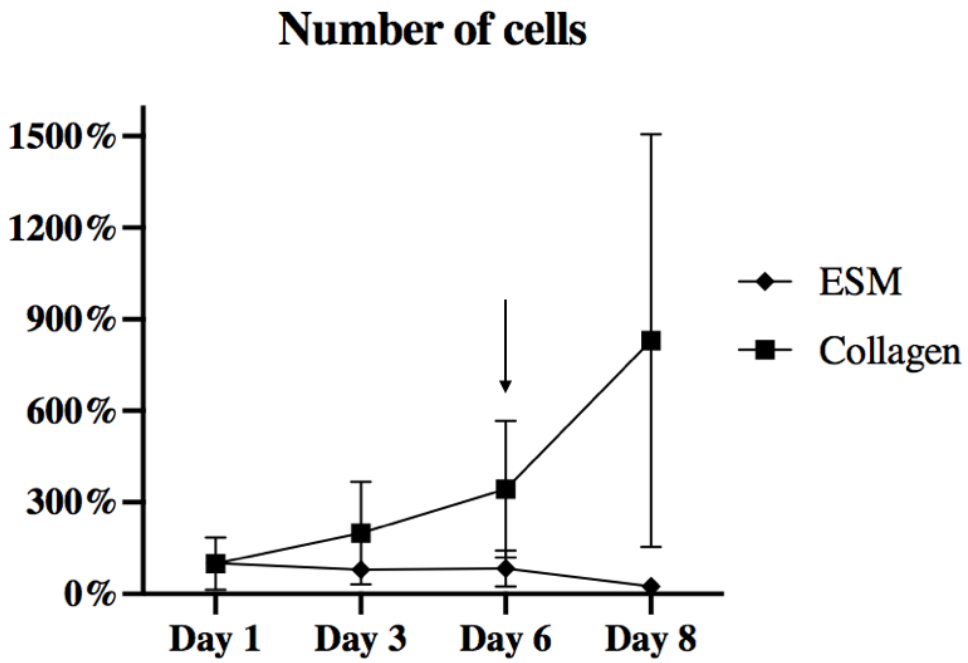

Figure 22: Number of cells on ESM and collagen beads in spinner flaks. *Cell numbers were counted in ImageJ with images from 2-6 replicates of two independent experiments. The black arrow indicates when the medium was changed and new microcarriers were added, after day 6. The number of cells were calculated to percent and normalised to day 1.*

The muscle cells on ESM were decreasing, while on the collagen beads the muscle cells increased a lot from day 1 (figure 22). Figure 22 showed a large standard deviation on day 8 on the collagen beads. With a safety factor of 95 %, the number of cells on ESM had a statistical significance between day 1 and 8. The number of cells on collagen had also a statistical significance between day 1 and 8 with a significant level of 0.05 (appendix 2).

4.2.3. Biochemical measurments in spinner flaks

DNA concentration

The total DNA concentration were measured by using Qubit™ 1X dsDNA (HS) assay kit with the Qubit 3.0 fluorometer. The result begins on day 3 because the concentration was too low to read on day 1, as well as the DNA concentrations of ESM and collagen beads.

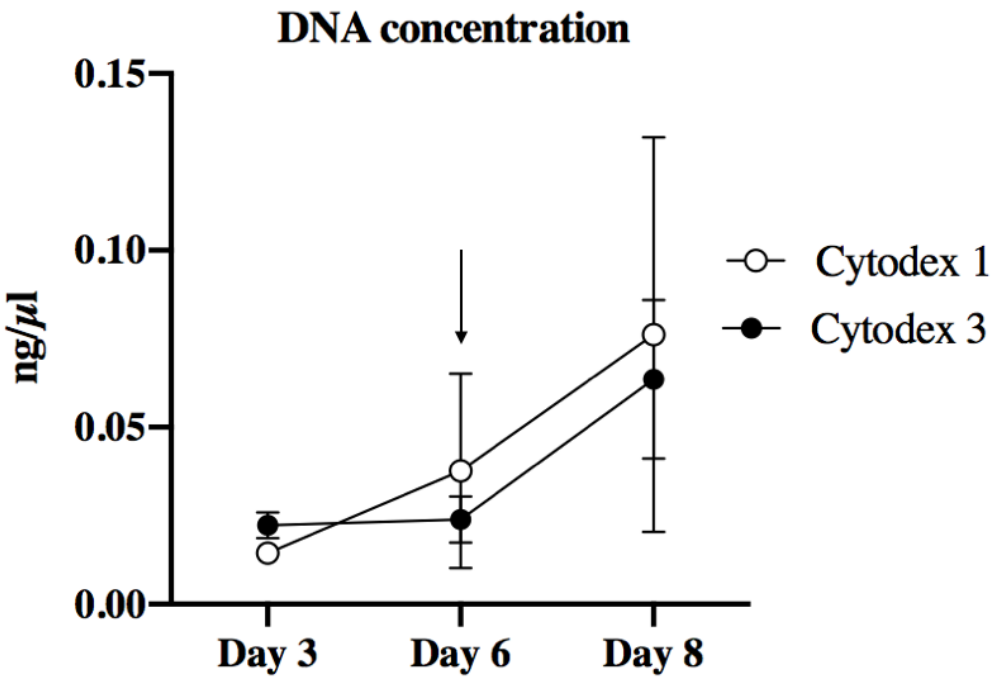

Figure 23: The total DNA concentration (ng/µl) of muscle cells grown on Cytodex 1 and 3 in spinner flasks. *The concentrations were analysed using Qubit™ 1X dsDNA (HS) assaykKit with frozen samples from two replications of two independent spinner flask experiments over a time-course of 8 days. The black arrow indicates when the medium was changed and new beads were added after day 6.*

The DNA concentrations in figure 23 increased from day 3 to day 8 in both Cytodex 1 and 3. Cytodex 1 were shown to be increasing more than Cytodex 3, but the concentration on Cytodex 1 have large standard deviation on day 6 and 8.

Protein production

The total concentration was measured using Bio-Rad DC™ protein assay kit I with a microplate reader to evaluate the protein amount from the muscle cells, attached on the microcarriers in the spinner flasks over a period of 8 days. The total protein concentration was calculated relative to a standard line.

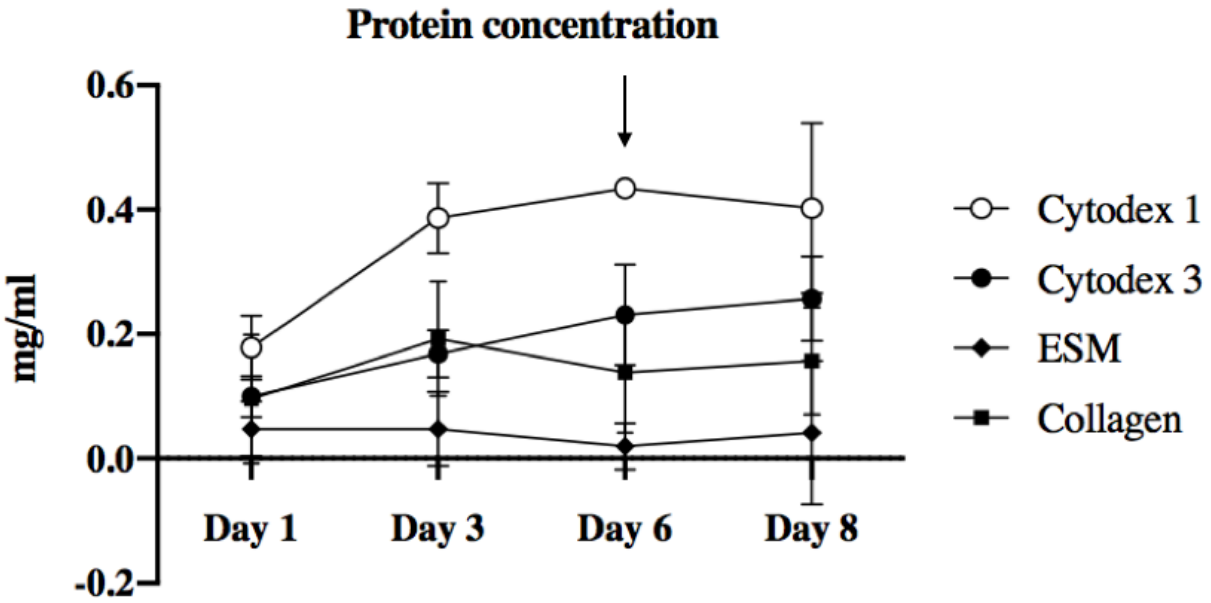

Figure 24: The total protein concentration (mg/ml) of muscle cells on different microcarrier in spinner flaskss. *Cytodex 1, Cytodex 3, eggshell membrane (ESM) powder and homemade collagen beads were measured using Bio-Rad DC™ protein assay kit I with frozen samples from two replications of two independent spinner flask experiments over a time-course of 8 days. The black arrow indicates when the medium was changed and new beads were added after day 6.*

The total protein concentration of muscle cells on Cytodex 1 and 3 were increasing throughout the period, while ESM and collagen beads kept a more stable line (figure 24). Protein concentration on day 1 was statistical significance from all the other days of Cytodex 1, with a 95 % safety factor. Day 1 of Cytodex 3 had a statistical significance between day 6 and 8, with a significant level of 0.05. There was no statistical significance within ESM and collagen beads. Between Cytodex 1 and 3 there was a statistical significance on day 3 and 6, with a significant level of 0.05 (appendix 2).

Glucose consumption

The total glucose level was analysed using glucose assay kit with a microplate reader, the same way as in the 2D systems, to evaluate how much glucose the cells were consuming over the time-course of 8 days.

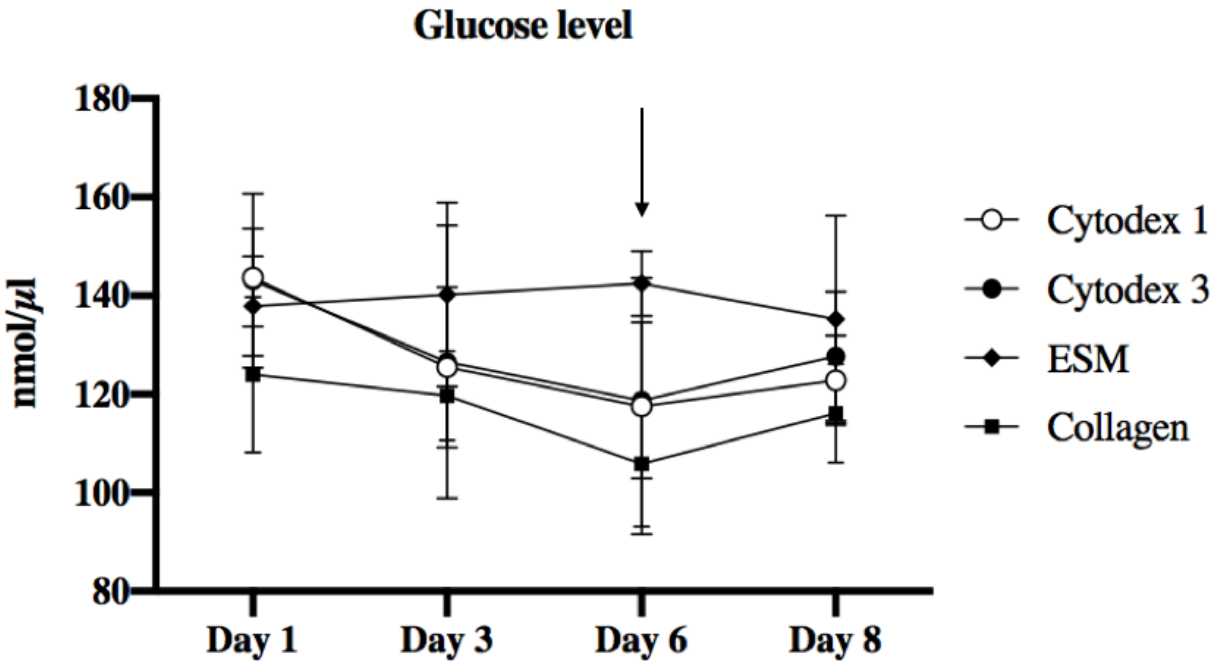

Figure 25: The total glucose level (nmol/µl) in medium from spinner flasks with muscle cells on different microcarriers. *The glucose level with Cytodex 1, Cytodex 3, eggshell membrane (ESM) and collagen beads were measured using glucose assay kit with frozen samples from one replicate of two independent spinner flask experiments over a time-course of 8 days. The black arrow indicates when the medium was changed and new beads were added after day 6.*

The total glucose levels measured from the medium with Cytodex 1, 3 and ESM were decreasing from day 1 to day 6, and then increasing till day 8 as a conceivable reaction of the new media added after day 6 (figure 25). While the collagen beads remained more stable, with a slight increase from day 1 till day 6, before falling till day 8 under the glucose level on day 1. No statistical significances were found within or between the glucose level from media with the different microcarriers (appendix 2).

Lactate level

The total lactate level was measured the same way as in the 2D systems, to analyse how much lactate the muscle cells on different microcarriers were producing into the media in spinner flasks.

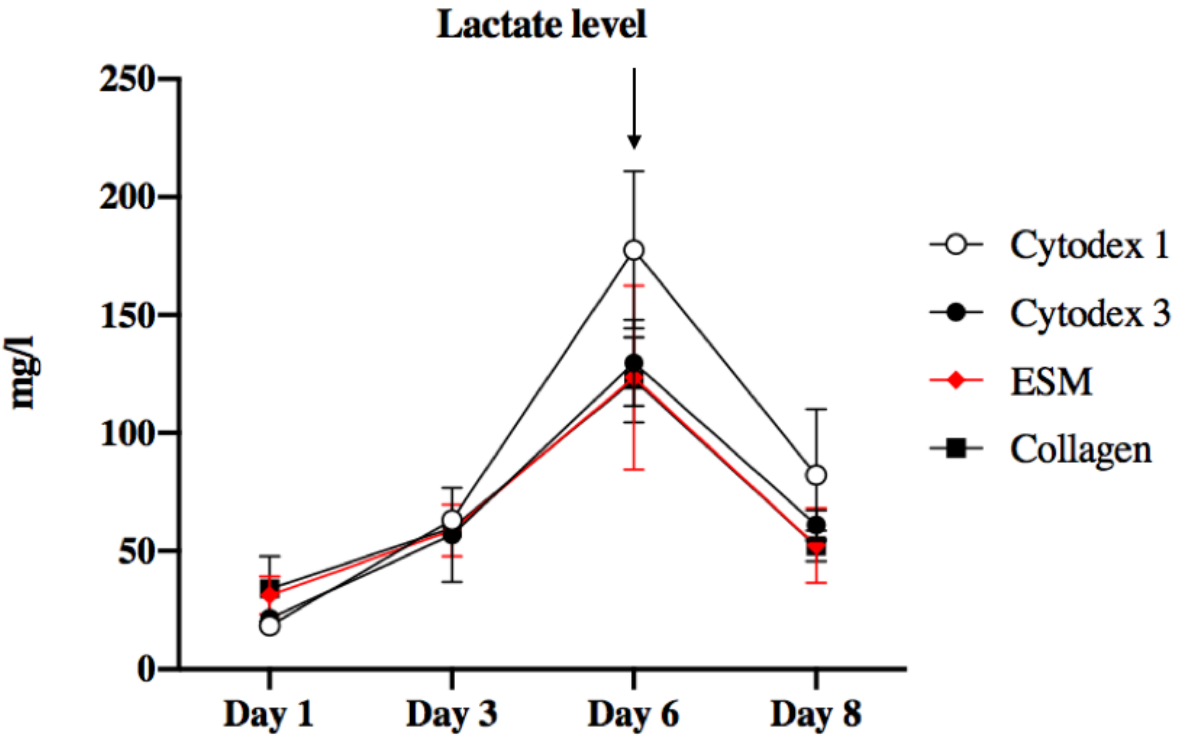

Figure 26: The total lactate level (mg/l) in medium from spinner flasks with muscle cells on different microcarriers. *Cytodex 1, Cytodex 3, eggshell membrane (ESM) and the collagen beads with muscle cells in media were measured directly from reflectometer RQflex plus10 with frozen samples from one replicate of two independent spinner flask experiments over a time-course of 8 days. The black arrow indicates when the medium was changed and new beads were added after day 6.*

The lactate concentrations increased in media of cell cultured on all the different microcarriers till day 6, before decreasing till day 8 (figure 26). From figure 26, it almost looks as if there are equal numbers of cells throughout the period. Cytodex 1 was the one that stood out from the other microcarriers, with a higher lactate level on day 6. The red line indicating lactate level in media with ESM were accentuated to show how it refers to be more similar to the other microcarriers then shown in all the other results over. The lactate level at day 6 in the media with Cytodex 1, 3 and collagen beads had a statistical significance from all the other days, with a significant level of 0.05. The media with ESM had only a statistical significance between day 1 and 6, with 0.05 as the significant level. With a 95 % safety factor, there were no statistical significance between Cytodex 1 and 3 on any days (appendix 2).

4.3. Up-scaling from spinner flasks to benchtop bioreactor with Cytodex 1 in cell culture

4.3.1. Proliferation and number of muscle cells on Cytodex 1 in benchtop bioreactor

The muscle cells nuclei on Cytodex 1 in benchtop bioreactor were stained with hoechst and characterised with a fluorescence microscope such as in figures 18-20. After day 6 the medium was changed and new batch of Cytodex 1 were added to the bioreactor to prevent cell aggregation and give them more surface to proliferate on. Every sampling day (day 0, 1, 3, 6, 7

and 8) three images were taken to characterise viable cells on the beads, and the most representative images were presented.

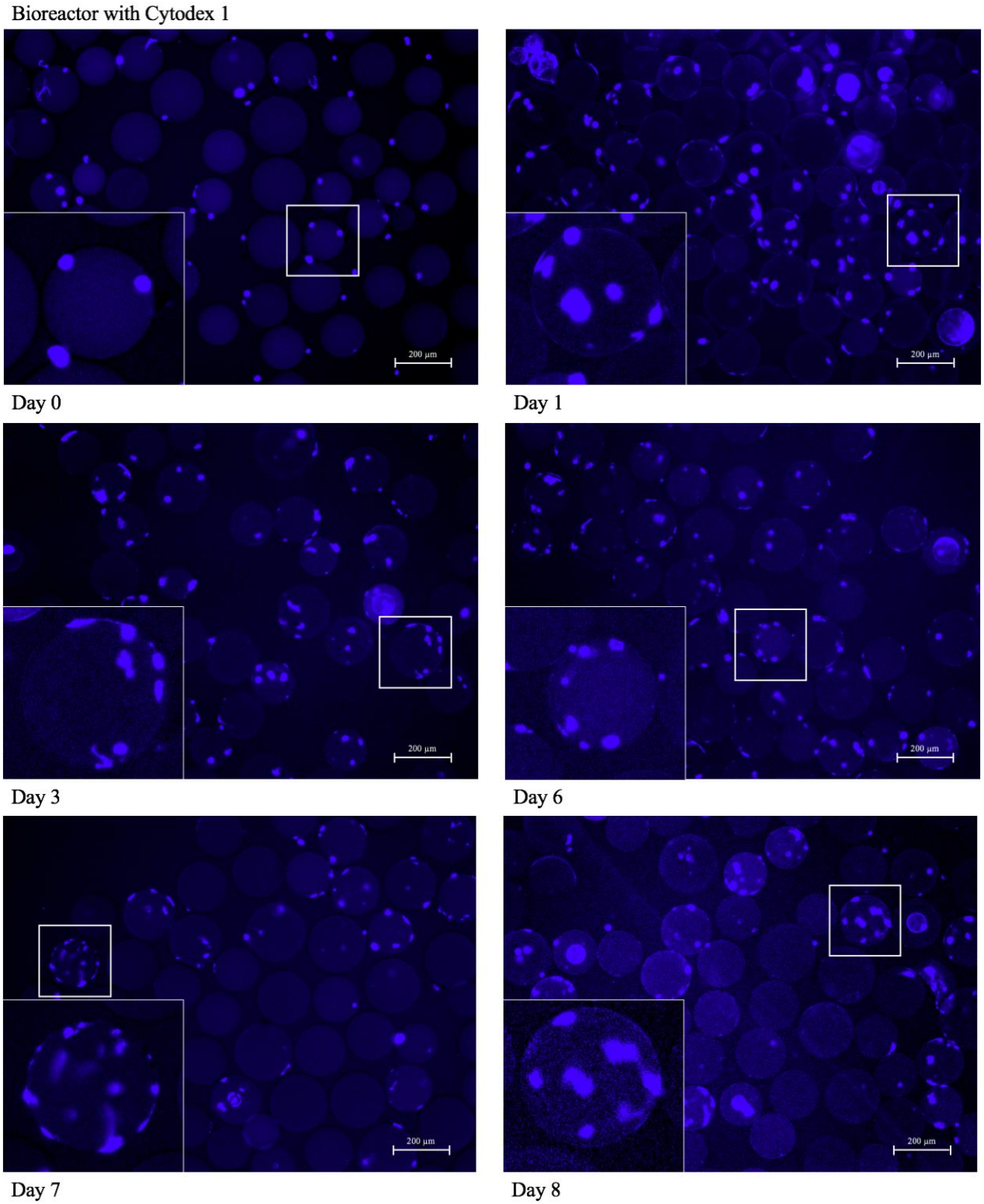

Figure 27: Hoechst stained muscle cells nuclei on Cytodex 1 in benchtop bioreactor. *Proliferation of muscle cells on Cytodex 1 in benchtop bioreactor over a time-course of 8 days. The medium was changed and new microcarriers were added after day 6. The representative images were selected from three images from one independent experiments. Images were taken using the Zeiss Zen software and fluorescence microscope with 5x magnification.*

The muscle cells nuclei in the benchtop bioreactor were attaching and proliferation on Cytodex 1 (figure 27). The images on day 7 and 8, clearly outline the number of empty beads added after day 6.

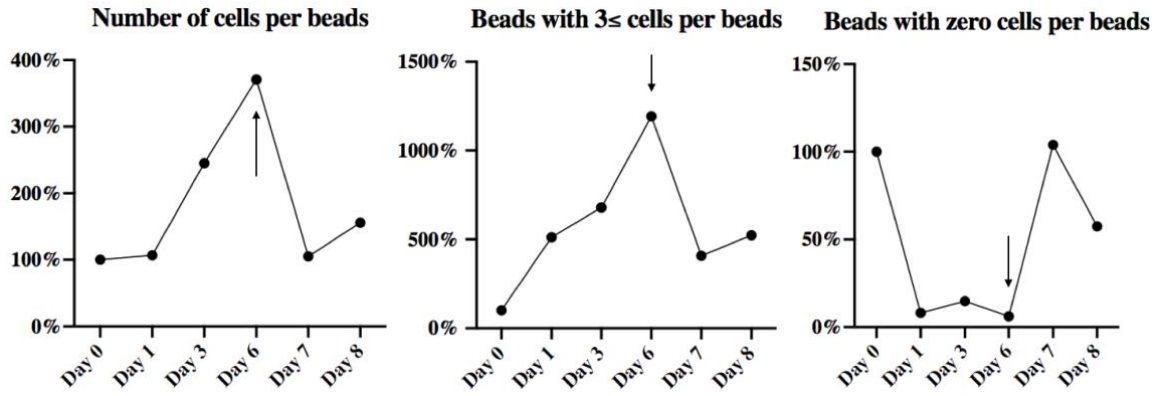

Figure 28: Number of cells, beads with 3≤ cells and empty beads in benchtop bioreactor. *The amounts were compared to the total number of beads over a time-course of 8 days. The results were collected from one image, with a total of 24 images assembled using Zeiss Zen software and fluorescence microscope with a 5x magnification, of one experiment. The black arrows indicate when the medium was changed and new beads were added, after day 6. The numbers were converted to percent and normalised to day 1.*

The results in figure 28 were counted exactly like in figure 21. The number of cells and beads with 3≤ cells per beads were increasing till day 6, meanwhile the number of empty beads were decreasing. After day 6, new beads were added to the benchtop bioreactor and number counted were based on additions of new beads, making the number of cells and 3≤ cells per beads to drop till day 7 before increasing till day 8. The number of beads with zero cells per beads were increasing after the new beads were added till day 7 before decreasing till day 8.

4.3.2. Biochemical measurements in benchtop bioreactor

DNA concentration

The DNA concentration from the bench bioreactor experiments used Qubit™ dsDNA (BR) assay kit with duplications of fresh samples in a Qubit 3.0 fluorometer by Principal Engineer Dimitrios Tzimorotas at Nofima AS in Ås. The concentration was measured to have additional parameters on how the cell proliferation went in an environment that's optimal for up-scale muscle cells production.

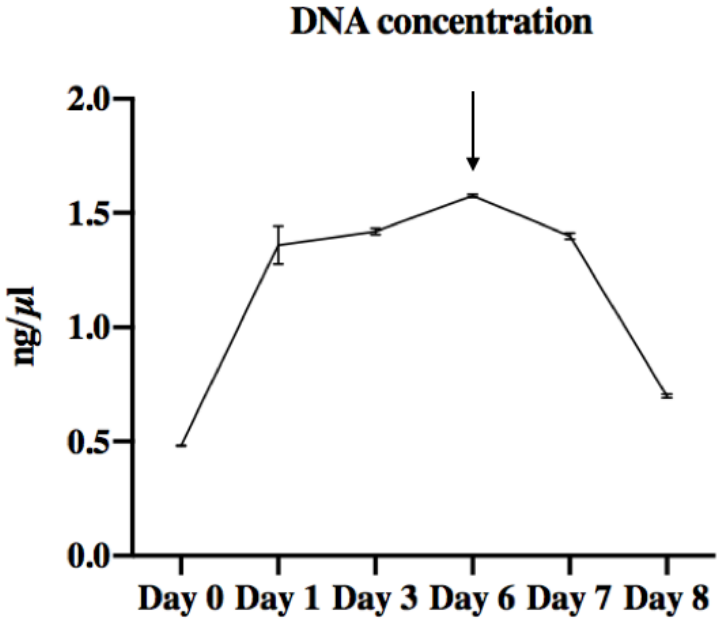

Figure 29: Total DNA concentration (ng/µl) of muscle cells on Cytodex 1 in benchtop bioreactor. *The concentration was measured with fresh samples taken over a time-course of 8 days. Qubit™ dsDNA assay kit with a Qubit 3.0 Fluorometer (broad range) was used to collect the results. The results from the graph over were assembled from two replications of one experiments. The black arrows indicate when the medium was changed and new beads were added after day 6.*

The results indicate that the DNA concentration increased and the cell proliferation was present till day 6, and after the new beads were added the concentration went down (figure 29). With a safety factor of 95 %, there was found statistical significance between most days, except between day 1, 3 and 7 (appendix 2).

Protein production

The total concentration was measured using Bio-Rad DC™ protein assay kit I with a microplate reader to evaluate the protein amount from the muscle cells, attached on the Cytodex 1. The total protein concentration was calculated relative to a standard line. The samples were duplicated and presented in the graph under (figure 30).

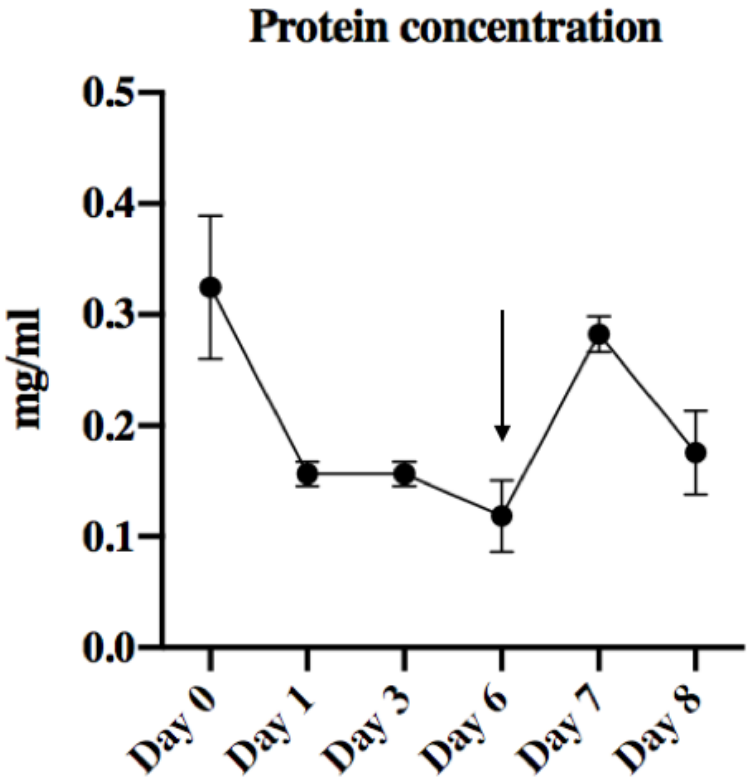

Figure 30: The total protein concentration (mg/ml) of muscle cells on Cytodex 1 in benchtop bioreactor. *The results were measured using Bio-Rad DC™ protein assay kit I with frozen samples from two replications of one experiments over a time-course of 8 days. The black arrow indicates when the medium was changed and new beads were added after day 6.*

The total protein concentration was decreasing till day 6, and rose immediately after the new beads were added, before it dropped again (figure 30). Only day 7 did not have a statistical significance between day 0, with a significant level of 0.05 (appendix 2).

Glucose consumption

The total glucose level was analysed using glucose assay kit with a microplate reader, the same way as in the 2D systems, to evaluate how much glucose the cells were consuming over the time-course of 8 days. The results were calculated against a standard curve.

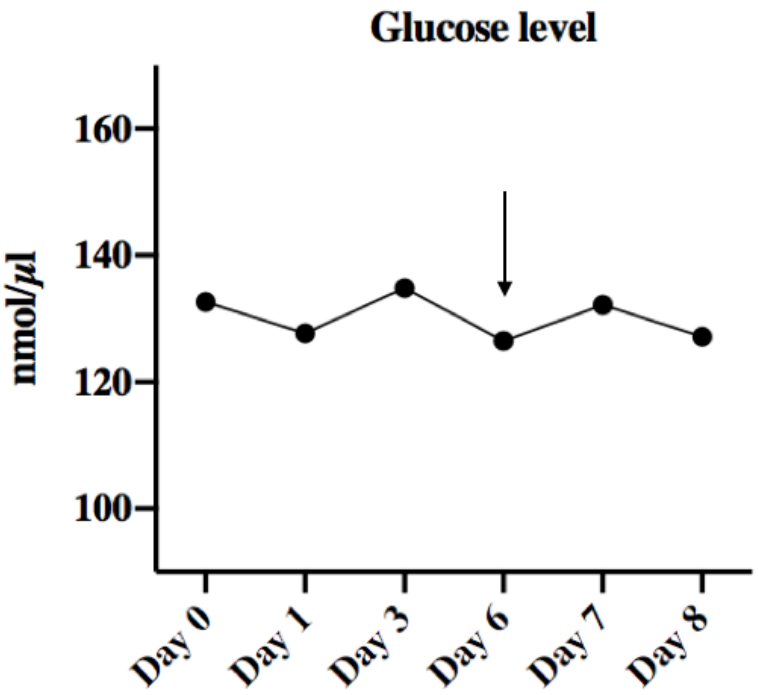

Figure 31: Total glucose level (nmol/µl) in media from benchtop bioreactor with muscle cells on Cytodex 1. *The glucose level was measured using glucose assay kit with frozen samples from one replicate of one experiments over a time-course of 8 days. The black arrow indicates when the medium was changed and new beads were added after day 6.*

The total glucose consumption in the proliferation medium remained virtually stable over the 8 days (figure 31).

Lactate production

The total lactate level was measured the same way as in the 2D systems to analyse how much lactate the muscle cells on Cytodex 1 was producing into the media in benchtop bioreactor.

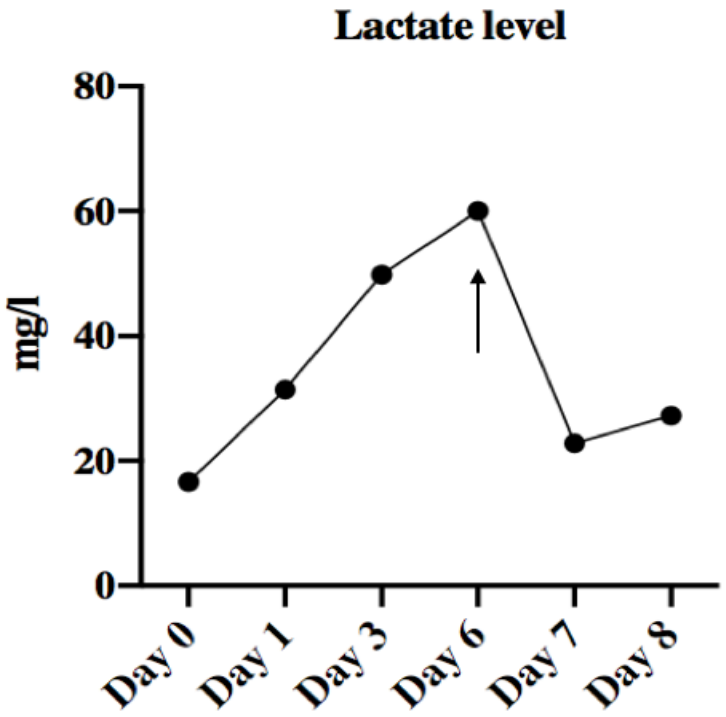

Figure 32: The total lactate level (mg/l) in media from benchtop bioreactor with muscle cells on Cytodex 1. *Cytodex 1 in cell culture was measured directly from reflectometer RQflex plus10 with frozen samples from one replicate of one experiments over a time-course of 8 days. The black arrow indicates when the medium was changed and new beads were added after day 6.*

The total lactate level was increasing from day 0 to day 6, before decreasing as a reaction of adding of new beads after day 6, and then increasing again from day 7 to 8 (figure 32).

L-glutamine and ammonia concentration

The L-glutamine and ammonia concentration were characterised by using the L-glutamine/ammonia (rapid) assay kit with a microplate reader, to evaluate how the L-glutamine spontaneously breaks down to L-glutamate and free ammonium ions, and how it affects to the cell proliferation. The experiment went over a period of 8 days, and results came from to replicates (frozen samples) of one experiment.

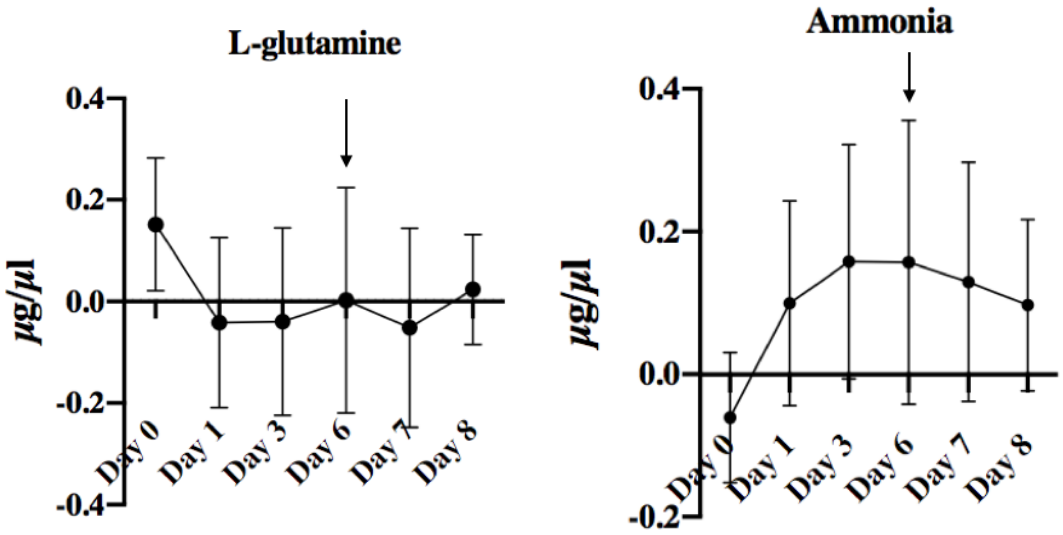

Figure 33: Ammonia and L-glutamine concentration (µg/µl) in media from benchtop bioreactor with muscle cells on Cytodex 1*. L-glutamine/ammonia (rapid) assay kit was used to measurement the ammonia and L-glutamine concentration from two replicates of one benchtop bioreactor experiment over a time-course of day 8 days. The black arrows indicate when the medium was changed and new beads were added after day 6.*

The graph over shows that when the L-glutamine breaks down, the ammonia level increases (figure 33). After the new medium was added the L-glutamine begins to increase eventually, and corollary the ammonia concentration starts to sink. The standard deviation was large in both measurement within all the days. No statistical significances were found between the days in none of the graphs (appendix 2).

5. Discussion

5.1. Characterisation of cell growth in 2D and 3D systems

In all experiment, primary muscle cells were used to give a more similar representation of the animal tissue, *in vivo* state. The primary cells were taken directly from the tissue of origin and had a limited lifespan, meaning it will die after a certain number of divisions. Cell line could be an option for extending the lifespan, because through genetic mutations or artificial modifications cell lines has acquired the ability to proliferate indefinitely. However, they will lose their characteristics of the original isolated tissue and are not preferred as a biologically option. The skeletal muscle cells are more difficult of cultivating then cell line, so it is important to establish optimised culture conditions (Merck, 2019c).

With age the skeletal muscle decreases in fibre number and loses its remaining muscle fibres by atrophy, which can potentially originate from proteolytic pathway. Decrease in muscle mass due to apoptosis, programmed cell death, is also an alternative (Dirks and Leeuwenburgh, 2002). To maintain cell population, apoptosis is an important part under normal aging of muscle cells. It is a defence mechanism during exposure to heat, radiation, cytotoxic compounds, infections and hypoxia. Apoptosis is triggered either by internal factors caused by cell stress or external stimuli induced by other cells signals (Rønning, 2017).

In both images from light microscopy and with hoechst stained muscle cells nuclei in 2D systems, the cells were proliferating and differentiating till almost 100 % confluence on day 8. Also, when counting the number of cells, it showed an increase in number which could ensure that the cells were alive and proliferating. The number of cells in 2D systems had a statistical significance between day 1 and 8, which meant there was a significant increase with a significance level of 5 % from day 1 till day 8. This was an expected result which have been done with different muscle cells several times before, with same outcome (Lambrechts et al., 2016). In figure 9 a spontaneous differentiation occurred on day 8, although differentiation of skeletal muscle cells *in vitro* are commonly controlled by adding differentiation medium to start the process (Mattick et al., 2015). The proliferation medium that was used in this experiment contained FBS which exhibits high levels of variations in batches, that could affect cellular differentiation. It has been demonstrated that different hormones in relation with serum origin, have resulted in a dramatic change in the spontaneous contractility in muscle cells, caused of a shift in calcium action (Aswad et al., 2016). The medium also contained the antibiotic PenStrep which have shown to enhance transcription factors known to have a key role in cell differentiation and proliferation (Ryu et al., 2017). By adding PenStrep in the proliferation medium, the muscle cells were not edible and were used for research only (Gstraunthaler, 2003).

Cytodex 1 and 3 (commercial microcarrier) were used in the experiment to gain an understanding of how the cells usually grow on 3D structures. The muscle cells were proliferating on both microcarriers viewed in figure 18, which was an expected result from the commercial microcarriers (Frauenschuh et al., 2007). Cytodex 1 appeared to be a more

appropriate matrix for the cells to grow on, as the Cytodex 1 assays gave higher cell viability then Cytodex 3. Cytodex 1 are designed to support production of primary cells and therefore was a better alternative for culturing bovine skeletal muscle cells in vitro, as expected (Healthcare, 2016). The number of cells per beads in figure 21 was counted only of Cytodex 1 and 3 because it was done manually in ImageJ. The number of cells on Cytodex 1 and 3 were increasing from day 1 till day 6 before dropping on day 8, along with the number of cells on each bead. The beads with no cells attached decreased in the period before more beads were added. These results provided additional evidence that the cells were proliferating till day 6, before new proliferation medium and new batch of beads was added.

5.2. Characterisation of cell growth on edible microcarriers

Previously microcarriers (as Cytodex 1 and 3) were made with synthetic materials (e.g. glass or polystyrene) or natural products (e.g. cross-linked dextran or collagen) have just been used as substrates for the cell culture and not as a part of the final comestible product (Marga et al., 2017). By making the microcarriers edible and digestible they could be incorporated into the final product without the step of removing the cells from the microcarriers. Using entirely edible materials in microcarriers is a novel technology for *in vitro* meat production, and could be a more sustainable alternative if the cell growth is somewhat similar to the commercial microcarriers.

ESM powder was made from natural biomaterial. It consists of collagens, glycoproteins, cysteine-rich eggshell membrane proteins (CREMPS), carbohydrate and antibacterial protein, which is similar to the skeletal muscle cells ECM. ESM powder is a new, microporous organic support material that is also cost effective, robust and an available material (Pundir et al., 2009). As shown in figure 16, the ESM powder has a network of cross-linked fibrillary structure. ESM have traditionally been used in wound healing for more than 400 years in Asian countries (Vuong et al., 2017). Primary muscle cells are adherent and requires attachment for growth. The muscle cells *in vivo* are surrounded by collagen fibrils which is the major structural protein in the muscles ECM (Gillies and Lieber, 2011). Knowing this, the ESM should be a suitable matrix alternative for the cells to proliferate on. From the hoechst stained nuclei on ESM in this study it appeared that the muscle cells kept the same amount until day 6. On day 8 the cells were almost not present, and only a few were located. Compared with the number of cells counted on ESM in figure 22, the number of cells slowly decreases till day 6, after dropping further to day 8. The aggregation in the spinner flasks were not optimal and every day the spinner flask was manually stirred to distribute the beads better. In a study by Ferrari et al., when he used microcarrier (Cytodex 1) in spinner flask, large microcarrier-cell-aggregates could occur, which could reduce the access of nutrients to the cells and lead to cell death (Ferrari et al., 2012). It may seem like the ESM concentration in comparison to the amount of cells were too high, in addition to the stirring not working as it could. When too much powder was added, it could have given the cells too must space. When the muscle cells were spread out, it could prevent the opportunity of meeting and dividing. The muscle cells nuclei were attaching sporadic to the ESM powder on day 1, while on day 3 the muscle cells nuclei looked more aligned. It could indicate differentiation when myoblasts merges into myotubes (Thomas et al.,

2015). Some cells detach the microcarriers when entering the differentiation stage, and this could potentially be the case in this experiment.

ECM supports the muscle cells, not only for structure but also for signaling, regulating activation and maintaining stem cell identity (Thomas et al., 2015). Edible porous scaffold of fish gelatin, alginate and other ingredients has newly been developed for myoblasts growth. The cells grew excellent, but they needed exogenous stimuli to differentiate the cells (Acevedo et al., 2018). An irregular surface, as the ESM powder has, could affect the biological function by the randomly distribution of cells (Li et al., 2014). A uniform cell alignment and reproducible architecture are needed to produce dense skeletal muscle tissue (Langelaan et al., 2010). However, pores, orientation and roughness of the biomaterials surface are also aspects that is important factors for cell development (Li et al., 2014). The collagen beads used in this study had a sponge like surface with several small holes (figure 17), which resembled the *in vivo* structure of skeletal muscles matrix (Klumpp et al., 2010).

The collagen beads made of residual raw materials of turkey was also an edible microcarrier, that were made for evaluating its potential in meat production with cell culture. The worlds consumption and food production have a long way to be fully sustainable. By recycling residual raw materials of turkey, the production of *in vitro* meat could get one step closer to becoming more sustainable (Jurgilevich et al., 2016). Unlike ESM in our experiment, the number of muscle cells on collagen beads appeared to continue proliferating throughout the period, and had a significant increase from day 1 till day 8 in figure 22, despite of the large standard deviation on day 8. A challenge with the collagen beads was that they were light and floated on the medium, unlike the other microcarriers. When the muscle cells were added, they sank to the bottom and it became difficult to get the cells to adhere to the floating beads. The solution was to add a small amount of medium the first 24 h and then fill up the flask so the cells got enough nutrition. When the muscle cells attached, and proliferated on the collagen beads, it became heavier and dropped to the bottom. The microcarriers were used to up-scale the primary muscle cells production and to provide a larger surface area for the cells to proliferate and differentiate on. The collagen beads were macroporous and in average larger than the other microcarriers because of their pores, which could be up to 400 µm wide. The lager carriers, the less surface area for the cells to grow on and the optimal size for smooth microcarriers is 100-300 µm (Healthcare, 2009). The collagen in this study had an average length of around 2500 µm (figure 15). The collagen beads were made with a droplet technique into liquid nitrogen to make the beads round and small, however it could be made even smaller to give the muscle cells a larger surface area by using a smaller needle.

5.3. Characterisation of biochemical processes in 2D and 3D systems

In the up-scaling of the muscle cell production, spinner flask and bioreactor was used. By up-scaling, the monitoring and control of an optimal culture conditions were tested. In the spinner flasks, which is a smaller up-scaling method, only temperature and stirring are commonly controlled. In our experiments with spinner flask the stirring glass bars (100 rpm) were placed on the bottom of the vessel to give a more accurate stirring speed. However, this could lead to

sedimentation of the microcarriers, which could affect the cells functions. In bioreactors, it is easier to control optimal culture conditions, by monitoring pH, oxygen, temperature, aggregation and measuring metabolites as lactate, glucose, glutamine and ammonia (Nilsson, 1988). In this study, we also measured DNA and protein concentration to get a better indication of how the muscle cells proliferate and develop. The concentration of nutrients is one of the crucial variables for controlling the cell growth, viability and differentiation. To improve the cell culture performance, fed-batch could be included to reduce the metabolite accumulation in the supernatant and perfusion (Hambor, 2012). When future commercializing the muscle cells, a new culture media should also be made without any antibiotic, and serum-free (Gstraunthaler, 2003).

The DNA concentration results in 2D systems were somewhat misleading compared to the other results. It had a decrease in concentration till day 5, which could indicate that the muscle cells were dying. However, the images taken with light and fluorescence microscope showed that the muscle cells were increasing in growth and only got more cells over the period (figure 12). The method used to measure DNA concentration in 2D systems and in the benchtop bioreactor, Qubit™ dsDNA (BR) Assay Kit, have been studied with frozen samples and the results demonstrated that divergence of quantification with Qubit depends on the salt concentration in the sample. In our samples the DNA concentration was low, and this could lead to inconsistencies in the quantification of DNA using the Qubit (Nakayama et al., 2016). The measurement of DNA concentration for Cytodex 1 and 3 was done using the high-sensitivity setting on the Qubit 3.0 Fluorometer, to get a result from the low DNA concentration. The results were in the lowest quantitation range of the assay in 2D systems, and there were too low concentrations on day 1 to get any results. However, it showed an increase in DNA concentration in both Cytodex 1 and 3, which could indicate cell growth and proliferations. Neither ESM or collagen beads had enough DNA to give any results. Which could indicate that the muscle cells were not alive or that we did not got enough DNA from the sampling. Small amounts of DNA in the sample gave uncertainty in the quantification, because Qubit-methods highly depends on the determination size by the bioanalysis, which is estimated from intensity of DNA determent at specific sizes (Robin et al., 2016). The amount of DNA in our samples were very low and perhaps the sampling could be done differently with higher number of beads with muscle cells attached. In the bioreactor, the DNA concentration was much higher than in the other systems. It gave the more expected results based on how the cells proliferated as shown in figure 29. The DNA concentration in the benchtop bioreactor peaked on day 6, such as the number of cells counted. The DNA measurement was done with fresh samples from the bioreactor, and it appeared to give a more stable result than with the frozen samples.

The protein production of the muscle cells had a significant increase from day 1 to day 5 in 2D systems, which also gave an indication of cell proliferation and that live cells were present. Protein denaturation, lactic acid accumulation and anaerobic glycolysis metabolic reactions, that is responsible for producing the textural quality, appearance and taste of meat (Datar and Betti, 2010). After the exponential growth till day 5 the protein concentration began to equalise. The muscle cells on Cytodex 1 and 3 in spinner flasks were producing scientifically more proteins from day 1 till day 6. When the new medium and beads where added, it diluted the

protein concentration in the medium and the results showed a decrease in protein concentration after day 6. However, this does not indicate that the cells were dying or resting. Instead, if the cells were dying this would have occurred immediately and this was not the case. The muscle cells were probably still proliferating till day 8. The results from the ESM and collagen beads were uncertain, because both the ESM powder and collagen beads were made of protein. This means that when the lysis buffer was used to get the protein of the muscle cells attached to the beads, the protein from the beads were probably contaminating the samples. The protein concentrations appeared to increase and decease every sampling day in figure 24, which could apply that the amount of muscle cells just stayed the same. The protein level in the bioreactor however decreased till day 6 before increasing till day 8, which was not an expected result. Maybe the protein from the medium was measured as well, which could explain why the protein level was increasing after the new medium was added after day 6.

Glucose from the proliferation medium added in all the experiments, modifies ATP through glycolysis. The conversion of glucose is happening in the mitochondria and are transferred by proteins in the plasma membrane (Moritz et al., 2015). The glucose level in 2D was slightly decreasing till day 5, but kept non-the less stable throughout the period. As well as in the spinner flasks and the benchtop bioreactor, none of the measurements had a statistical significance. In the spinner flasks, the glucose level decreased more with a peak on day 6 in Cytodex 1, 3 and ESM. The supernatants glucose level with collagen beads was in the other hand slightly increasing till day 6, before falling to the starting level. The quite stable lines could indicate that the systems had more than enough proliferation medium added, because the cells only used some. In the benchtop bioreactor, the glucose level was also quite stable throughout the period, and no major change after the new medium changed after day 6. Bioreactor provides a steadier environment, due to its high level of proliferation medium and the controlled modified conditions. The possibilities of recycling culture medium will be an important factor for an up-scale system, but it has not been studied enough for large-scale cell production (Moritz et al., 2015).

Both in the spinner flasks and bioreactor the proliferation medium was change after day 6 and then the lactate level in the supernatant decreased in all cases (figures 26 and 32). The lactate is the final product of anaerobic glycogen, which accumulate when the muscle must produce energy in a survival situation (Pösö and Puolanne, 2005). It is a by-product produced by the cells when they consume glucose (Moritz et al., 2015). This is a burden for the bioreactor's pH control system, and a base addition is required. By reducing the waste-product, lactate, in the medium, it has been shown to lead to higher cell productivity (Xu et al., 2018). The lactate level was just increasing with muscle cells grown in 2D systems (figure 13). In the spinner flasks and benchtop bioreactor, the lactate production from the muscle cells also increased before changing the medium and lowering the concentration for a longer life-span of the muscle cells. Other studies have also shown that the lactic acid has increased in hypoxic conditions (Chakravarthy et al., 2001).

An important amino acid for the muscle cells is glutamine and when it is consumed by the muscle cells it produces another by-product, ammonia (Moritz et al., 2015). In figure 33, it is

clear to see that when the L-glutamine decreased, the ammonia concentration was rising in the benchtop bioreactor on day 1. Regulation of the glutamine are preferred so the ammonia concentration is reduced, because of its inhibition of cells in small concentration. It has also been shown that lactate consumption could be regulated by glutamine concentration. Degradation of lactate was starting when the glutamate was lowered (Zagari et al., 2013). The refreshment of medium when cultivating muscle cells are necessary, due to its ability to regulate both glucose, lactate, glutamine and the consumption/production of ammonia (Schop et al., 2008).

6. Conclusion and future work

The muscle cells in 2D systems were proliferating as expected. The cell growth on Cytodex 1 and 3 in spinner flasks gave similar trends in growth. However, Cytodex 1 appeared to give a higher cell density which aligns with earlier studies. The edible collagen beads appeared to give a suitable matrix for the muscle cells to proliferate on. Although the lactate level in ESM was increasing over time indicating that the cells were active, the cells where hardly observed in fluorescence microscope after adding the new beads. The biochemical processes in 2D and 3D systems gave a good indication of the cells viability, however, some of the measurements had a few inconsistencies due to low concentration and frozen samples. The up-scaled production in benchtop bioreactor was more stable due to the large access of nutrients and growth area.

This study arrives one step closer to the *in vitro* meat production, however, there are several challenges that must be solved before it reaches a consumer's market. The challenges in making the production more cost-efficient, ethical and in a more sustainable way must be solved. Is it possible to recycle the medium to save money? Making the medium serum-free must be done. The biochemical processes need to be monitored further so that we can achieve an optimal environment for the skeletal muscle cells. The up-scaled production is in its infancy and more research is needed. Sterile techniques when cultivating the meat is also an important factor. This was shown in our first experiments using the benchtop bioreactor, where an infection due to unknown factors was found. The aspect of reducing the environmental damages related to the production and understanding the health benefits, limits its commercial viability. At last, the taste and acceptance from the costumers must be taken in consideration in order to make *in vitro* meat production a part of the future food industry.

Referances

ABCAM. 2018. Picro Sirius Red Stain Kit (Connective Tissue Stain) [Online]. Available: https://www.abcam.com/ps/products/150/ab150681/documents/ab150681_Picro%20Sirius%20Red%20Stain%20Kit%20(Connective%20Tissue%20Stain)%20v3b%20(website).pdf [Accessed]

ABCAM. 2019. *Glucose Assay Kit (ab65333)* [Online]. abcam.com. Available: https://www.abcam.com/glucose-assay-kit-ab65333.html?productWallTab=ShowAll [Accessed].

ACEVEDO, C. A., ORELLANA, N., AVARIAS, K., ORTIZ, R., BENAVENTE, D. & PRIETO, P. 2018. Micropatterning Technology to Design an Edible Film for In Vitro Meat Production. *Food and bioprocess technology***,** 1-7.

ALEXANDER, P., BROWN, C., ARNETH, A., DIAS, C., FINNIGAN, J., MORAN, D. & ROUNSEVELL, M. D. A. 2017. Could consumption of insects, cultured meat or imitation meat reduce global agricultural land use?

ARGILÉS, J. M., CAMPOS, N., LOPEZ-PEDROSA, J. M., RUEDA, R. & RODRIGUEZ-MANAS, L. 2016. Skeletal muscle regulates metabolism via interorgan crosstalk: roles in health and disease. *Journal of the American Medical Directors Association,* 17**,** 789-796.

ASWAD, H., JALABERT, A. & ROME, S. 2016. Depleting extracellular vesicles from fetal bovine serum alters proliferation and differentiation of skeletal muscle cells in vitro. *BMC biotechnology,* 16**,** 32.

BACH, A., BEIER, J., STERN-STAETER, J. & HORCH, R. 2004. Skeletal muscle tissue engineering. *Journal of cellular and molecular medicine,* 8**,** 413-422.

BADENES, S., FERNANDES-PLATZGUMMER, A., RODRIGUES, C., DIOGO, M., DA SILVA, C. & CABRAL, J. 2016. Microcarrier Culture Systems for Stem Cell Manufacturing. *Stem Cell Manufacturing.* Elsevier.

BERTOLO, A., ARCOLINO, F., CAPOSSELA, S., TADDEI, A. R., BAUR, M., PÖTZEL, T. & STOYANOV, J. 2015. Growth factors cross-linked to collagen microcarriers promote expansion and chondrogenic differentiation of human mesenchymal stem cells. *Tissue engineering Part A,* 21**,** 2618-2628.

BHAT, Z. F., KUMAR, S. & FAYAZ, H. 2015. In vitro meat production: Challenges and benefits over conventional meat production. *Journal of Integrative Agriculture,* 14**,** 241-248.

BHUTDA, S., SURVE, M. V., ANIL, A., KAMATH, K., SINGH, N., MODI, D. & BANERJEE, A. 2016. Histochemical Staining of Collagen and Identification of Its Subtypes by Picrosirius Red Dye in Mouse Reproductive Tissues. *PLOS Pathogens*.

BIO-RAD. 2019. *Bio-Rad Protein Assay* [Online]. bio-rad.com. Available: http://www.bio-rad.com/en-no/product/bio-rad-protein-assay?ID=d4d4169a-12e8-4819-8b3e-ccab019c6e13 [Accessed].

BIOMATE. *Fermentation Design Technology* [Online]. Available: https://biomateindia.tradeindia.com/fermentation-design-technology-1598582.html [Accessed].

CADENA-HERRERA, D., ESPARZA-DE LARA, J. E., RAMÍREZ-IBAÑEZ, N. D., LÓPEZ-MORALES, C. A., PÉREZ, N. O., FLORES-ORTIZ, L. F. & MEDINA-RIVERO, E.

2015. Validation of three viable-cell counting methods: manual, semi-automated, and automated. *Biotechnology Reports,* 7**,** 9-16.
CHAKRAVARTHY, M., SPANGENBURG, E. & BOOTH, F. 2001. Culture in low levels of oxygen enhances in vitro proliferation potential of satellite cells from old skeletal muscles. *Cellular and Molecular Life Sciences CMLS,* 58**,** 1150-1158.
COMPTON, S. J. & JONES, C. G. 1985. Mechanism of dye response and interference in the Bradford protein assay. *Analytical biochemistry,* 151**,** 369-374.
DATAR, I. & BETTI, M. 2010. Possibilities for an in vitro meat production system. *Innovative Food Science & Emerging Technologies,* 11**,** 13-22.
DIRKS, A. & LEEUWENBURGH, C. 2002. Apoptosis in skeletal muscle with aging. *American Journal of Physiology-Regulatory, Integrative and Comparative Physiology,* 282**,** R519-R527.
DOS SANTOS, F., ANDRADE, P., DA SILVA, C. & CABRAL, J. 2013. Scaling-up ex vivo expansion of mesenchymal stem/stromal cells for cellular therapies. *Mesenchymal Stem Cell Therapy.* Springer.
FERNANDES, A., FERNANDES, T., DIOGO, M., DA SILVA, C. L., HENRIQUE, D. & CABRAL, J. 2007. Mouse embryonic stem cell expansion in a microcarrier-based stirred culture system. *Journal of biotechnology,* 132**,** 227-236.
FERRARI, C., BALANDRAS, F., GUEDON, E., OLMOS, E., CHEVALOT, I. & MARC, A. 2012. Limiting cell aggregation during mesenchymal stem cell expansion on microcarriers. *Biotechnology progress,* 28**,** 780-787.
FRAUENSCHUH, S., REICHMANN, E., IBOLD, Y., GOETZ, P. M., SITTINGER, M. & RINGE, J. 2007. A microcarrier-based cultivation system for expansion of primary mesenchymal stem cells. *Biotechnology progress,* 23**,** 187-193.
GALUSKY, W. 2014. Technology as responsibility: Failure, food animals, and lab-grown meat. *Journal of agricultural and environmental ethics,* 27**,** 931-948.
GERBER, P. J., STEINFELD, H., HENDERSON, B., MOTTET, A., OPIO, C., DIJKMAN, J., FALCUCCI, A. & TEMPIO, G. 2013. *Tackling climate change through livestock: a global assessment of emissions and mitigation opportunities*, Food and Agriculture Organization of the United Nations (FAO).
GHARAIBEH, B., LU, A., TEBBETS, J., ZHENG, B., FEDUSKA, J., CRISAN, M., PÉAULT, B., CUMMINS, J. & HUARD, J. 2008. Isolation of a slowly adhering cell fraction containing stem cells from murine skeletal muscle by the preplate technique. *Nature protocols,* 3**,** 1501.
GIBCO™. 2019. *Trypan Blue Solution, 0.4%* [Online]. thermoficher.com. Available: https://www.thermofisher.com/order/catalog/product/15250061 [Accessed].
GILLIES, A. R. & LIEBER, R. L. 2011. Structure and function of the skeletal muscle extracellular matrix. *Muscle & nerve,* 44**,** 318-331.
GODFREY, M. 2009. Extracellular matrix. *Asthma and COPD: Basic Mechanisms and Clinical Management,* 2**,** 265-71.
GOODWIN, J. N. & SHOULDERS, C. W. 2013. The future of meat: A quantitative analysis of cultured meat media coverage. *Elsivier,* 95**,** 445-450.
GRZELKOWSKA-KOWALCZYK, K. 2016. The importance of extracellular matrix in skeletal muscle development and function. *Composition and Function of the Extracellular Matrix in the Human Body.* IntechOpen.
GSTRAUNTHALER, G. 2003. Alternatives to the use of fetal bovine serum: serum-free cell culture. *ALTEX-Alternatives to animal experimentation,* 20**,** 275-281.
GUPTA, P., ISMADI, M.-Z., VERMA, P. J., FOURAS, A., JADHAV, S., BELLARE, J. & HOURIGAN, K. 2016. Optimization of agitation speed in spinner flask for microcarrier

structural integrity and expansion of induced pluripotent stem cells. *Cytotechnology,* 68**,** 45-59.
HAMBOR, J. E. 2012. Bioreactor design and bioprocess controls for industrialized cell processing. *BioProcess Int,* 10**,** 22-33.
HAUGDAHL, M. 2014. *Learn more about in vitro meat* [Online]. Nofima.no. Available: https://nofima.no/en/nyhet/2008/04/61431701152917714 97/ [Accessed].
HEALTHCARE, G. 2005. *Microcarrier Cell Culture - Principles and Methods* [Online]. Gelifesciences.co. Avilable: http://www.gelifesciences.co.kr/wp-content/uploads/2016/07/023.8_Microcarrier-Cell-Culture.pdf [Accessed]
HEALTHCARE, G. 2009. CytodexTM surface microcarriers. *Data file***,** 18-1060 [Online]. Gelifesciences.co. Available: https://www.gelifesciences.co.jp/catalog/pdf/18106061_cytodex.pdf [Accessed]
HEALTHCARE, G. 2016. Cytodex™ 1 Gamma and Cytodex 3 Gamma [Online]. Gelifesciences.co. Available: https://www.gelifesciences.co.jp/catalog/pdf/29158445AB.pdf [Accessed]
HENCHION, M., HAYES, M., MULLEN, A., FENELON, M. & TIWARI, B. 2017. Future Protein Supply and Demand: Strategies and Factors Influencing a Sustainable Equilibrium. Basel, Switzerland :.
HOSIOS, AARON M., HECHT, VIVIAN C., DANAI, LAURA V., JOHNSON, MARC O., RATHMELL, JEFFREY C., STEINHAUSER, MATTHEW L., MANALIS, SCOTT R. & VANDER HEIDEN, MATTHEW G. 2016. Amino Acids Rather than Glucose Account for the Majority of Cell Mass in Proliferating Mammalian Cells. *Developmental Cell,* 36**,** 540-549.
HUGHES, D. C., STEWART, C. E., SCULTHORPE, N., DUGDALE, H. F., YOUSEFIAN, F., LEWIS, M. P. & SHARPLES, A. P. 2016. Testosterone enables growth and hypertrophy in fusion impaired myoblasts that display myotube atrophy: deciphering the role of androgen and IGF-I receptors. *Biogerontology,* 17**,** 619-639.
HUKILL, T. 2006, july 12. *Would you eat lab grown meat?* [Online]. AlterNet. Available: http://www.alternet.org/environment/38755?page=1 [Accessed].
INVITROGEN™ 2005. Hoechst Stains [Online]. Thermofisher.com. Available: https://www.thermofisher.com/order/catalog/product/62249 [Accessed]
INVITROGEN™ 2017. QubitTM 1X dsDNA HS Assay Kits [Online]. Thermofisher.com. Available: https://www.thermofisher.com/order/catalog/product/Q33230 [Accessed]
INVITROGEN™. 2019a. *NucBlue™ Live ReadyProbes™ Reagent* [Online]. Thermoficher.com. Available: https://www.thermofisher.com/order/catalog/product/R37605 [Accessed].
INVITROGEN™. 2019b. *Trypan Blue Stain (0.4%) for use with the Countess™ Automated Cell Counter* [Online]. Thermoficher.com. Available: https://www.thermofisher.com/order/catalog/product/T10282 [Accessed].
JURGILEVICH, A., BIRGE, T., KENTALA-LEHTONEN, J., KORHONEN-KURKI, K., PIETIKÄINEN, J., SAIKKU, L. & SCHÖSLER, H. 2016. Transition towards circular economy in the food system. *Sustainability,* 8**,** 69.
KLUMPP, D., HORCH, R. E., KNESER, U. & BEIER, J. P. 2010. Engineering skeletal muscle tissue–new perspectives in vitro and in vivo. *Journal of cellular and molecular medicine,* 14**,** 2622-2629.
LAMBRECHTS, T., PAPANTONIOU, I., VIAZZI, S., BOVY, T., SCHROOTEN, J., LUYTEN, F. & AERTS, J.-M. 2016. Evaluation of a monitored multiplate bioreactor

for large-scale expansion of human periosteum derived stem cells for bone tissue engineering applications. *Biochemical engineering journal,* 108**,** 58-68.
LANDGREBE, D., HAAKE, C., HÖPFNER, T., BEUTEL, S., HITZMANN, B., SCHEPER, T., RHIEL, M. & REARDON, K. F. 2010. On-line infrared spectroscopy for bioprocess monitoring. *Applied microbiology and biotechnology,* 88**,** 11-22.
LANGELAAN, M. L., BOONEN, K. J., POLAK, R. B., BAAIJENS, F. P., POST, M. J. & VAN DER SCHAFT, D. W. 2010. Meet the new meat: tissue engineered skeletal muscle. *Trends in food science & technology,* 21**,** 59-66.
LI, G., ZHAO, X., ZHAO, W., ZHANG, L., WANG, C., JIANG, M., GU, X. & YANG, Y. 2014. Porous chitosan scaffolds with surface micropatterning and inner porosity and their effects on Schwann cells. *Biomaterials,* 35**,** 8503-8513.
LISTRAT, A., LEBRET, B., LOUVEAU, I., ASTRUC, T., BONNET, M., LEFAUCHEUR, L., PICARD, B. & BUGEON, J. 2016. How muscle structure and composition influence meat and flesh quality. *The Scientific World Journal,* 2016.
LÓPEZ-MEZA, J., ARAÍZ-HERNÁNDEZ, D., CARRILLO-COCOM, L. M., LÓPEZ-PACHECO, F., DEL REFUGIO ROCHA-PIZAÑA, M. & ALVAREZ, M. M. 2016. Using simple models to describe the kinetics of growth, glucose consumption, and monoclonal antibody formation in naive and infliximab producer CHO cells. *Cytotechnology,* 68**,** 1287-1300.
MARGA, F. S., PURCELL, B. P., FORGACS, G. & FORGACS, A. 2017. Edible and animal-product-free microcarriers for engineered meat. Google Patents.
MARTINELLO, T., BRONZINI, I., MACCATROZZO, L., MOLLO, A., SAMPAOLESI, M., MASCARELLO, F., DECAMINADA, M. & PATRUNO, M. 2011. Canine adipose-derived-mesenchymal stem cells do not lose stem features after a long-term cryopreservation. *Research in veterinary science,* 91**,** 18-24.
MATHENY, J. 2005. In Vitro-Cultured Meat Production. *TISSUE ENGINEERING,* 11.
MATTICK, C. S., LANDIS, A. E., ALLENBY, B. R. & GENOVESE, N. J. 2015. Anticipatory life cycle analysis of in vitro biomass cultivation for cultured meat production in the United States. *Environmental science & technology,* 49**,** 11941-11949.
MEDCHEMEXPRESS 2019. Hoechst 33342 trihydrochloride [Online]. Medchemexpress.com. Available: https://www.medchemexpress.com/Hoechst-33342-trihydrochloride.html [Accessed]
MEGAZYME 2018. L-GLUTAMINE / AMMONIA (Rapid) ASSAY PROCEDURE.
MEILIANA, A., DEWI, N. M. & WIJAYA, A. 2015. Molecular Regulation and Rejuvenation of Muscle Stem (Satellite) Cell Aging. *The Indonesian Biomedical Journal,* 7**,** 73-86.
MERCK. 2019a. *Cell Dissociation with Trypsin* [Online]. sigmaaldrich.com. Available: https://www.sigmaaldrich.com/technical-documents/articles/biology/cell-dissociation-with-trypsin.html [Accessed].
MERCK 2019b. Lactic Acid Test [Online]. Merckmillipore.com. Available: http://www.merckmillipore.com/NO/en/product/Lactic-Acid-Test,MDA_CHEM-116127?ReferrerURL=https%3A%2F%2Fwww.google.com%2F [Accessed]
MERCK. 2019c. *Primary cell culture bascis* [Online]. Available: https://www.sigmaaldrich.com/technical-documents/articles/biology/primary-cell-culture.html [Accessed].
MIDGLEY, C. 2008, May 9. Meat without feet. *The Times*.
MORITZ, M. S., VERBRUGGEN, S. E. & POST, M. J. 2015. Alternatives for large-scale production of cultured beef: A review. *Journal of Integrative Agriculture,* 14**,** 208-216.
NAKAYAMA, Y., YAMAGUCHI, H., EINAGA, N. & ESUMI, M. 2016. Pitfalls of DNA quantification using DNA-binding fluorescent dyes and suggested solutions. *PLoS One,* 11**,** e0150528.

NIENOW, A. W. 2006. Reactor engineering in large scale animal cell culture. *Cytotechnology,* 50**,** 9.
NILSSON, K. 1988. Microcarrier cell culture. *Biotechnology and genetic engineering reviews,* 6**,** 404-439.
NZYTECH™ 2014. L-Glutamine/Ammonia, UV method. nzytech.com.
PENN, J. 2018. "Cultured Meat": Lab-Grown Beef and Regulating the Future Meat Market. *UCLA Journal of Environmental Law & Policy,* 36**,** 104.
POST, M. 2018. Proteins in cultured beef. *Proteins in Food Processing.* Elsevier.
POST, M. J. 2012. Cultured meat from stem cells: Challenges and prospects. *Meat Science,* 92**,** 297-301.
POST, M. J. 2014. An alternative animal protein source: cultured beef. *Annals of the New York Academy of Sciences,* 1328**,** 29-33.
POST, M. J. & HOCQUETTE, J. F. 2017. Chapter 16 - New Sources of Animal Proteins: Cultured Meat. *In:* PURSLOW, P. P. (ed.) *New Aspects of Meat Quality.* Woodhead Publishing.
PROBES, M. 2015. Qubit® dsDNA BR Assay Kits [Online]. Thermofisher.com. Available: https://www.thermofisher.com/order/catalog/product/Q32853 [Accessed]
PUNDIR, C., BHAMBI, M. & CHAUHAN, N. S. 2009. Chemical activation of egg shell membrane for covalent immobilization of enzymes and its evaluation as inert support in urinary oxalate determination. *Talanta,* 77**,** 1688-1693.
PUOLANNE, E. Lactic acid in muscle and its effects on meat quality. 55^< th> Annu. Recip. Meats Conf., 2002, 2002. 57-62.
PÖSÖ, A. R. & PUOLANNE, E. 2005. Carbohydrate metabolism in meat animals. *Meat science,* 70**,** 423-434.
RABI MD, Y., FRCPC, KOWAL RRT, D., AMBALAVANAN MBBS, N. & MD 2017. 10 - Blood Gases: Technical Aspects and Interpretation. *Elsevier***,** 80-96.
ROBIN, J. D., LUDLOW, A. T., LARANGER, R., WRIGHT, W. E. & SHAY, J. W. 2016. Comparison of DNA quantification methods for next generation sequencing. *Scientific reports,* 6**,** 24067.
RYU, A. H., ECKALBAR, W. L., KREIMER, A., YOSEF, N. & AHITUV, N. 2017. Use antibiotics in cell culture with caution: genome-wide identification of antibiotic-induced changes in gene expression and regulation. *Scientific reports,* 7**,** 7533.
RØNNING, S. B., ANDERSEN, P. V., PEDERSEN, M. E. & HOLLUNG, K. 2017. Primary bovine skeletal muscle cells enters apoptosis rapidly via the intrinsic pathway when available oxygen is removed. *PloS one,* 12**,** e0182928.
RØNNING, S. B., PEDERSEN, M. E., ANDERSEN, P. V. & HOLLUNG, K. 2013. The combination of glycosaminoglycans and fibrous proteins improves cell proliferation and early differentiation of bovine primary skeletal muscle cells. *Differentiation,* 86**,** 13-22.
SANES, J. R. 2003. The basement membrane/basal lamina of skeletal muscle. *Journal of Biological Chemistry,* 278**,** 12601-12604.
SCHAEFER, G. O. & SAVULESCU, J. 2014. The ethics of producing in vitro meat. *Journal of Applied Philosophy,* 31**,** 188-202.
SCHOP, D., JANSSEN, F., BORGART, E., DE BRUIJN, J. D. & VAN DIJKHUIZEN-RADERSMA, R. 2008. Expansion of mesenchymal stem cells using a microcarrier-based cultivation system: growth and metabolism. *Journal of tissue engineering and regenerative medicine,* 2**,** 126-135.
SECIU, A.-M., GASPAR, A., STEFAN, L. M., MOLDOVAN, L., CRACIUNESCU, O. & ZARNESCU, O. 2016. RIBOFLAVIN CROSS-LINKING OF COLLAGEN POROUS SCAFFOLDS FOR PERIODONTAL REGENERATION. *Studia Universitatis Vasile Goldis Seria Stiintele Vietii (Life Sciences Series),* 26.

SHUTTLEWORTH, A. 1998. Extracellular Matrix.
SINHA, I., SAKTHIVEL, D. & VARON, D. E. 2017. Systemic regulators of skeletal muscle regeneration in obesity. *Frontiers in endocrinology,* 8**,** 29.
SONS, J. W. 2008. Cell and Molecular Biology Fifth Edition CHAPTER 5 Part 1 Aerobic Respiration and the Mitochondrion Copyright 2008 by John Wiley & Sons, Inc. Gerald.
SOUZA, M. C. D. O., FREIRE, M. D. S. & CASTILHO, L. D. R. 2005. Influence of culture conditions on Vero cell propagation on non-porous microcarriers. *Brazilian archives of biology and technology,* 48**,** 71-77.
STERN, R. A. & MOZDZIAK, P. E. 2019. Differential ammonia metabolism and toxicity between avian and mammalian species, and effect of ammonia on skeletal muscle: A comparative review. *Journal of animal physiology and animal nutrition*.
TEBB, T. A., TSAI, S.-W., GLATTAUER, V., WHITE, J. F., RAMSHAW, J. A. & WERKMEISTER, J. A. 2006. Development of porous collagen beads for chondrocyte culture. *Cytotechnology,* 52**,** 99-106.
TECHONLOGIES, L. 2014. Qubit® 3.0 Fluorometer (user guide). thermoficher.com. Available: http://tools.thermofisher.com/content/sfs/manuals/qubit_3_fluorometer_man.pdf [Accessed]
THERMOFISHER 2019a. Amphotericin B. *In:* GIBCO™ (ed.) [Online]. Thermofisher.com. Available: https://www.thermofisher.com/order/catalog/product/15290018 [Accessed]
THERMOFISHER. 2019b. *Freezing Cells* [Online]. Available: https://www.thermofisher.com/no/en/home/references/gibco-cell-culture-basics/cell-culture-protocols/freezing-cells.html - 1 [Accessed].
THOMAS, K., ENGLER, A. J. & MEYER, G. A. 2015. Extracellular matrix regulation in the muscle satellite cell niche. *Connective tissue research,* 56**,** 1-8.
TIRABASSI, R. 2017. *Surviving the Big Chill: Freezing and Thawing Mammalian Cells* [Online]. bitesizebio.com. Available: https://bitesizebio.com/13684/freezing-and-thawing-mammalian-cells-tutorial/ [Accessed].
TUOMISTO, H. L. 2019. The eco-friendly burger: Could cultured meat improve the environmental sustainability of meat products? *EMBO reports,* 20**,** e47395.
TUOMISTO, H. L. & DE MATTOS, M. J. T. 2011. Environmental impacts of cultured meat production. *Environmental science & technology,* 45**,** 6117.
TUOMISTO, H. L., ELLIS, M. J. & HAASTRUP, P. Environmental impacts of cultured meat: alternative production scenarios. Proceedings of the 9th international conference on life cycle assessment in the agri-food sector, 2014. 8-10.
VAN DER VALK, J., BIEBACK, K., BUTA, C., COCHRANE, B., DIRKS, W., FU, J., HICKMAN, J., HOHENSEE, C., KOLAR, R., LIEBSCH, M., PISTOLLATO, F., SCHULZ, M., THIEME, D., WEBER, T., WIEST, J., WINKLER, S. & GSTRAUNTHALER, G. 2018. Fetal Bovine Serum (FBS): Past – Present – Future. *ALTEX,* 35**,** 1-596x.
VAN DER WEELE, C. & TRAMPER, J. 2014. Cultured meat: every village its own factory? *Trends in biotechnology,* 32**,** 294-296.
VEISETH-KENT, E., HØST, V. & PEDERSEN, M. E. 2019. Preparation of Proliferated Bovine Primary Skeletal Muscle Cells for Bottom-Up Proteomics by LC-MSMS Analysis. *Myogenesis.* Springer.
VERBRUGGEN, S., LUINING, D., VAN ESSEN, A. & POST, M. J. 2018. Bovine myoblast cell production in a microcarriers-based system. *Cytotechnology,* 70**,** 503-512.
VUONG, T. T., RØNNING, S. B., SUSO, H.-P., SCHMIDT, R., PRYDZ, K., LUNDSTRÖM, M., MOEN, A. & PEDERSEN, M. E. 2017. The extracellular matrix of eggshell

displays anti-inflammatory activities through NF-κB in LPS-triggered human immune cells. *Journal of inflammation research,* 10**,** 83.

WEGNER, K. A., KEIKHOSRAVI, A., ELICEIRI, K. W. & VEZINA, C. M. 2017. Fluorescence of picrosirius red multiplexed with immunohistochemistry for the quantitative assessment of collagen in tissue sections. *Journal of Histochemistry & Cytochemistry,* 65**,** 479-490.

WIGMORE, P. & STICKLAND, N. 1983. Muscle development in large and small pig fetuses. *Journal of anatomy,* 137**,** 235.

WILL, K., SCHERING, L., ALBRECHT, E., KALBE, C. & MAAK, S. 2015. Differentiation of bovine satellite cell-derived myoblasts under different culture conditions. *In Vitro Cellular & Developmental Biology-Animal,* 51**,** 885-889.

WUXI, B. 2018. *WuXi Biologics to Install Industry's Largest Single-Use Bioreactor from ABEC at its New Commercial Manufacturing Facility* [Online]. Available: https://www.prnewswire.com/news-releases/wuxi-biologics-to-install-industrys-largest-single-use-bioreactor-from-abec-at-its-new-commercial-manufacturing-facility-300617206.html [Accessed].

XU, S., JIANG, R., MUELLER, R., HOESLI, N., KRETZ, T., BOWERS, J. & CHEN, H. 2018. Probing lactate metabolism variations in large-scale bioreactors. *Biotechnology progress,* 34**,** 756-766.

YABLONKA-REUVENI, Z. & DAY, K. 2011. Skeletal muscle stem cells in the spotlight: the satellite cell. *Regenerating the heart.* Springer.

YAO, L., PHAN, F. & LI, Y. 2013. Collagen microsphere serving as a cell carrier supports oligodendrocyte progenitor cell growth and differentiation for neurite myelination in vitro. *Stem cell research & therapy,* 4**,** 109.

ZAGARI, F., JORDAN, M., STETTLER, M., BROLY, H. & WURM, F. M. 2013. Lactate metabolism shift in CHO cell culture: the role of mitochondrial oxidative activity. *New biotechnology,* 30**,** 238-245.

ZAMMIT, P. S., PARTRIDGE, T. A. & YABLONKA-REUVENI, Z. 2006. The skeletal muscle satellite cell: the stem cell that came in from the cold. *Journal of Histochemistry & Cytochemistry,* 54**,** 1177-1191.

Appendix 1: Laboratory instruments and equipments

Instrument	Supplier
Alpha 1-2 LDplus Entry Laboratory Freeze Dryer	Christ
AG204 DeltaRange®	Mettler Toledo
Axio observer. Z1 (fluorecence microscope)	Zeizz
BioFlo® 120 bioprocess control station	Eppendorf
Biofuge fresco	Heraeus
Canon ESO 550D (camera)	Canon
Centrifuge 5430	Eppendorf
Countess™ Automated Cell Counter	Invitrogen
Digital Heatblock	VWR
Digital IR Vortex Mixer	Velp Scientifica
Galaxy 170R/170S (Incubator)	New Brunswick
Tomy SX-700E (High-pressure steam steriliser)	Tomy Digital Biology
Incubator cabnite	Termarks
Inverted Laboratory Microscope Leica DM IL LED	Leica
Leica DMIL LED, type: 11090 137001 (light microscope)	Leica
Microcentrifuge, MiniStar	VWR Collection
POLYLUX PT Dental Polymeriser	Dreve
Qubit 3.0 Fluorometer	Invitrogen
RQflex plus 10	Merck
See-saw rocker SSL4	Stuart
SW22 (heated water bath)	Julaba
Synergy H1 (microplate reader)	BioTek
VACUSAFE™ Vaccum Aspiration System, INTEGRA Biosciences	VWR
VARIOMAG® Magnetic Stirrers	Thermo Scientific
AG204 DeltaRange®	Mettler Toledo
Axio observer. Z1 (fluorecence microscope)	Zeizz
BioFlo® 120 bioprocess control station	Eppendorf
Biofuge fresco	Heraeus
Canon ESO 550D (camera)	Canon
Centrifuge 5430	Eppendorf
Countess™ Automated Cell Counter	Invitrogen
Digital Heatblock	VWR
Digital IR Vortex Mixer	Velp Scientifica
Galaxy 170R/170S (Incubator)	New Brunswick

Equipment	Supplier
6-, 24- and 96-well cell culture plates	Sarstedt
Accu-jet® pro Pipette Controller	BrandTech Scientific.
Cell Scraper (25 cm, 39 cm)	BD Falcon
Countess® cell counter chamber slides	Invitrogen
Microscope Cover Glasses 24 x 50 mm	ThermoFicher
Eppendorf tubes (1.5 ml, 2 ml)	Eppendorf
Falcon tubes (15 ml, 50 ml)	VWR
Glass beaker (5 ml - 100 ml)	Merck
Glass pasteur pipettes	VWR
Glass Reagent bottles (25 ml, 100 ml, 200 ml)	Merck
Microcentrifuge, MiniStar	VWR Collection
VWR® Microscope Slides	VWR
Nunclon Surface 25 cm^2, 75 cm^2 and 175 cm^2 cell growth flask	Starstedt
Pipette tips	ART, Sarstedt and Thermo Scientific
Sterican® Insulin needle (6 mm)	Braun
Sterile Cell Filter Strainers (100 µm)	Life science products

Software	**Supplier**
Zeiss Zen (blue edition)	Carl Zeiss Microscopy GmbH
GraphPad Prism 8	GraphPad
Leica Application Suite (version 4)	Leica
Microsoft Office Excel	Microsoft
Microsoft Office PowerPoint	Microsoft
Gen5™	BioTek

Chemicals	**Supplier**
AEBSF, $C_8H_{10}FNO_2S$•HCl	Sigma-Aldrich
ECL, Cell attachment matrix	Millipore
Ethanol, C_2H_5OH	GE Healthcare
Trypan blue stain 0.4 %	Life technologies
0.05 % Trypsin-EDTA	Life technologies
NucBlue™ Live Cell Stain ReadyProbes ™	Invitrogen
Ethanol 75 %	Antibac
Water	Millipore
Phosphatase coctail	abcam
Dimethyl sulfoxide (DMSO)	Sigma-Aldrich
Dulbecco's Phosphate Buffered Saline (DPBS/PBS)	Sigma-Aldrich
1 % Riboflavin	

Buffer RLT Plus	Qiagen
NP-40 lysis buffer	Thermo Fisher

Medium	Components	Supplier
Collagenase medium	200 ml DMEM with GlutaMAX™-1 1 ml Penicillin Streptomycin (PenStrep) 1 ml Amphotericin B (Fungizone) 142 mg Collagenase	Life technologies
Proliferation medium (PM) 12 % FBS	500 ml DMEM with GlutaMAX™-1 60 ml Fetal Bovine Serum (FBS) 2.5 ml Penicillin Streptomycin (PenStrep) 2.5 ml Amphotericin B (Fungizone)	Life technologies
Proliferation medium (PM) 2 % Ultroser/FBS	500 ml DMEM with GlutaMAX™-1 10 ml Fetal Bovine Serum (FBS) 10 ml Ultroser ™ G 2.5 ml Penicillin Streptomycin (PenStrep) *2.5 ml Amphotericin B (Fungizone)*	Life technologies Life sciences (Ultroser)
Seeding medium	100 DMEM with GlutaMAX™-1 10 ml Fetal Bovine Serum (FBS) 0.5 ml Penicillin Streptomycin (PenStrep) 2.5 ml Amphotericin B (Fungizone)	Life technologies

Kit	Contents	Supplier
Bio-Rad DC™ Protein Assay Kit I	DC™ Protein Assay Reagent A DC™ Protein Assay Reagent B DC™ Protein Assay RC Reagent I DC™ Protein Assay RC Reagent II DC™ Protein Assay Reagent S	Bio-Rad
Glucose Assay Kit	Assay Buffer Glucose Enzyme Mix (lyophilised) Glucose Probe (in DMSO) Glucose Standard (100 nmol/µl)	Abcam
L-Glutamine/Ammonia (Rapid) Assay Kit	Bottle 1: Buffer pH 4.9, plus sodium azide Bottle 2: Buffer pH 8.0, plus sodium azide Bottle 3: NADPH Bottle 4: Glutamine suspension Bottle 5: Glutamate dehydrogenase Bottle 6: Ammonia standard solution Bottle 7: L-glutamine control powder	Megazyme
Picro sirius Red Stain Kit	Phosphomofybdic Acid, Solution A Picro sirius Red F3BA, Solution B 0.1 N Hydrochloric Acid, Solution C	Polysciences

Qubit™ dsDNA BR Assay Kit	Qubit™ assay tubes Qubit™ dsDNA BR Buffer Qubit™ dsDNA BR Reagent Qubit™ dsDNA BR Standard #1 Qubit™ dsDNA BR Standard #2	Invitrogen
Qubit™ 1X dsDNA HS Assay Kit	Qubit™ 1X dsDNA HS Working Solution Qubit™ assay tubes	Invitrogen

Appendix 2: Statistical calculations

Statistical calculations of bioprocesses in 2D systems

Table 1: Tukey's multiple comparisons test on normalised number of cells in 2D systems. *Measured with a significant level of 0.05.*

Tukey's multiple comparisons test	Mean Diff,	95,00% CI of diff,	Significant?	Adjusted P Value
Day 1 vs. Day 3	-111,7	-381,3 to 157,8	No	0,6276
Day 1 vs. Day 5	-195,7	-506,9 to 115,5	No	0,2969
Day 1 vs. Day 8	-392,2	-678,1 to -106,4	Yes	0,0069
Day 3 vs. Day 5	-84	-395,2 to 227,2	No	0,8567
Day 3 vs. Day 8	-280,5	-566,4 to 5,353	No	0,0551
Day 5 vs. Day 8	-196,5	-522,0 to 129,0	No	0,329

Table 2: Tukey's multiple comparisons test on DNA concentration in 2D systems. *Measured with a significant level of 0.05.*

Tukey's multiple comparisons test	Mean Diff,	95,00% CI of diff,	Significant?	Adjusted P Value
Day 1 vs. Day 3	0,2388	-0,6808 to 1,158	No	0,866
Day 1 vs. Day 5	0,3315	-0,5880 to 1,251	No	0,7131
Day 1 vs. Day 8	0,1358	-0,7838 to 1,055	No	0,9706
Day 3 vs. Day 5	0,09275	-0,8268 to 1,012	No	0,9902
Day 3 vs. Day 8	-0,103	-1,023 to 0,8165	No	0,9867
Day 5 vs. Day 8	-0,1958	-1,115 to 0,7238	No	0,9197

Table 3: Tukey's multiple comparisons test on protein concentration in 2D systems. *Measured with a significant level of 0.05.*

Tukey's multiple comparisons test	Mean Diff,	95,00% CI of diff,	Significant?	Adjusted P Value
Day 1 vs. Day 3	-0,1374	-0,2459 to -0,02889	Yes	0,0091
Day 1 vs. Day 5	-0,2779	-0,3827 to -0,1731	Yes	<0,0001
Day 1 vs. Day 8	-0,2974	-0,4023 to -0,1926	Yes	<0,0001
Day 3 vs. Day 5	-0,1405	-0,2490 to -0,03200	Yes	0,0075
Day 3 vs. Day 8	-0,16	-0,2685 to -0,05153	Yes	0,0021
Day 5 vs. Day 8	-0,01953	-0,1244 to 0,08529	No	0,956

Table 4: Tukey's multiple comparisons test on glucose level in 2D systems. *Measured with a significant level of 0.05.*

Tukey's multiple comparisons test	Mean Diff,	95,00% CI of diff,	Significant?	Adjusted P Value
Day 1 vs. Day 3	0,3929	-1,682 to 2,468	No	0,9273
Day 1 vs. Day 5	1,816	-0,2588 to 3,892	No	0,0879
Day 1 vs. Day 8	1,018	-1,057 to 3,093	No	0,4443
Day 3 vs. Day 5	1,424	-0,6517 to 3,499	No	0,2037
Day 3 vs. Day 8	0,625	-1,450 to 2,700	No	0,7725
Day 5 vs. Day 8	-0,7985	-2,874 to 1,277	No	0,6256

Table 5: Tukey's multiple comparisons test on lactate level in 2D systems. *Measured with a significant level of 0.05.*

Tukey's multiple comparisons test	Mean Diff,	95,00% CI of diff,	Significant?	Adjusted P Value
Day 1 vs. Day 3	-36	-238,4 to 166,4	No	0,9384
Day 1 vs. Day 5	-62	-264,4 to 140,4	No	0,764
Day 1 vs. Day 8	-174	-376,4 to 28,42	No	0,0943
Day 3 vs. Day 5	-26	-228,4 to 176,4	No	0,975
Day 3 vs. Day 8	-138	-340,4 to 64,42	No	0,2074
Day 5 vs. Day 8	-112	-314,4 to 90,42	No	0,3515

Statistical calculations of microcarriers size and bioprocesses in spinner flask

Table 6: Tukey's multiple comparisons test on the different microcarriers size in spinner flasks. *Measured with a significant level of 0.05.*

Tukey's multiple comparisons test	Mean Diff,	95,00% CI of diff,	Significant?	Adjusted P Value
Cytodex 1 vs. Cytodex 3	-61,33	-341,9 to 219,2	No	0,938
Cytodex 1 vs. ESM	-51,94	-369,2 to 265,4	No	0,9725
Cytodex 1 vs. Collagen	-2293	-2556 to -2030	Yes	<0,0001
Cytodex 3 vs. ESM	9,394	-338,3 to 357,1	No	0,9999
Cytodex 3 vs. Collagen	-2232	-2531 to -1932	Yes	<0,0001
ESM vs. Collagen	-2241	-2575 to -1907	Yes	<0,0001

Table 7: Tukey's multiple comparisons test on normalised number of cells on ESM in spinner flasks.
Measured with a significant level of 0.05.

Tukey's multiple comparisons test	Mean Diff,	95,00% CI of diff,	Significant?	Adjusted P Value
Day 1 vs. Day 3	20,07	-39,27 to 79,41	No	0,75
Day 1 vs. Day 6	16,76	-47,33 to 80,85	No	0,8636
Day 1 vs. Day 8	75,73	19,44 to 132,0	Yes	0,0083
Day 3 vs. Day 6	-3,307	-67,40 to 60,78	No	0,9986
Day 3 vs. Day 8	55,66	-0,6295 to 112,0	No	0,0529
Day 6 vs. Day 8	58,97	-2,313 to 120,3	No	0,0606

Table 8: Tukey's multiple comparisons test on normalised number of cells on collagen in spinner flasks.
Measured with a significant level of 0.05.

Tukey's multiple comparisons test	Mean Diff,	95,00% CI of diff,	Significant?	Adjusted P Value
Day 1 vs. Day 3	-99,06	-1004 to 805,9	No	0,9892
Day 1 vs. Day 6	-243,4	-1069 to 582,7	No	0,836
Day 1 vs. Day 8	-729,9	-1421 to -38,74	Yes	0,0365
Day 3 vs. Day 6	-144,3	-1122 to 833,1	No	0,9743
Day 3 vs. Day 8	-630,8	-1497 to 235,6	No	0,2026
Day 6 vs. Day 8	-486,5	-1270 to 297,2	No	0,3232

Protein concentration

Table 9: Tukey's multiple comparisons test on protein concentration with Cytodex 1 in spinner flasks.
Measured with a significant level of 0.05.

Tukey's multiple comparisons test	Mean Diff,	95,00% CI of diff,	Significant?	Adjusted P Value
Day 1 vs. Day 3	-0,2075	-0,3719 to -0,04318	Yes	0,0128
Day 1 vs. Day 6	-0,2559	-0,4202 to -0,09154	Yes	0,0028
Day 1 vs. Day 8	-0,2237	-0,3880 to -0,05930	Yes	0,0077
Day 3 vs. Day 6	-0,04836	-0,2127 to 0,1160	No	0,8183
Day 3 vs. Day 8	-0,01612	-0,1805 to 0,1482	No	0,991
Day 6 vs. Day 8	0,03224	-0,1321 to 0,1966	No	0,9355

Table 10: Tukey's multiple comparisons test on protein concentration with Cytodex 3 in spinner flasks. *Measured with a significant level of 0.05.*

Tukey's multiple comparisons test	Mean Diff,	95,00% CI of diff,	Significant?	Adjusted P Value
Day 1 vs. Day 3	-0,06851	-0,1910 to 0,05401	No	0,3845
Day 1 vs. Day 6	-0,131	-0,2535 to -0,008446	Yes	0,035
Day 1 vs. Day 8	-0,1572	-0,2797 to -0,03464	Yes	0,0115
Day 3 vs. Day 6	-0,06246	-0,1850 to 0,06006	No	0,4599
Day 3 vs. Day 8	-0,08865	-0,2112 to 0,03387	No	0,1932
Day 6 vs. Day 8	-0,02619	-0,1487 to 0,09633	No	0,9188

Table 11: Tukey's multiple comparisons test on protein concentration with eggshell membrane (ESM) in spinner flasks. *Measured with a significant level of 0.05.*

Tukey's multiple comparisons test	Mean Diff,	95,00% CI of diff,	Significant?	Adjusted P Value
Day 1 vs. Day 3	-0,09671	-0,3003 to 0,1069	No	0,5081
Day 1 vs. Day 6	-0,04231	-0,2459 to 0,1613	No	0,9217
Day 1 vs. Day 8	-0,06112	-0,2810 to 0,1588	No	0,8362
Day 3 vs. Day 6	0,0544	-0,1492 to 0,2580	No	0,8512
Day 3 vs. Day 8	0,0356	-0,1843 to 0,2555	No	0,9604
Day 6 vs. Day 8	-0,01881	-0,2387 to 0,2011	No	0,9937

Table 12: Tukey's multiple comparisons test on protein concentration with collagen in spinner flasks. *Measured with a significant level of 0.05.*

Tukey's multiple comparisons test	Mean Diff,	95,00% CI of diff,	Significant?	Adjusted P Value
Day 1 vs. Day 3	0	-0,1490 to 0,1490	No	>0,9999
Day 1 vs. Day 6	0,02821	-0,1208 to 0,1772	No	0,9414
Day 1 vs. Day 8	0,006045	-0,1429 to 0,1550	No	0,9993
Day 3 vs. Day 6	0,02821	-0,1208 to 0,1772	No	0,9414
Day 3 vs. Day 8	0,006045	-0,1429 to 0,1550	No	0,9993
Day 6 vs. Day 8	-0,02216	-0,1711 to 0,1268	No	0,97

Glucose level

Table 13: Tukey's multiple comparisons test on glucose level with Cytodex 1 in spinner flasks. *Measured with a significant level of 0.05.*

Tukey's multiple comparisons test	Mean Diff,	95,00% CI of diff,	Significant?	Adjusted P Value
Day 1 vs. Day 3	37,07	-26,14 to 100,3	No	0,2214
Day 1 vs. Day 6	26,07	-37,14 to 89,28	No	0,4363
Day 1 vs. Day 8	20,81	-42,40 to 84,02	No	0,5885
Day 3 vs. Day 6	-11	-74,21 to 52,21	No	0,889
Day 3 vs. Day 8	-16,26	-79,47 to 46,95	No	0,735
Day 6 vs. Day 8	-5,262	-68,47 to 57,95	No	0,9847

Table 14: Tukey's multiple comparisons test on glucose level with Cytodex 3 in spinner flasks. *Measured with a significant level of 0.05.*

Tukey's multiple comparisons test	Mean Diff,	95,00% CI of diff,	Significant?	Adjusted P Value
Day 1 vs. Day 3	16,46	-62,33 to 95,24	No	0,8297
Day 1 vs. Day 6	24,35	-54,44 to 103,1	No	0,629
Day 1 vs. Day 8	15,31	-63,48 to 94,09	No	0,8557
Day 3 vs. Day 6	7,893	-70,90 to 86,68	No	0,9743
Day 3 vs. Day 8	-1,148	-79,94 to 77,64	No	>0,9999
Day 6 vs. Day 8	-9,041	-87,83 to 69,75	No	0,9625

Table 15: Tukey's multiple comparisons test on glucose level with ESM in spinner flasks. *Measured with a significant level of 0.05.*

Tukey's multiple comparisons test	Mean Diff,	95,00% CI of diff,	Significant?	Adjusted P Value
Day 1 vs. Day 3	-2,392	-64,74 to 59,96	No	0,9984
Day 1 vs. Day 6	-4,592	-66,94 to 57,76	No	0,9893
Day 1 vs. Day 8	2,679	-59,67 to 65,03	No	0,9978
Day 3 vs. Day 6	-2,2	-64,55 to 60,15	No	0,9988
Day 3 vs. Day 8	5,07	-57,28 to 67,42	No	0,9857
Day 6 vs. Day 8	7,271	-55,08 to 69,62	No	0,9608

Table 16: Tukey's multiple comparisons test on glucose level with collagen in spinner flasks. *Measured with a significant level of 0.05.*

Tukey's multiple comparisons test	Mean Diff,	95,00% CI of diff,	Significant?	Adjusted P Value
Day 1 vs. Day 3	4,257	-59,01 to 67,52	No	>0,9999
Day 1 vs. Day 6	18,08	-45,19 to 81,35	No	0,9969
Day 1 vs. Day 8	7,893	-55,37 to 71,16	No	>0,9999
Day 3 vs. Day 6	13,82	-49,44 to 77,09	No	0,9998
Day 3 vs. Day 8	3,635	-59,63 to 66,90	No	>0,9999
Day 6 vs. Day 8	-10,19	-73,46 to 53,08	No	>0,9999

Lactate level

Table 17: Tukey's multiple comparisons test on lactate level with Cytodex 1 in spinner flasks. *Measured with a significant level of 0.05.*

Tukey's multiple comparisons test	Mean Diff,	95,00% CI of diff,	Significant?	Adjusted P Value
Day 1 vs. Day 3	-44,75	-133,8 to 44,26	No	0,3078
Day 1 vs. Day 6	-159	-248,0 to -69,99	Yes	0,0066
Day 1 vs. Day 8	-63,75	-152,8 to 25,26	No	0,1344
Day 3 vs. Day 6	-114,3	-203,3 to -25,24	Yes	0,0216
Day 3 vs. Day 8	-19	-108,0 to 70,01	No	0,8211
Day 6 vs. Day 8	95,25	6,242 to 184,3	Yes	0,0401

Table 18: Tukey's multiple comparisons test on lactate level with Cytodex 3 in spinner flasks. *Measured with a significant level of 0.05.*

Tukey's multiple comparisons test	Mean Diff,	95,00% CI of diff,	Significant?	Adjusted P Value
Day 1 vs. Day 3	-35,45	-91,84 to 20,94	No	0,1879
Day 1 vs. Day 6	-108,2	-164,6 to -51,81	Yes	0,005
Day 1 vs. Day 8	-39,7	-96,09 to 16,69	No	0,1408
Day 3 vs. Day 6	-72,75	-129,1 to -16,36	Yes	0,0213
Day 3 vs. Day 8	-4,25	-60,64 to 52,14	No	0,9885
Day 6 vs. Day 8	68,5	12,11 to 124,9	Yes	0,0262

Table 19: Tukey's multiple comparisons test on lactate level with ESM in spinner flasks. *Measured with a significant level of 0.05.*

Tukey's multiple comparisons test	Mean Diff,	95,00% CI of diff,	Significant?	Adjusted P Value
Day 1 vs. Day 3	-27,35	-117,2 to 62,52	No	0,6386
Day 1 vs. Day 6	-92,2	-182,1 to -2,332	Yes	0,046
Day 1 vs. Day 8	-21,05	-110,9 to 68,82	No	0,7813
Day 3 vs. Day 6	-64,85	-154,7 to 25,02	No	0,1318
Day 3 vs. Day 8	6,3	-83,57 to 96,17	No	0,9907
Day 6 vs. Day 8	71,15	-18,72 to 161,0	No	0,1018

Table 20: Tukey's multiple comparisons test on lactate level with collagen in spinner flasks. *Measured with a significant level of 0.05.*

Tukey's multiple comparisons test	Mean Diff,	95,00% CI of diff,	Significant?	Adjusted P Value
Day 1 vs. Day 3	-25,6	-74,01 to 22,81	No	0,2777
Day 1 vs. Day 6	-88,4	-136,8 to -39,99	Yes	0,006
Day 1 vs. Day 8	-18,1	-66,51 to 30,31	No	0,5031
Day 3 vs. Day 6	-62,8	-111,2 to -14,39	Yes	0,0209
Day 3 vs. Day 8	7,5	-40,91 to 55,91	No	0,917
Day 6 vs. Day 8	70,3	21,89 to 118,7	Yes	0,014

Table 21: Tukey's multiple comparisons test on DNA concentration with Cytodex 1 in benchtop bioreactor. *Measured with a significant level of 0.05.*

Tukey's multiple comparisons test	Mean Diff,	95,00% CI of diff,	Significant?	Adjusted P Value
Day0 vs. Day1	-0,879	-1,022 to -0,7362	Yes	<0,0001
Day0 vs. Day3	-0,939	-1,082 to -0,7962	Yes	<0,0001
Day0 vs. Day6	-1,094	-1,237 to -0,9512	Yes	<0,0001
Day0 vs. Day7	-0,919	-1,062 to -0,7762	Yes	<0,0001
Day0 vs. Day8	-0,219	-0,3618 to -0,07621	Yes	0,0067
Day1 vs. Day3	-0,06	-0,2028 to 0,08279	No	0,5893
Day1 vs. Day6	-0,215	-0,3578 to -0,07221	Yes	0,0074
Day1 vs. Day7	-0,04	-0,1828 to 0,1028	No	0,8596
Day1 vs. Day8	0,66	0,5172 to 0,8028	Yes	<0,0001
Day3 vs. Day6	-0,155	-0,2978 to -0,01221	Yes	0,0351
Day3 vs. Day7	0,02	-0,1228 to 0,1628	No	0,9906
Day3 vs. Day8	0,72	0,5772 to 0,8628	Yes	<0,0001
Day6 vs. Day7	0,175	0,03221 to 0,3178	Yes	0,0202
Day6 vs. Day8	0,875	0,7322 to 1,018	Yes	<0,0001
Day7 vs. Day8	0,7	0,5572 to 0,8428	Yes	<0,0001

Table 22: Tukey's multiple comparisons test on protein concentration with Cytodex 1 in benchtop bioreactor. *Measured with a significant level of 0.05.*

Tukey's multiple comparisons test	Mean Diff,	95,00% CI of diff,	Significant?	Adjusted P Value
Day0 vs. Day1	0,1679	0,03037 to 0,3053	Yes	0,0205
Day0 vs. Day3	0,1679	0,03037 to 0,3053	Yes	0,0205
Day0 vs. Day6	0,206	0,06852 to 0,3435	Yes	0,0075
Day0 vs. Day7	0,04196	-0,09552 to 0,1794	No	0,8169
Day0 vs. Day8	0,1488	0,01130 to 0,2863	Yes	0,0356
Day1 vs. Day3	0	-0,1375 to 0,1375	No	>0,9999
Day1 vs. Day6	0,03815	-0,09933 to 0,1756	No	0,8639
Day1 vs. Day7	-0,1259	-0,2634 to 0,01159	No	0,0717
Day1 vs. Day8	-0,01907	-0,1566 to 0,1184	No	0,991
Day3 vs. Day6	0,03815	-0,09933 to 0,1756	No	0,8639
Day3 vs. Day7	-0,1259	-0,2634 to 0,01159	No	0,0717
Day3 vs. Day8	-0,01907	-0,1566 to 0,1184	No	0,991
Day6 vs. Day7	-0,164	-0,3015 to -0,02655	Yes	0,0228
Day6 vs. Day8	-0,05722	-0,1947 to 0,08026	No	0,5973
Day7 vs. Day8	0,1068	-0,03067 to 0,2443	No	0,1322

Table 23: Tukey's multiple comparisons test on ammonia concentration with Cytodex 1 in benchtop bioreactor. *Measured with a significant level of 0.05.*

Tukey's multiple comparisons test	Mean Diff,	95,00% CI of diff,	Significant?	Adjusted P Value
Day 0 vs. Day 1	-0,16	-0,7639 to 0,4439	No	0,883
Day 0 vs. Day 3	-0,2185	-0,8224 to 0,3854	No	0,7079
Day 0 vs. Day 6	-0,2175	-0,8214 to 0,3864	No	0,7112
Day 0 vs. Day 7	-0,19	-0,7939 to 0,4139	No	0,7998
Day 0 vs. Day 8	-0,1575	-0,7614 to 0,4464	No	0,8891
Day 1 vs. Day 3	-0,0585	-0,6624 to 0,5454	No	0,9983
Day 1 vs. Day 6	-0,0575	-0,6614 to 0,5464	No	0,9984
Day 1 vs. Day 7	-0,03	-0,6339 to 0,5739	No	>0,9999
Day 1 vs. Day 8	0,0025	-0,6014 to 0,6064	No	>0,9999
Day 3 vs. Day 6	0,001	-0,6029 to 0,6049	No	>0,9999
Day 3 vs. Day 7	0,0285	-0,5754 to 0,6324	No	>0,9999
Day 3 vs. Day 8	0,061	-0,5429 to 0,6649	No	0,9979
Day 6 vs. Day 7	0,0275	-0,5764 to 0,6314	No	>0,9999
Day 6 vs. Day 8	0,06	-0,5439 to 0,6639	No	0,9981
Day 7 vs. Day 8	0,0325	-0,5714 to 0,6364	No	0,9999

Table 24: Tukey's multiple comparisons test on L-glutamine concentration with Cytodex 1 in benchtop bioreactor. *Measured with a significant level of 0.05.*

Tukey's multiple comparisons test	Mean Diff,	95,00% CI of diff,	Significant?	Adjusted P Value
Day 0 vs. Day 1	0,193	-0,4937 to 0,8797	No	0,8581
Day 0 vs. Day 3	0,191	-0,4957 to 0,8777	No	0,8628
Day 0 vs. Day 6	0,1495	-0,5372 to 0,8362	No	0,942
Day 0 vs. Day 7	0,203	-0,4837 to 0,8897	No	0,8338
Day 0 vs. Day 8	0,128	-0,5587 to 0,8147	No	0,9684
Day 1 vs. Day 3	-0,002	-0,6887 to 0,6847	No	>0,9999
Day 1 vs. Day 6	-0,0435	-0,7302 to 0,6432	No	0,9998
Day 1 vs. Day 7	0,01	-0,6767 to 0,6967	No	>0,9999
Day 1 vs. Day 8	-0,065	-0,7517 to 0,6217	No	0,9985
Day 3 vs. Day 6	-0,0415	-0,7282 to 0,6452	No	0,9998
Day 3 vs. Day 7	0,012	-0,6747 to 0,6987	No	>0,9999
Day 3 vs. Day 8	-0,063	-0,7497 to 0,6237	No	0,9987
Day 6 vs. Day 7	0,0535	-0,6332 to 0,7402	No	0,9994
Day 6 vs. Day 8	-0,0215	-0,7082 to 0,6652	No	>0,9999
Day 7 vs. Day 8	-0,075	-0,7617 to 0,6117	No	0,997

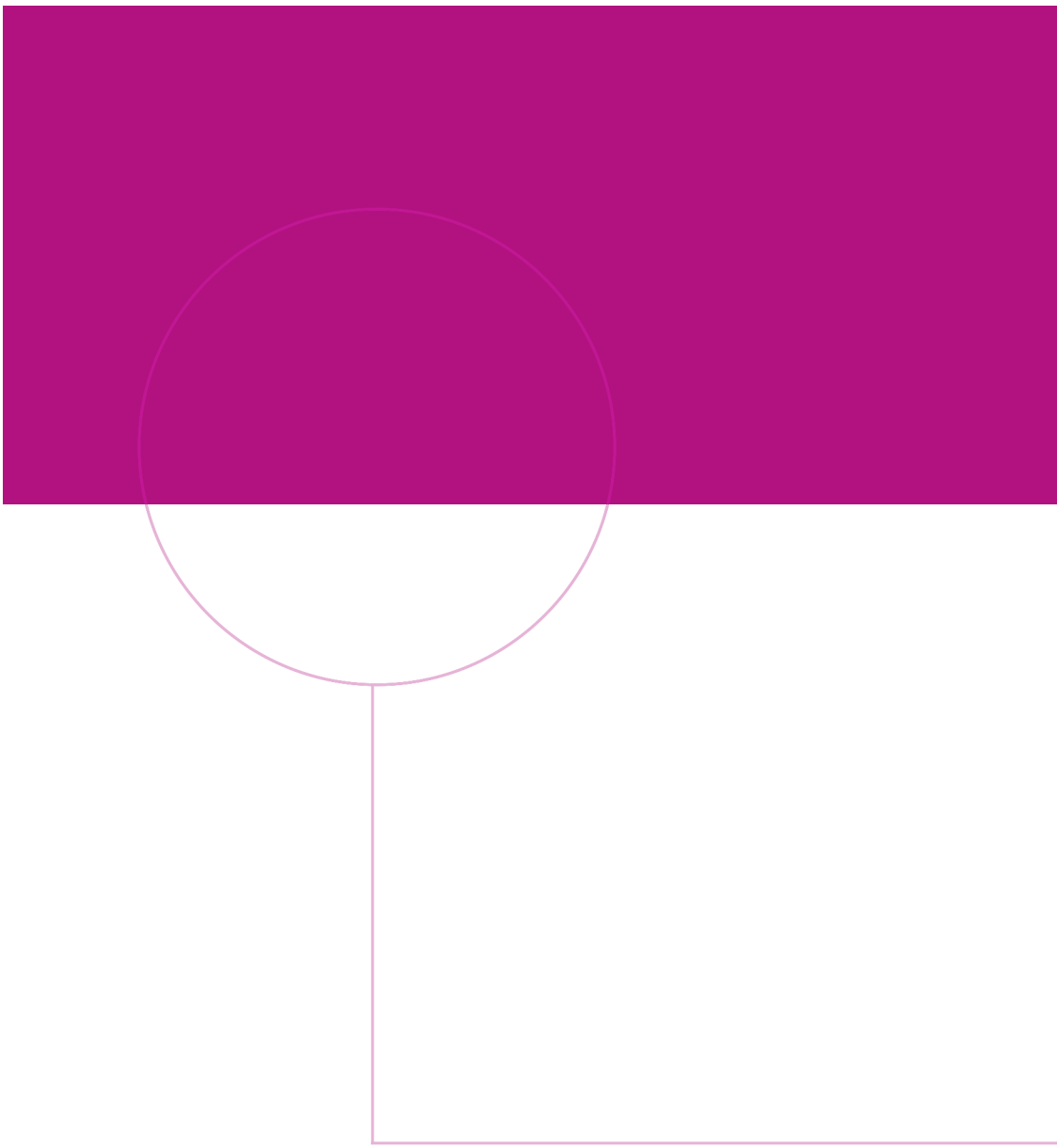

NTNU
Norwegian University of
Science and Technology